TEMPORAL DYNAMICS OF VANCOUVER'S URBAN HEAT ISLAND

by

KATHRYN ELIZABETH RUNNALLS

B.Sc., McMaster University, 1993

A THESIS SUBMITTED IN PARTIAL FULFILLMENT OF

THE REQUIREMENTS FOR THE DEGREE OF

MASTER OF SCIENCE

in

THE FACULTY OF GRADUATE STUDIES

(Department of Geography)

We accept this thesis as conforming
to the required standard

THE UNIVERSITY OF BRITISH COLUMBIA

August 1995

In presenting this thesis in partial fulfilment of the requirements for an advanced degree at the University of British Columbia, I agree that the Library shall make it freely available for reference and study. I further agree that permission for extensive copying of this thesis for scholarly purposes may be granted by the head of my department or by his or her representatives. It is understood that copying or publication of this thesis for financial gain shall not be allowed without my written permission.

Department of Geography

The University of British Columbia
Vancouver, Canada

Date August 28, 1995.

DE-6 (2/88)

ABSTRACT

A study of the urban heat island of Vancouver, British Columbia is reported. Hourly urban and rural air temperature observations are used to investigate the daily cycle of heat island growth, seasonal variations of nocturnal heat island intensity, and important controls on heat island magnitude. Urban - rural differences in nocturnal cooling are analyzed and related to heat island dynamics. Seasonal variations of rural thermal admittance are estimated from soil properties, and the relationship between thermal admittance, cooling potential, and heat island magnitude is explored.

The heat island of Vancouver is found to be most significant at night, with the daily cycle of heat island magnitude linked to urban - rural differences in cooling/warming rates. Nocturnal heat island magnitude is shown to vary significantly from day-to-day, and seasonally, but the causes of these variations are not obvious. The inverse square root of wind speed and a measure of cloud amount and type are shown to be linearly related to heat island intensity on average, but cannot be used to predict heat island intensity on any particular occasion.

Distinct seasonal variations in rural thermal admittance are observed, and although they are physically capable of producing significant seasonal variability of heat island magnitude, only a weak relationship between the two measures is found. It is concluded that while heat island magnitude behaves predictably on average, the magnitude of the urban - rural temperature difference on any particular occasion is unpredictable as a result of other unknown influences, or random effects.

TABLE OF CONTENTS

LIST OF TABLES

LIST OF FIGURES

ACKNOWLEDGEMENTS

Even though my name rests as the sole author of this work, it would never have come to exist in its present state without the help of several people. I would like to thank my supervisor, Dr. Tim Oke, for his guidance and encouragement throughout, and most importantly, for his unwavering confidence that I would eventually be able to make something of a rather uncooperative data set. I also thank my committee members, Drs. Andy Black and Douw Steyn who were always willing to discuss problems, and who provided many helpful comments along the way.

Special thanks to Jamie Voogt for patiently answering thousands of questions, explaining the mysteries of meteorological instruments, and being a limitless source of advice. Dr. Rachel Spronken-Smith was also of great assistance in setting up the field program, and Jessica North was instrumental to its successful completion. Thanks also to the Nottingham Family for accommodating the instruments in the midst of their fields.

Finally, I would like to thank Brett for 'volunteering' as emergency field assistant and proof-reader, and most importantly for the tremendous support and encouragement he has always given me.

Financial support from the Natural Science and Engineering Research Council of Canada in the form a graduate scholarship is gratefully acknowledged. Funding for Dr. Oke's research is provided by the Natural Science and Engineering Research Council of Canada, and the Atmospheric Environment Service.

Chapter 1

INTRODUCTION

Urban heat islands are undoubtedly the best known and most studied aspect of urban climatology. As early as 1833, Luke Howard proposed a list of probable causes of the increased warmth of urban areas. Despite the numerous heat island studies which have occurred since, there is much still to be learned about urban heat islands and their behaviour. This thesis presents the results of a study which describes the dynamics of the heat island of Vancouver, British Columbia; particularly its seasonal variations and how they relate to the thermal properties of its surrounding rural area. This first chapter defines urban heat islands and discusses their causes and the problems associated with the measurement of urban effects on climate. It then considers factors which affect the magnitude of heat islands and presents evidence suggesting the importance of rural thermal properties as a control on heat island magnitude. Finally, an overview of the purpose of this research project is given and limitations of the study are discussed.

1.1 Urban heat islands: definition and causes

Urban heat islands are simply defined as the relative warmth of an urban area compared to its rural surroundings. Heat island magnitude, or intensity, is calculated as the difference between urban and rural temperatures, ΔT_{u-r}. Different types of heat island are defined depending on whether temperatures of the soil, surface, or air - above or below roof level- are used to calculate the heat island magnitude (Oke, 1995). The most common heat island studied, and the one of

concern in this study, is determined by the temperature of the air below the average roof level, that is, in the Urban Canopy Layer (UCL).

A typical temperature transect in the UCL across a city is shown in Figure 1.1. The temperature increases sharply on the upwind boundary of the city, and continues to increase until it reaches its maximum, usually slightly downwind of the urban centre. It then decreases gradually returning to rural temperatures slightly downwind of the urban-rural boundary. The heat island magnitude is shown on the diagram as the difference between the maximum urban temperature and the minimum rural temperature.

Heat island magnitude varies significantly over a 24 hour period. Figure 1.2 shows typical diurnal cycles of urban and rural temperatures, heating and cooling rates, and the resulting heat island intensity. The time scale is arbitrary in that the actual timing of the onset of cooling or warming depends on the times of sunset and sunrise, and therefore varies seasonally. Typically, urban and rural temperatures are similar in the daytime, but begin to diverge when cooling starts in the late afternoon. Rural temperatures decrease rapidly at first, then more slowly after midnight, while urban cooling is less, but fairly constant throughout the night. These differences in cooling rates result in rapid growth of the heat island between sunset and midnight, when the maximum usually occurs. Heat island magnitude stays about the same or slowly decays during the rest of the night because the cooling rates are essentially the same. Following sunrise the rural area warms more rapidly than the urban area initially, but the rates are similar during most of the day, resulting in small, or occasionally negative, urban-rural temperature differences.

Because heat island magnitude is largest at night, and because this is when the practical implications are significant with respect to heat stress, space heating requirements and air pollutant dispersion, most research focuses on the nocturnal heat island. The focus of this thesis

Figure 1.1 Typical spatial variation of temperature in the UCL of a hypothetical city, along cross section AB. The resulting heat island intensity is ΔT_{u-r}. (From Oke, 1982).

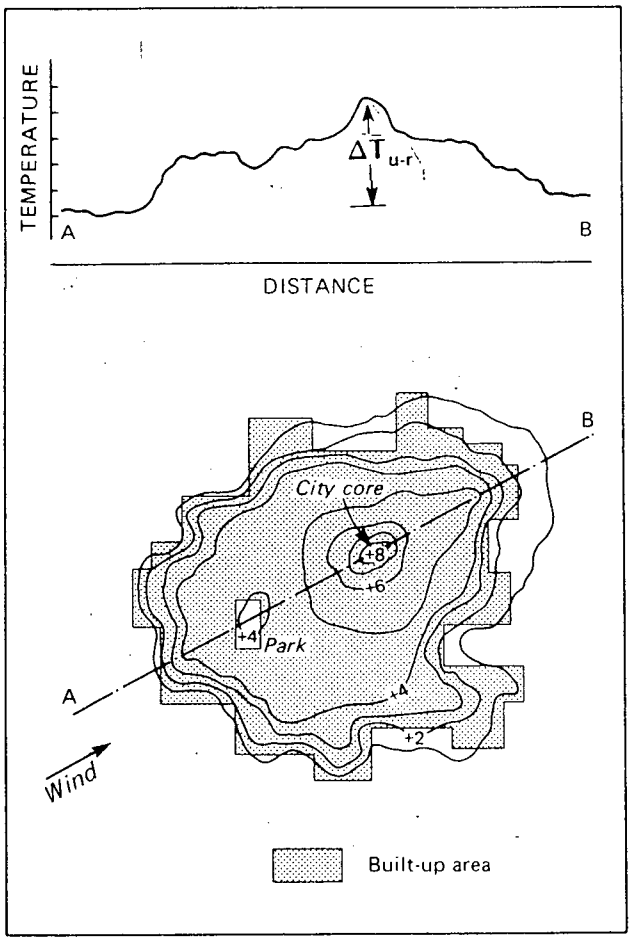

Figure 1.2 Temporal variation of urban and rural temperatures, cooling/warming rates and the magnitude of the heat island. (From Oke, 1982).

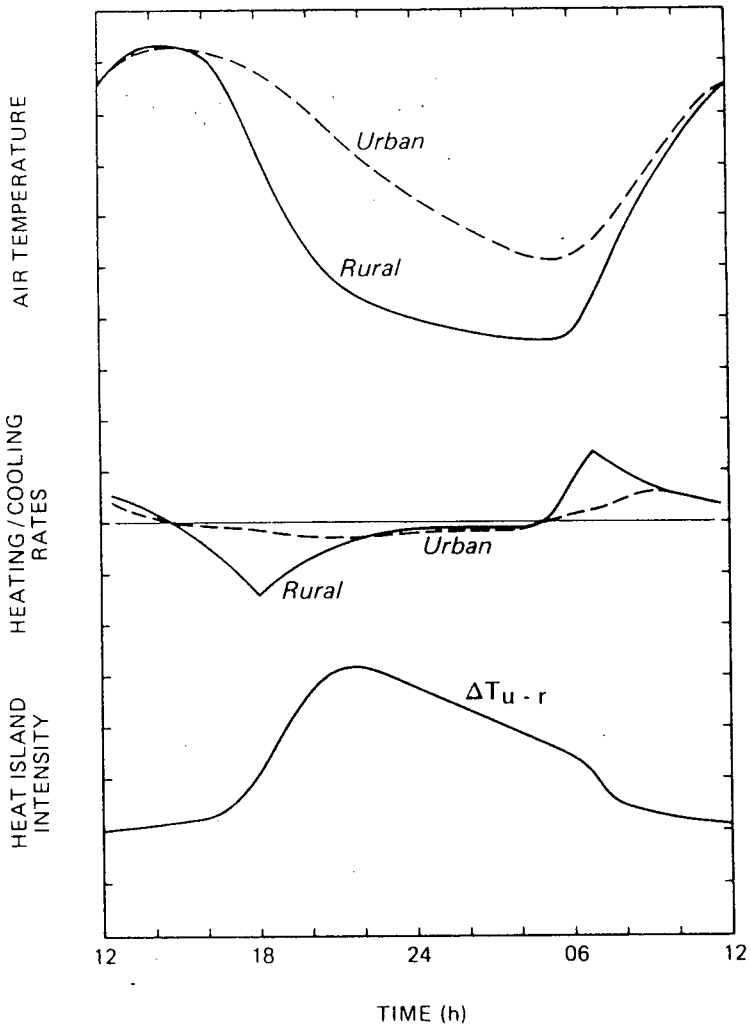

is also largely, but not exclusively, on the nocturnal heat island and causes of seasonal variations in its magnitude.

Because the magnitude changes continuously and depends on the location of observations within and outside the city, it is necessary to maintain consistent observation methods when studying heat islands. For example, to compare the magnitudes of heat islands, it is important to ensure that the measurements are consistently from the same time of day, and it is important to know the spatial variability of temperatures within and outside of the city in order to ensure the maximum difference is observed.

Because urban heat islands are a feature of the built environment, it is appealing to think of them as effects of urban development. That is, the rural temperature is often considered to be the background value, *i.e.* the temperature that would occur if the urban area were not present. However, as Lowry (1977) points out, urban-rural temperature differences are not necessarily a good measure of urban effects on temperature. Urban and rural areas are likely to experience microclimatic differences because of different topography, or the rural area itself may be influenced by the urban area. The only true method of measuring urban effects is to have pre- and post- urban observations stratified by synoptic type. Unfortunately pre-urban observations are rarely available, and urban-rural differences must be substituted. Recognizing this limitation, the urban heat island measurements in this study should be considered contemporaneous urban - rural differences only; they are not necessarily a measure of how urbanization has changed the local climate.

Causes of the increased warmth of urban areas are well known (Table 1.1). These features of the urban environment vary in their relative importance in different cities, and at different times within a particular city. For example, anthropogenic heat may be more important during the

winter in high-latitude cities. The amount and type of macroclimate, industry, transportation and population in a given city dictate the relative importance of anthropogenic heat.

Table 1.1 Causes of urban heat islands (Source: Oke, 1982).

Feature of the Urban Environment	Effect on Energy Balance and Temperature
Canyon Geometry	Greater surface area and vertical surfaces increase reflection and absorption of solar radiation.
Canyon Geometry	Tall buildings obscure the sky, reducing the sky view factor. This lowers the amount of long-wave radiation lost at night; warm buildings emit long-wave radiation back to surface to offset cooling.
Pollution, Urban 'Greenhouse' Effect	Polluted air absorbs long-wave radiation, warms, and emits more radiation back to surface (increases net radiation).
Anthropogenic Heat	Waste heat from space heating, cars, industry and people warms the urban air.
Reduced Vegetation	Evapotranspiration is reduced; more energy is available to heat the air or to be stored in the ground.
Thermal Properties	Urban materials are better able to store heat during the day and release it at night to offset cooling.
Increased Shelter	Turbulent transport and advection of heat is reduced; less efficient transport of heat out of the urban environment.

As previously noted, this thesis focuses mainly on causes of variations in nocturnal heat island intensity. Although each city is unique, canyon geometry and surface thermal properties are thought to be particularly important in generating the nocturnal heat island in most cities (Oke *et al.*, 1991). The sky view factor is a measure of canyon geometry. It is defined as the ratio of the area of sky visible from a point to the total area of the hemisphere above the point (Oke, 1987). Closely spaced, tall buildings in city centres lead to low sky view factors and decreased radiative cooling at night compared to the more open (larger sky view factors) surrounding rural areas.

Thermal properties of urban surfaces are also important because they determine the amount of heat transported to the substrate by day which is then available at night to offset cooling. The thermal admittances (square root of the product of heat capacity and thermal conductivity) of most urban surface materials are typically larger than those of relatively dry rural surfaces, but not necessarily larger when the soils are wet (Table 1.2). The thermal admittance determines the rate of surface temperature change in response to heat gains or losses. The lower the thermal admittance, the larger the surface temperature change. The larger the urban-rural difference of thermal admittance, the greater the effect on differential warming/cooling rates. The importance of thermal admittance in heat island intensity is discussed further in Section 1.3.

Typically, the combination of the city's lower sky view factor and larger thermal admittance (compared to rural values) results in less urban cooling after sunset, as shown in Figure 1.2.

Table 1.2 Thermal admittance values for typical urban and rural surfaces (Oke, 1987).

Material	Thermal admittance ($J\ m^{-2}\ s^{-1/2}\ K^{-1}$)
Asphalt	1205
Concrete	1785
Steel	14475
Glass	1110
Sandy soil: dry	620
saturated	2550
Clay soil: dry	600
saturated	2210
Peat soil: dry	190
saturated	1420
Snow	130

1.2 Factors Affecting Heat Island Magnitude

The geographic location (*e.g.* climate, proximity to water bodies, local topography and land use) and characteristics of the city itself (*e.g.* size, population, population density, building density or sky-view factor, amount and type of industry, *etc.*) are largely responsible for between-city differences of heat island characteristics such as magnitude and seasonality. Ludwig (1970) found $\Delta T_{u\text{-}r}$ to be proportional to the fourth root of population, which is related to the radius of the city. Oke (1973) showed that $\Delta T_{u\text{-}r(max)}$ (observed under 'ideal', calm and clear conditions) is proportional to the logarithm of the population, but that the relationship is slightly different for North American and European cities. Later Oke (1981) showed that some of the variability in $\Delta T_{u\text{-}r(max)}$ is related to the street geometry of the city core (*i.e.* its sky-view factor). Since European cities tend to have more open geometries than North American cities with the same population, population alone cannot predict heat island intensity.

The day - to -day variability of heat island magnitude in a particular city has been shown to be strongly influenced by weather, especially wind speed and cloud cover. Sundborg (1950) found for Uppsala, Sweden, that

$$\Delta T_{u\text{-}r} = (a\text{-}bn)u^{-1} \qquad (1.1)$$

where n is the cloud amount, u is the regional wind speed and a and b are constants specific to each city. Oke (1973) showed that heat island intensity in several cities is inversely proportional to the square root of wind speed. Other studies have demonstrated that cloud type, as well as the amount, is important in determining heat island intensity. For a given fractional cloud cover, low cloud is more effective at limiting heat island intensity than high cloud. Ludwig (1970) and Lee (1975) found that atmospheric stability, which incorporates cloud and wind effects, is also correlated to heat island intensity.

Because meteorological variables exert significant control on heat island intensity, it is difficult to make meaningful comparisons unless the heat island observations are made under similar weather conditions. Other things being equal, heat island intensity is largest under calm, clear conditions and decreases with increasing wind speed and cloud cover. Calm and clear conditions are therefore referred to as 'ideal' heat island conditions throughout this thesis. This is when the maximum intensity is observed ($\Delta T_{u\text{-}r(max)}$), so it is common to compare heat island intensities observed under these 'ideal' conditions.

1.3 Seasonal Variations of Heat Island Magnitude

In addition to the day-to-day variations of magnitude caused by changing synoptic weather conditions, heat island magnitudes in many cities also vary seasonally. This is perhaps not surprising given that synoptic conditions also often vary seasonally. That is, 'ideal' conditions are more frequent at certain times of the year. However, even after stratifying by synoptic conditions, or only considering heat islands which occur under 'ideal' conditions, seasonality is still apparent. In many mid-latitude cities, larger heat island intensities and/or greater rural cooling rates have been observed to occur in the warmer part of the year. *e.g.* London (Chandler, 1965; Lee, 1975; Lee 1979), Montreal, Vancouver (Oke and Maxwell, 1975), and Birmingham (Unwin, 1980). However, Hage (1972) found that Edmonton's heat island magnitude exhibited only a small annual variation, and that weak maxima occurred in both January and June. Similarly, some tropical cities experience their largest heat island magnitude in the cool season. However, moisture, not temperature, appears to be the important seasonal variable for tropical cities, because the maximum heat island magnitude usually occurs in the dry season. *e.g.* Johannesburg (Tyson *et al.*, 1972), Bombay (Philip *et al.*, 1973), Delhi (Bahl and Padmanabhamurty, 1979), Mexico City (Jauregui, 1986), Guadalajara (Jauregui *et al.*, 1992).

Large heat island intensities occurring in the warmer half of the year are often attributed to the increase of solar radiation available for storage in the urban fabric during the day, and its release at night to offset cooling. In the rural case, increased absorbed solar radiation leads to higher surface temperatures, and greater surface-sky temperature contrasts at the onset of cooling, resulting in large radiative losses. Other explanations of the causes of seasonal variations in magnitude may be elucidated by re-examining Table 1.1.

Clearly, the canyon geometry of a city does not vary significantly from season to season and cannot explain the variations discussed above. While the amount and type of air pollution may vary seasonally, there is still debate as to the net effect of air pollution on urban temperatures (Estournel, *et al.*, 1982; *Oke et al.*, 1991). Although a layer of pollutants may increase the net long-wave radiation at the urban surface, it also reflects solar radiation during the day. These two effects are offsetting, and may produce only a small net effect on the urban temperature.

Anthropogenic heat is a possible control on seasonal variations of heat island intensity in mid- and high- latitude cities with large winter space-heating requirements. This may be the reason for the maximum heat island in Edmonton (Hage, 1972) and Fairbanks (Bowling and Benson, 1978) occurring in winter. However, since most mid-latitude cities experience maximum heat island magnitudes in the warmer part of the year, anthropogenic heat does not appear to be a factor of general importance. The effects of reduced vegetation and increased shelter are likely to exert similar control on the heat island magnitude in all seasons.

The final possible control, the thermal properties of the substrate, is potentially important in producing seasonal variations of heat island intensity. Although urban thermal properties are likely to remain fairly constant throughout the year, rural surfaces can undergo significant seasonal variations in thermal properties due to changes in soil moisture, vegetation cover, or the presence of snow. In particular, the thermal admittance, the property which determines the rate

of cooling following a step change in heat flux, is very different for wet and dry soils (Table 1.2). Hence rural cooling rates may be vary considerably between the wet and dry seasons, or in some areas, between the snow-covered and snow-free seasons. The following section examines evidence of the importance of rural thermal admittance in determining heat island intensity.

1.4 The Role of Rural Thermal Admittance in Determining Heat Island Intensity

Much of the work aimed at understanding heat island intensity has focused on features of the city believed to cause its greater warmth. However it is important to keep in mind that the heat island is a measure of the difference between urban and rural temperatures, and therefore the rural temperatures are equally important in determining the heat island magnitude. That is, no matter how warm the urban area is, if the rural area is the same temperature and cools off at the same rate as the urban area, a heat island will not occur . Because the nocturnal heat island develops when the urban area cools down more slowly than the surrounding rural area, (Figure 1.2) the rural cooling rate is an important control on the heat island intensity. Since cooling rates are controlled in part by the surface thermal admittance it seems this factor should also be considered in empirical estimates of heat island intensity. Oke (1981) showed in a physical modeling study that cooling differences between surfaces with different thermal admittances produce 'heat islands' which behave in a similar way to real world heat islands. Clearly urban - rural differences in thermal admittance and cooling potential are important in heat island development.

Figure 1.3 (Oke *et al.*, 1991) shows heat island intensity determined by the numerical model SHIM (Surface Heat Island Model). It shows the effects of both canyon geometry (sky view factor) and urban-rural thermal admittance differences and that heat island intensity is approximately equally sensitive to both factors. It also shows that the absolute thermal

Figure 1.3 Model predictions of maximum nocturnal surface heat island intensity in relation to sky view factor of the urban canyons (ψ) and urban - rural thermal admittance difference ($\Delta\mu_{u-r}$). Each of three sets of curves is for a different absolute value of rural thermal admittance (μ_r). (From Oke *et al.*, 1991).

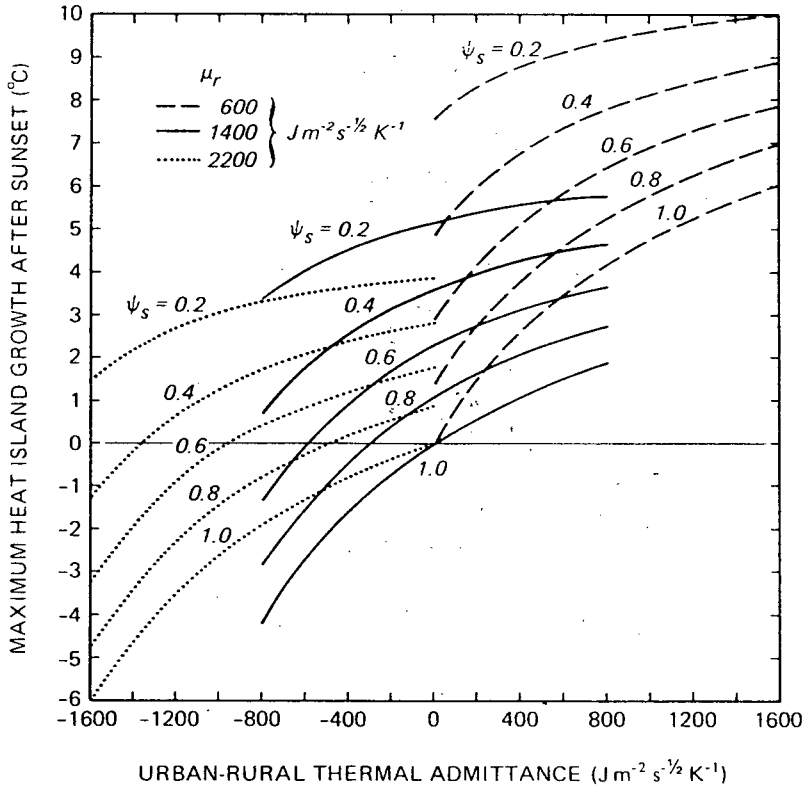

admittance of one of the environments sets the overall context for heat island potential. The largest heat island intensity (10 °C) occurs when the sky-view factor is small, the urban-rural thermal admittance difference is large, and the rural admittance is small. With small sky-view factors (*e.g.* 0.2), heat island intensity is approximately half the maximum value of that when there is no difference between the urban and rural thermal admittances. If rural thermal admittances are greater than urban values, negative heat island intensities can occur. If the rural admittance is large, the ability to develop a positive urban-rural temperature difference is limited. Although these model results are for surface temperatures, they are expected to apply to near-surface air temperatures as well.

Because most city centres are built from similar types of materials (asphalt, concrete, brick, *etc.*), thermal admittance differences between cities are probably relatively small. However, since rural thermal admittances are controlled by soil moisture, soil type, vegetation cover and the presence or absence of snow, differences in rural rather than urban thermal admittances are more likely to explain differences in heat island intensities between cities.

Evidence of the importance of rural thermal admittance is given in Figure 1.4 (Oke *et al.*, 1991) where maximum observed heat island intensities ('ideal' conditions) are plotted against sky-view factors for different cities. Two distinct linear relationships emerge: one for North American, European and Australasian cities, and a different one for Asian cities. Oke *et al.* (1991) suggested that the reason these Asian cities experience smaller heat islands at a given sky-view factor is related to the rural thermal admittance. Because most of these Asian cities are surrounded by paddy fields with high soil moisture and large thermal admittances, the rural cooling potential is limited, and smaller heat islands result.

Figure 1.4 Relationship between the maximum heat island observed and the sky view factor of the city centre (ψ). Data are for summer only. (From Oke *et al.*, 1991).

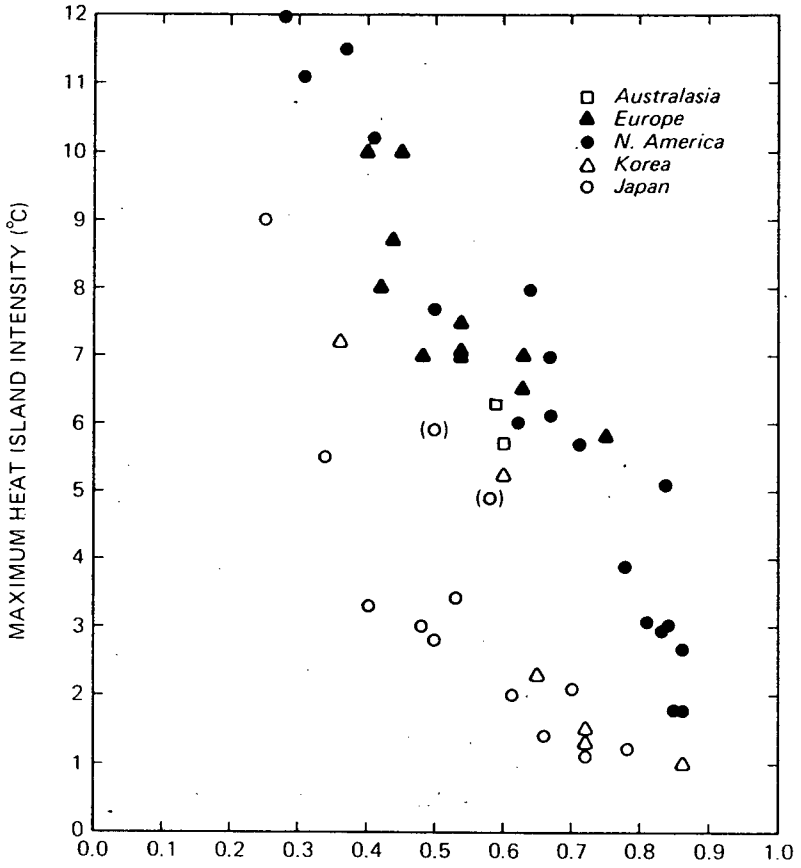

A further implication of these findings is that the seasonal variations in rural thermal admittance previously discussed (soil moisture variations, vegetation cover and snow cover) are likely to produce a component of the seasonal variations in heat island intensities. Assuming that the urban thermal admittance remains relatively constant throughout the year, low thermal admittances of dry rural soils can explain the observations of large heat island intensities in tropical cities during the dry season (Tyson *et al.*, 1972; Philip *et al.*, 1973; Bahl and Padmanabhamurty, 1979; Jauregui, 1986, Jauregui *et al.*, 1992). As mid-latitude cities may also experience significant seasonal variations in rural thermal admittance due to soil moisture changes or the presence or absence of a plant or snow cover, this pattern should be reflected in the seasonal variation of heat island magnitude.

1.5 Research Design

Recognizing the probable importance of rural thermal admittance as a control on heat island intensity, research is undertaken to investigate it further. The aim is to show from observations that seasonal variations in rural thermal admittance are related to seasonal variations in heat island intensity. In order to do this, a thorough understanding of the temporal dynamics of the heat island is necessary. Observations of heat island intensities and thermal admittances for a period of at least one year are required.

1.5.1 Location of the Study

Vancouver, British Columbia has an adequate data base of heat island measurements and was chosen for the site of the study. Vancouver is situated on the south-west coast of continental British Columbia, Canada (Figure 1.5). The greater metropolitan region covers 2750 km^2 at the mouth of the Fraser River, and is home to more than 1.5 million people. The most intensively

built up area and commercial centre is located on the Burrard Peninsula, towards the western end of the metropolitan region. Vancouver is bordered by Georgia Strait to the west and the Coastal Mountains to the north. A mix of agricultural and residential areas lie to the south and east.

Figure 1.5 Location of Vancouver, British Columbia, Canada.

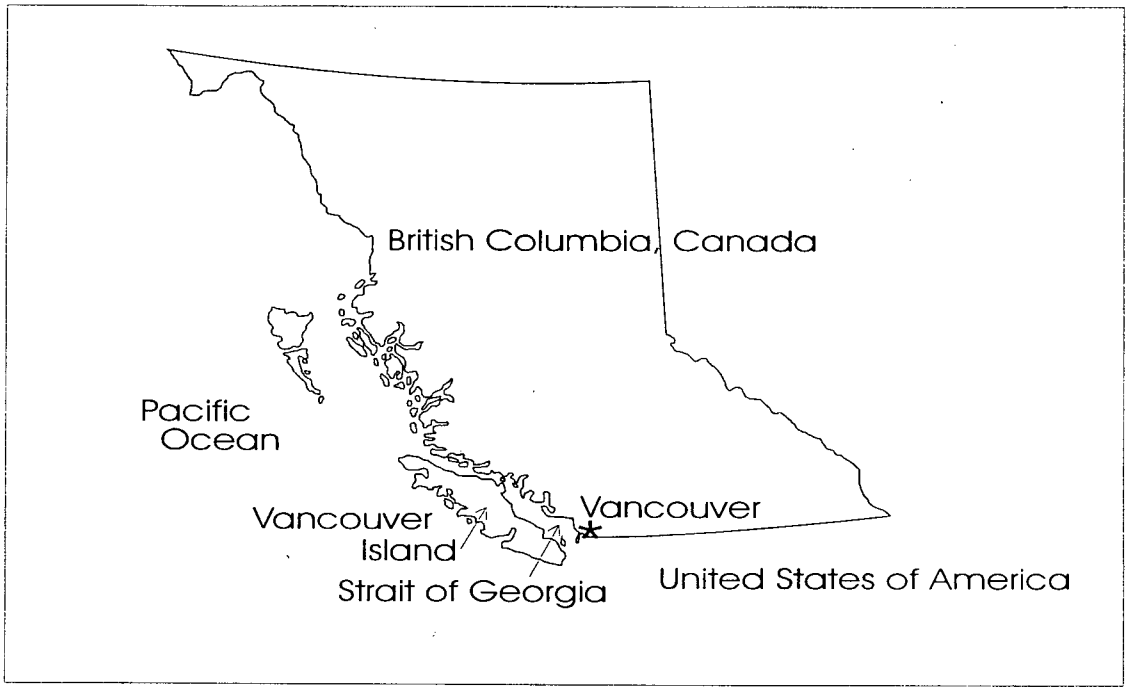

Vancouver's climate (described by Oke and Hay, 1994) is largely governed by its mid-latitude location on the west coast of a large continent. The proximity to the Pacific Ocean provides Vancouver with a significantly milder climate than most Canadian cities. The mean daily temperature recorded at the Vancouver International Airport (1961-1990) is 9.9 °C. 1117 mm of the 1167 mm of precipitation each year falls as rain. The rain is mainly confined to the cooler half of the year.

Since Vancouver is located at the mouth of a coastal valley, in the absence of strong regional winds both land/sea and mountain/valley circulations act together to produce landward directed winds by day, and seaward winds at night.

The mountains also influence the climate by channeling and deflecting winds, causing cold air drainage downslope and variations of temperature and solar radiation with increasing elevation. Urban development is another important feature that affects the local climate.

1.5.2 Vancouver's Urban Heat Island

Although Vancouver's urban heat island has been the subject of several short-term studies the data have not been available to adequately describe extended day-to-day or seasonal variations.

Emslie (1972) described regional variations in mean monthly maximum and minimum temperatures from 25 standard climate stations in the Lower Mainland. Both maximum and minimum temperatures in the downtown core of Vancouver (Burrard Peninsula) were found to exceed the airport temperatures by more than 2°C at all times of the year. The apparent coldest region was located in Delta, south-east of Vancouver (near the rural observation site used in this thesis), where mean minimum temperatures were more than 5 °C colder than the airport temperatures.

Field (1973) using vehicle traverses also found the highest nocturnal temperatures to be in the downtown core. He investigated the relationship between heat island intensity and cloud height for completely overcast conditions with very light or calm airflow. The largest heat island intensity (9°C) was observed under calm, clear conditions. Heat island intensity did not seem to be affected by high cloud. However, heat island magnitude was approximately halved with middle-level clouds, and virtually eliminated under low clouds. He suggested that the presence of

low and middle-level clouds significantly reduces cooling in the rural areas which limits the size of the urban-rural temperature difference.

Oke and Maxwell (1975) measured heat island intensity and heating/cooling rates by hourly traverses through a range of land uses for a short period. They found that the heat island magnitude increases rapidly after sunset, reaches a maximum 3 to 5 hours after sunset, then gradually declines through the night. The maximum observed heat island magnitude was 10.2 °C (Oke, 1981). Rural cooling rates at sunset were found to be greater in the summer, which was attributed to greater storage of daytime heat. In Montreal, urban cooling rates were found to be smaller, and essentially linear through the night during the summer, while no urban cooling took place for 5 hours after sunset in the winter. This lack of cooling was attributed to the release of heat during the evening rush-hour, which occurs around the time of sunset in winter.

Oke (1976) again used traverses to measure the urban heat island in order to test two models. There was a tendency for slightly greater heat island magnitudes to occur at a given wind-speed in the warmer half of the year.

Oke and Hay (1994) provide a general description of the urban influence on the region's climate. They report a rapid increase in temperature at the limits of the built up area. The core of the heat island, or highest urban temperature is located downtown, as observed in the previous studies, but secondary 'hot-spots' are found in other densely built-up areas. They also report that the mean annual air temperature is only slightly higher over the urban centre than the rural area, and that the daytime heat island intensity is small (around 1 °C). However, as discussed previously, the heat island intensity is usually greater at night, and in Vancouver, can exceed 10 °C.

1.5.3 Research Goals:

The aim of this thesis is to extend knowledge of Vancouver's urban heat island by describing the nature of short- and long-term variations in its magnitude. This description is possible because of a data base of hourly urban and rural temperatures made between December 1991 and September 1994. An attempt is also made to explain the causes of such variations. In particular, the relationship between seasonal variations in rural thermal admittance and heat island magnitude (and cooling rates) is examined.

The availability of the extensive data base compensated for the somewhat less than ideal location of Vancouver for heat island studies. Vancouver's proximity to the oceans, mountains and the Fraser River introduces complications such as sea breezes and air drainage from the Fraser River Valley. The varied rural surroundings of Vancouver prevent the selection of a 'representative' rural site. Also, being a coastal city, it experiences relatively small seasonal variations in climate, particularly temperature, so it is likely to have smaller seasonal variations in its heat island intensity than continental cities. However, with relatively dry summers and wet winters the seasonal variations in rural soil moisture and thermal admittance are significant, and likely to exert some influence on heat island intensity. Details of the research methodology are outlined in Chapter 2.

Chapter 2

DATA AND METHODS

2.1 Research Objectives

The aims of this research are to characterize the temporal dynamics of Vancouver's heat island and to understand its relationship to rural nocturnal cooling. In particular, the role of soil thermal admittance in controlling rural cooling is investigated. These goals were approached in the following stages: description of the typical characteristics of Vancouver's urban heat island in terms of daily and seasonal variations, and investigation of the controlling factors; description of the nature of rural and urban nocturnal cooling; and an attempt to measure the rural thermal admittance, its annual range and variations, in order to relate it to cooling and heat island intensity.

2.2 Heat Island Observations: Fixed Point vs Vehicle Traverse Methods

The typical characteristics of Vancouver's urban heat island were determined from differences between hourly averaged temperatures in downtown Vancouver, and a rural site in Delta, approximately 25 km south-east of the city. (Figure 2.1). The data set provides a fairly continuous record (except for occasional equipment failure) from December 1991 to September 1994. These air temperature observations are also used to investigate urban and rural cooling rates.

Figure 2.1 Location of urban and rural observation sites and Vancouver International Airport.

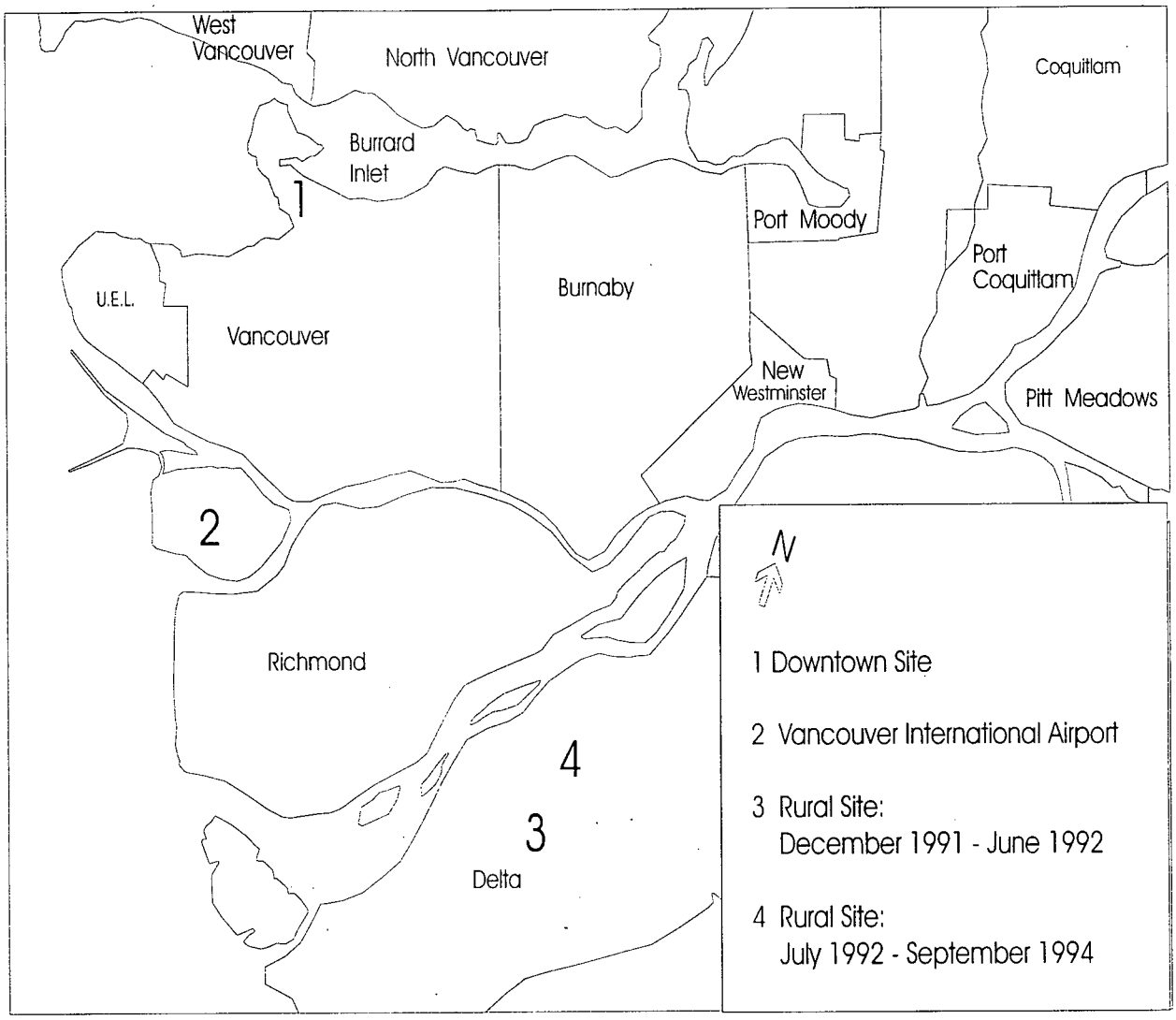

Previous heat island studies in Vancouver have used the vehicle traverse method of temperature observation rather than fixed point measurements (Field, 1973; Oke and Maxwell, 1975; Oke, 1976). The vehicle traverse method allows the spatial characteristics of the temperature field to be determined, and therefore increases the likelihood that the maximum urban-rural temperature difference will be observed. However this method is not practical when observations over a long period of time are required. The use of fixed point temperature measurements in this research allowed heat island and temperature variations on multiple hourly to seasonal time scales to be analyzed. Simultaneous observations from both methods were compared to determine how results of the analysis are affected by the method of observation.

Figure 2.2 shows maximum nocturnal heat island intensities calculated from the fixed station and vehicle traverse approaches between January 24 and February 9, 1994. The temperature sensor for the vehicle traverse consists of a thermocouple housed in an insulated, ventilated cylinder, mounted on the back of a truck and driven between the downtown and the rural site. Temperatures were sampled every second, averaged over 4 seconds, and recorded by a Campbell Scientific (CSI) 21X data logger. A correction was applied to account for cooling over the time of the traverse, and the heat island intensity was determined as the difference between the maximum downtown temperature and the temperature at the rural site. Instrumentation at the fixed sites is described below.

There is good agreement between the intensities, but the vehicle traverse method tends to yield slightly larger values. The difference is usually less than 1 °C, but on one occasion, it is slightly more than 1.5°C. Differences are expected since the fixed point observations are hourly averaged temperatures, whereas the vehicle traverse data are 4 second averages and are more likely to capture short-term temperature variations. The height of measurement is lower for the

vehicle traverses which might also be expected to affect temperature observations, particularly if a strong rural temperature inversion is present.

Figure 2.2 Comparison of heat island magnitudes determined from fixed point and vehicle traverse observations of air temperature.

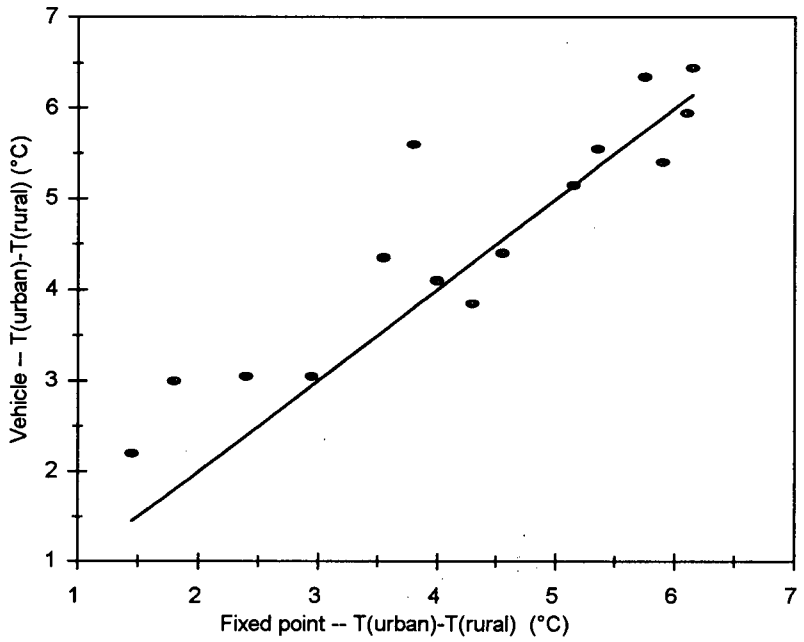

Table 2.1 compares 'simultaneous' temperature observations at both the urban and rural sites. The temperatures are not strictly simultaneous because the fixed point observations are hourly averages, whereas the traverse observations are 4 second averages. The maximum heat island intensity which occurred before midnight is also listed for each method. On two nights, the heat island intensities differ by more than 3 °C.

Table 2.1. Comparison of 'simultaneous' temperature observations (°C) from fixed point (hourly average) and vehicle traverse (4 second average), and the maximum heat island intensity observed between sunset and midnight.

Date	Urban Temperature		Rural Temperature		Maximum ΔT_{u-r}	
	Fixed	Vehicle	Fixed	Vehicle	Fixed	Vehicle
May 18, 1994	17.3	19.2	12.3	11.2	5.0	8.1
May 19, 1994	17.0	18.3	13.6	13.5	3.6	4.3
May 22, 1994	16.3	17.6	11.1	10.3	4.3	8.5
August 11, 1994	20.1	20.6	16.6	16.9	5.0	6.0

The observations reveal that the vehicle traverses generally record higher urban temperatures and lower rural temperature than the fixed point observations, systematically resulting in larger heat island intensities. Clearly, the longer averaging times at the fixed sites do not capture extremes in temperature variation, whereas the traverse method does. Since the traverse method may also capture short bursts of heat from vehicle exhaust, it might be argued that the fixed point method is more representative of the average conditions in the urban setting. The lower rural temperatures observed by the traverse method may be a result of the lower height of observation if a strong inversion is present, in which case the difference in averaging times is not as important.

Although heat island magnitudes from fixed point observations are smaller than those observed by vehicle traverses, both methods are likely to display the same temporal variability. Therefore, the use of fixed point rather than vehicle traverse observations in this study provides an adequate data base from which to study temporal dynamics of Vancouver's heat island, but absolute values are not strictly comparable with those from the previously reported vehicle-based studies.

2.3 Urban Site and Instrumentation

The downtown station is located just west of the intersection of Burrard and Georgia streets in the commercial centre of Vancouver (Figures 2.3 - 2.5). Air temperature was measured with a thermistor (CSI 101) and wind speed and direction with an anemometer (CSI Met One 014A) and wind vane (024A). These instruments were attached at 10 m above ground on a lamp post on the south side of Georgia Street, which runs approximately east-west. Observations were made once per minute, averaged over 1 hour and recorded by a data logger (CSI CR21X). Spatial surveys of nocturnal air temperatures in Vancouver have indicated that the highest nocturnal temperatures occur in this area of the city, and therefore the station is located near the core of the heat island. (Field, 1973; Oke and Maxwell, 1975; Oke and Hay, 1994; this study). As shown in Figure 2.5, the site is also surrounded by very tall buildings, giving it a low sky-view factor of approximately 0.41 (Steyn, 1980).

2.4 Rural Site and Instrumentation

Initially the rural station was located in the Delta works yard on Highway 99 (Figure 2.1). In July 1992 the instruments were moved approximately 1.5 km north-east into the midst of agricultural fields on the Nottingham farm (Figures 2.6, 2.7). Because simultaneous temperature data from both rural sites is not available, it is difficult to determine how the continuity of the rural data series was affected by the move. Comparison of temperature and heat island magnitudes before and after the move do not reveal obvious differences between the sites. The mean, standard deviation and range of heat island magnitudes from February to June 1992 (before the move) are intermediate to those in the same months of 1993 and 1994. If temperature differences between the rural sites do exist, they are smaller than the inter-annual variability at the present site.

Figure 2.3 Location of the urban observation site in downtown Vancouver.

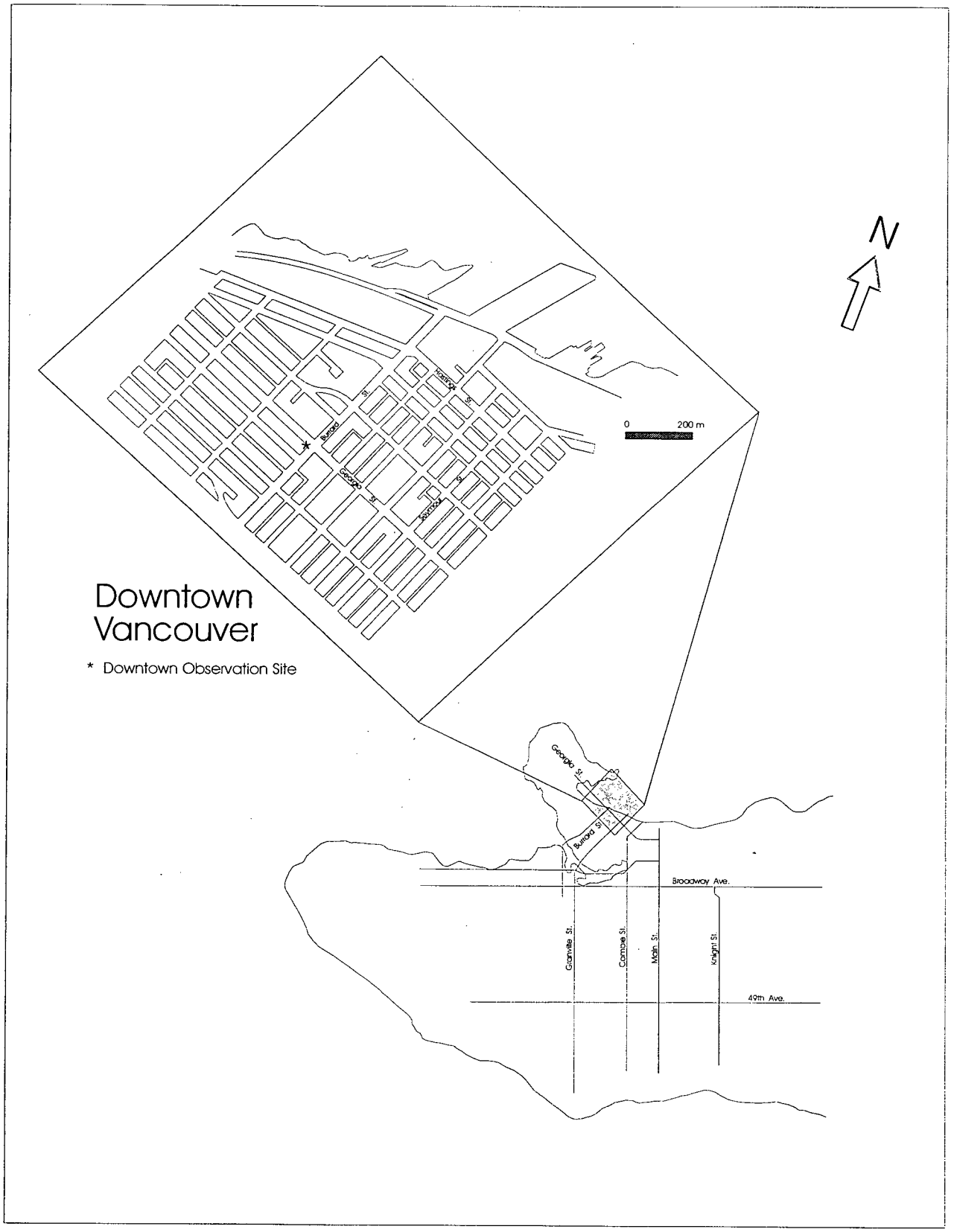

Figure 2.4 Aerial view of urban observation site on Georgia Street in downtown Vancouver.

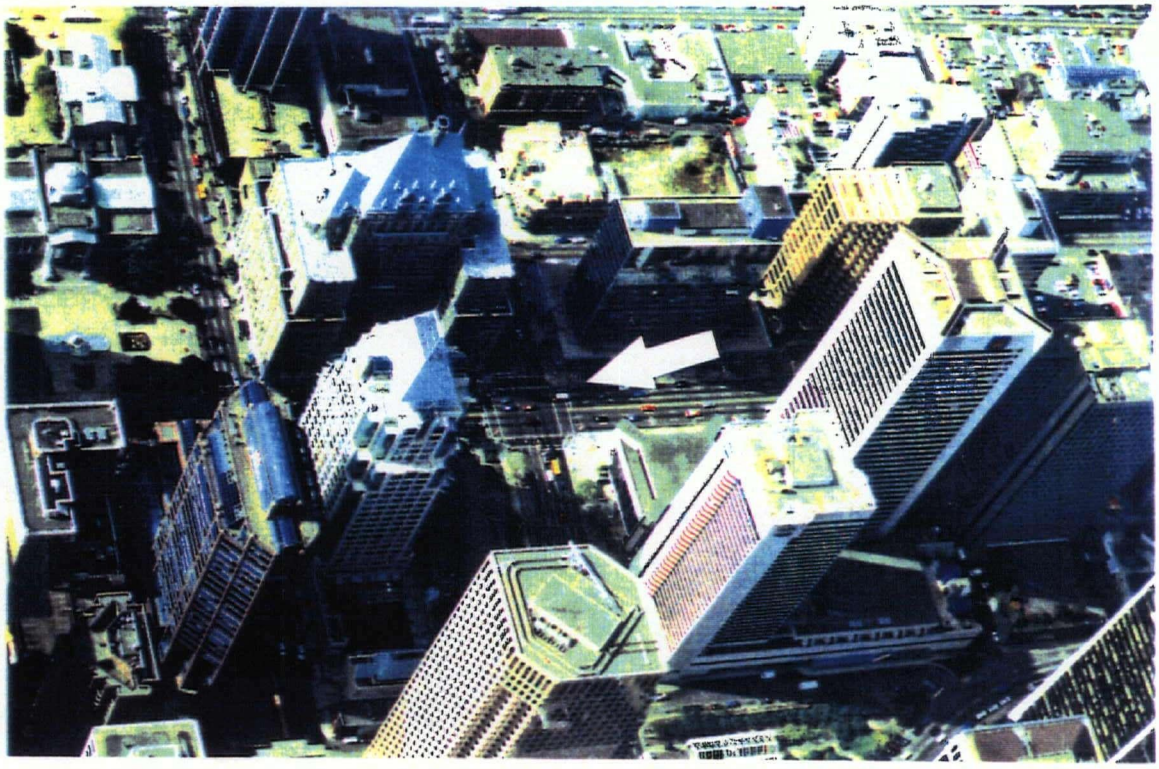

Figure 2.5 'Fish-eye' view showing relative proportions of sky and buildings visible from the surface at the downtown site. The instruments are located on the lamp-post in the lower centre of the picture.

Figure 2.6 Aerial view of typical farm land in Delta around the rural observation site.

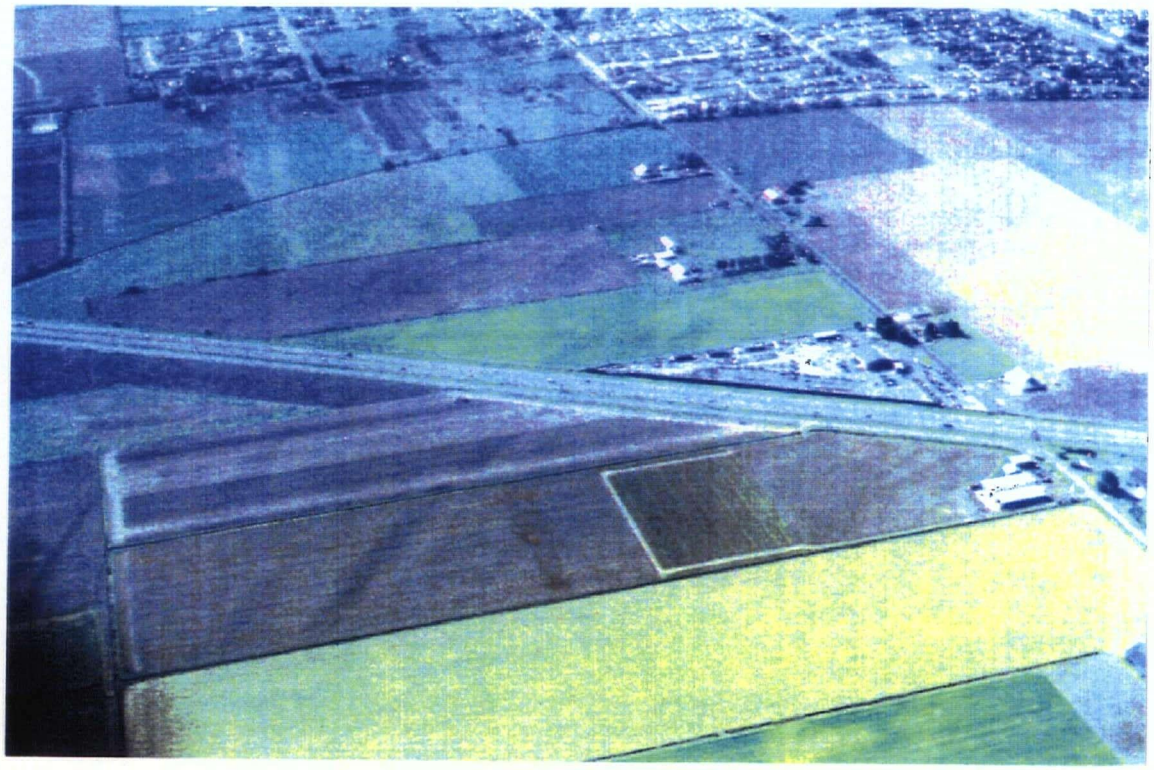

Figure 2.7 Instrumentation for energy balance measurements at the rural site.

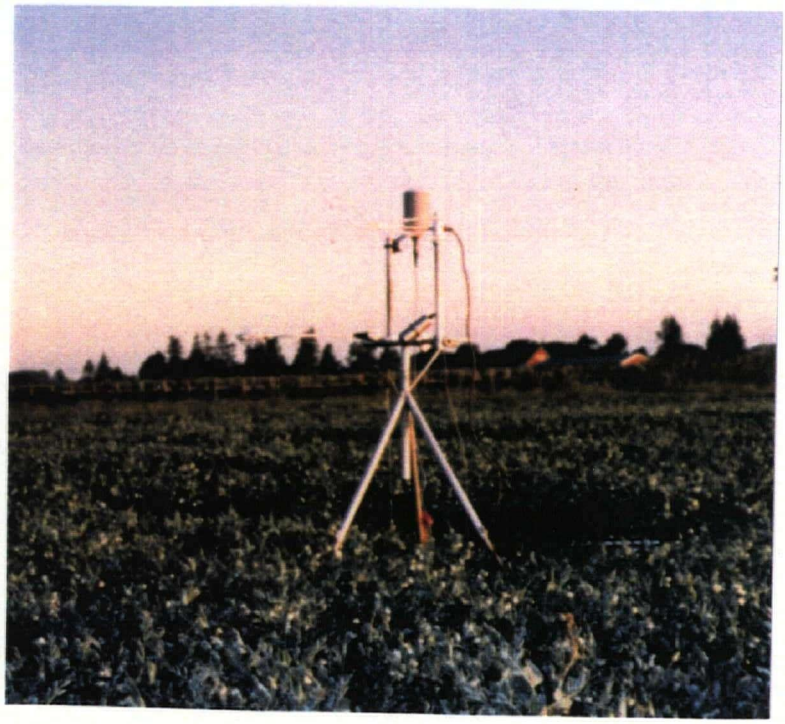

The site is located so as to minimize the influence of the ocean at Boundary Bay to the south, and the south arm of the Fraser River to the north. It is also located in the area where Emslie (1972) found the coolest average night-time temperatures in the greater Vancouver area. Land use is predominantly agricultural, although Burn's bog is approximately 2 km to the east, and the Vancouver landfill is approximately 5 km to the south-east.

The instruments are located at the junction of four cultivated fields, and there is an uninterrupted fetch over similar surfaces of at least 500 to 1000 m all directions. During the summer of 1994 the crops planted at the site were peas to the north-east and south-east, and corn to the north-west and south-west. In other years beans, peas or corn have been planted. In the fall of each year winter wheat was planted and harvested early in the spring. The soil was therefore not entirely bare during the winter. The predominant soil type in this area is a silt loam formed from deltaic deposits overlain by 0.1 to 0.15 m of organic matter.

Air temperature, relative humidity (Vaisala temperature-humidity probe), and wind speed and direction (R.M. Young 03001-10 wind sentry set) were measured at 2 m height. In addition, gravimetric soil moisture measurements were made in the fields surrounding the instruments. The frequency of soil moisture observations varied from daily to monthly.

Because rural observations were made at only one site, they are not representative of all of Vancouver's surroundings. However, given the heterogeneous surroundings of Vancouver (ocean, mountains, agricultural and industrial lands), it is difficult to define a representative rural surface. Undoubtedly different characteristics may have emerged from this study if observations from other sites had also been analyzed. Nevertheless, the three year record of rural temperatures at this site is considered adequate to describe the relationship between surface

thermal properties, nocturnal cooling and the resulting urban-rural temperature differences at a site which conforms to the 'rural' setting of many mid-latitude cities.

2.4.1 Energy Balance Measurements

On several nights during the summer of 1994 surface temperatures and components of the surface energy balance were measured at the rural site (Figure 2.7). These observations were made to obtain the data to calculate surface thermal admittance using the Brunt (1932) equation (Chapter 5). Turbulent sensible heat flux density was measured with a sonic anemometer-thermometer system placed 1.5 m above the crop surface. The sampling rate was 10 Hz and 15 minute averages were determined. Soil heat fluxes at 0.10 m were measured using Middleton soil heat flux plates and integrating thermometers at 0.02 and 0.04 m to determine heat storage in the soil above the plates. Net radiation at a height of 1 m was measured with a Swistecco net pyrradiometer (model S1). The latent heat was then calculated by residual. These measurements were conducted to verify that on 'ideal' calm and clear nights, the soil heat flux is the only significant non-radiative component of the energy balance, and therefore the Brunt equation is applicable.

The turbulent sensible heat flux and the vertical temperature gradient were also required in order to calculate the atmospheric thermal admittance (Chapter 5). The vertical temperature gradient was measured as the difference between air temperature at 1.5 m (Vaisala temperature-humidity probe) and the surface temperature, which was calculated from the upward longwave radiation ($L\uparrow$) measured by a downward-facing Eppley pyrgeometer ($L\uparrow = \varepsilon_o \sigma T_o^4$).

These surface temperature measurements are subject to errors due to the choice of the surface emissivity, ε_o. A surface emissivity of 0.98 was chosen for the rural surface, in accordance with the range of values given in Oke (1987) for agricultural crops (0.90 to 0.99) and dry soils (0.98). For an upward long-wave flux of 395 W m^{-2} (a typical value observed at the rural site), surface temperature differences of 0.5 °C (approximately 3 %) result when the emissivity value changes from 0.95 and 0.99. This much uncertainty in the temperature gradient leads to an uncertainty in the atmospheric thermal admittance of 30 per cent for typical 'ideal' conditions observed in this study.

2.4.2 Thermal Admittance Estimates From Soil Properties

As discussed in Chapter 1, thermal admittance ($\mu = (kC)^{1/2}$, the square root of the product of thermal conductivity and heat capacity) is an important control on the amount of cooling that occurs at a surface. Therefore, seasonal differences in rural cooling following sunset are likely to be related to seasonal variations in the surface thermal admittance. In order to study this relationship it was necessary to estimate seasonal variations of the rural thermal admittance.

One approach is to calculate μ from the site soil properties and soil moisture. The equations used to estimate thermal admittance by this method are outlined in Chapter 5. Soil moisture was measured by the gravimetric method which determines soil moisture on a percent per dry weight basis. To calculate thermal properties, however, moisture on a percent volume basis is needed. Volumetric moisture content was obtained by multiplying the gravimetric moisture content by the bulk density of the soil. Bulk density was measured several times during the year as the weight of oven dried soil divided by the volume of the undisturbed sample. The

bulk density was assumed to increase linearly from a low value (800 kg m^{-3}) at the beginning of May (following spring cultivation) to its maximum value in October (1100 kg m^{-3}). It is assumed to remain high throughout the winter. This model of variable bulk density agrees with the observations made at this site, and also with van Wijk and Derksen's (1966) observations of the effects of tillage on soil bulk density.

Moisture samples were taken at depths of 0 to 0.05 m, 0.05 to 0.10 m, and 0.10 to 0.15 m, and averaged. During most of the year, there is little variation of moisture content with depth, because the soil is saturated during the winter. However, in the summer, the top 0.05 m layer dries considerably, while moisture remains high at 0.15 m. For example, on July 5, 1994, the first clear day following several days of rain, soil moisture was approximately 35 per cent in all three layers. By July 20, the top layer had a moisture content of only 12 per cent, while the lowest layer remained at 31 per cent moisture. Because the lower layers of soil remain quite moist during the summer, the soil moisture estimates averaged over the top 0.15 m are higher than expected from the appearance of the top of the soil.

Averaging the moisture content and bulk density over the top 0.15 m has the effect of assuming the soil is homogeneous to this depth, which is not necessarily true particularly during the summer. This assumption may have implications for the calculation of a surface thermal admittance (Byrne and Davis, 1980). However this top 0.05 m layer with low soil moisture and low bulk density has such a small thermal admittance (449 J m^{-2} $s^{-1/2}$ K^{-1} for soil moisture of 12 percent and bulk density of 600 kg m^{-3}), and is so thin, that the lower, moist, dense layers must exert significant control on the nocturnal cooling. Therefore the effective thermal admittance of the soil probably lies somewhere between that of the dry top layer and the moist lower layer. The decision was made to assume a homogeneous layer of soil by averaging the moisture and bulk

density in the top 0.15 m, rather than attempting to calculate thermal admittance of a layered soil (Byrne and Davis, 1980), since the necessary data were not available.

Another limitation of the soil moisture observations is that soil moisture in the early morning can be as much as 6 percent higher than the previous evening due to the effects of dew alone (*i.e.* even though no precipitation occurs). This amount of moisture variation leads to a 10 percent change in the calculated thermal admittance. This implies that it is not possible to reliably interpolate soil moisture and the corresponding thermal admittances between the observations, particularly if precipitation occurs. Nevertheless, a significant number of soil moisture observations are available which can provide an indication of the gross features of the annual variation of rural thermal admittance.

Other soil analyses required for thermal admittance estimates include determination of organic and mineral content. Organic content was measured by burning a known mass of dry soil at 350 °C for 8 hours. Assuming all organic matter burns off at this temperature, the mass difference is the organic content. X-ray diffraction was used on the soil remaining after the organic burn-off to determine the quartz content of the mineral portion of the soil.

2.5 Local Weather Data

Hourly weather data collected by the Atmospheric Environment Service at the Vancouver International Airport (Figure 2.1) were used to identify synoptic influences on the heat island. It was necessary to identify calm, clear nights for the heat island and cooling analysis. Nights were classified as 'clear' if the net radiation was not reduced by more than 5 percent of the cloudless sky net radiation value. Using the Bolz long-wave correction this corresponded to less than 6/10 cirrus coverage, or less than 3/10 other cloud coverage. Nights were considered 'calm' if the wind speed never exceeded 2 m s^{-1}.

Chapter 3

CLIMATOLOGY OF VANCOUVER'S URBAN HEAT ISLAND

3.1 Introduction

This chapter presents the results of an analysis of Vancouver's urban heat island climatology. Hourly averaged air temperature data from downtown Vancouver and a rural site in Delta are used to describe urban-rural differences in maximum and minimum daily temperatures and the daily cycle of heat island magnitude. In particular, the seasonal variability of these measures is explored. The effects of weather conditions on heat island magnitude are also presented. In most cases long-term averages with maximum and minimum ranges are presented to show typical characteristics of Vancouver's heat island, and where possible, statistical significance of results are determined.

Unfortunately it is not possible to ensure that every aspect of the climatological analysis is based on exactly the same data. In some cases the entire data set is used to obtain averages, while in others only part is used. This inconsistency is necessary because some data are missing due to equipment failure. Therefore in some cases it may be possible to derive a monthly averaged urban or rural temperature, but not possible to determine an average heat island for the same month if sufficient simultaneous urban and rural temperatures are not available. The data used for each analysis are identified in the discussion to avoid confusion arising from comparisons between dissimilar data.

3.2 Urban and Rural Maximum and Minimum Daily Temperatures

Although it is customary to think of urban temperature effects in terms of simultaneous urban-rural temperature differences (the urban heat island), this section follows Unwin's (1980) analysis of Birmingham's urban heat island by considering urban-rural differences in maximum and minimum daily temperatures. Because these measures are not necessarily simultaneous, that is, maximum/minimum daily temperatures do not necessarily occur at exactly the same time at both sites, they should not be thought of as 'urban heat island' measurements. However, by looking at maximum and minimum temperatures, urban - rural differences in the daily temperature range can be determined. It is important to keep this distinction in mind. Differences in maximum daily temperatures can be thought of as $T_{Max\ U} - T_{Max\ R}$, whereas the maximum daily heat island is the largest observed difference between simultaneous urban and rural temperatures, and is commonly given the notation $\Delta T_{Urban\ -\ Rural\ (max)}$. The maximum daily heat island is related to the difference in minimum daily temperatures, since the largest heat islands typically occur at night. Similarly, the minimum daily heat island often occurs close to the time of maximum daily temperature.

3.2.1 Means, Variability and Ranges

Table 3.1 lists the overall statistics of urban and rural maximum and minimum daily temperatures during the study period from December 1991 to September 1994. Because they do not span an entire three year period and because some data are missing (for example there are relatively few data for November), the following statistics do not represent yearly averages, but are simply representative of the available data.

The mean hourly temperature observed over the entire period (all hours) was 13.7 °C at the urban site, and 12.3 °C at the rural site. This 1.4 °C difference represents the average urban heat island intensity for Vancouver, and is statistically significant at the 95% confidence level.

Variability is nearly the same at both sites. As expected, the urban site is warmer than the rural site on average. However, the maximum values recorded during the period are approximately equal at both sites, whereas the absolute minimum is 4.2 °C lower at the rural site.

Table 3.1 Summary of temperature data for all hours, and minimum and maximum daily temperatures, December 1991 - September 1994.

	Temperature (°C):					
	All Hours		Maximum Daily		Minimum Daily	
	Urban	Rural	Urban	Rural	Urban	Rural
Mean	13.7	12.3	16.08	16.15	10.9	8.1
Standard Deviation	5.2	5.7	5.5	5.7	4.4	4.6
Minimum	-2.8	-7.0	1.7	0.4	-2.8	-7.0
Maximum	30.5	30.8	30.5	30.8	21.2	17.9
n	17 877	17 735	782	782	782	782

The summary of statistics for the maximum and minimum daily temperatures further illustrates the nature of urban - rural differences in daily temperature range. Means for the entire period of observation show that the urban - rural differences in maximum daily temperatures are not large, and are not statistically significant at the 95 % confidence level. Standard deviations of maximum daily temperatures, as well as the range of values are similar at both sites. The largest differences occur in the minimum daily temperatures. The mean minimum daily temperature for the urban site is significantly larger than the rural value (10.9 and 8.1 °C respectively; 95% confidence level). While standard deviations are similar at both sites, the maximum and minimum observed values are slightly lower at the rural site.

These general results indicate that the increased warmth of Vancouver compared to its rural surroundings is most significant at night. The city experiences warmer night time temperatures than its surroundings, but daytime temperatures are similar in both settings. One consequence of warmer urban nights may be particularly interesting to gardeners: minimum

temperatures of 0 °C or less occurred on 46 occasions over the entire period at the rural site, whereas only 5 nights experienced freezing temperatures at the urban site.

3.2.2 Seasonal Variability

As discussed in Chapter 1, a number of factors can produce seasonal variations in the relative warmth of urban areas. These factors include seasonal variations in weather, net radiation, anthropogenic heat production, and soil moisture and thermal properties. This section describes seasonal variability of urban - rural differences in temperature ranges.

Figure 3.1 shows urban - rural differences in monthly averaged daily maximum and minimum temperatures. Again, these differences are intended to show urban - rural differences in daily temperature ranges, which are not the same as heat island magnitudes. Simultaneous temperature differences (urban heat island) are presented in Figure 3.2 for comparison. This figure further emphasizes the point that the major difference between urban and rural temperatures occurs in the minimum, rather than the maximum daily temperatures.

The monthly mean and median daily maximum temperature differences are close to zero all through the year. As stated earlier, the average difference in means for the entire record is not significantly different from zero. However, the urban and rural means are significantly different during January, March, April, May, September and December (95 % confidence level). The urban - rural difference is often negative, implying that rural maximum daily temperatures often exceed the maximum urban temperature.

Seasonal variations in differences of maximum daily temperatures are small, and the January and December mean differences are the only statistically significant positive values. The slightly higher urban daytime temperatures in December and January could result from increased anthropogenic heat in the winter months. It has been suggested that the cause of the lower urban

maximum daily temperatures (present during the rest of the year) might be due to shading of urban surfaces, especially at street-level, by tall buildings (Oke, 1982). The statistically significant negative values occur in March, April, May and September, when the Sun is lower in the sky and shading could be important. In summer, when the Sun is overhead and days are longer, more solar radiation could penetrate to the urban canyon floor, making shading less important, and possibly explaining the lack of significant difference between maximum temperatures in June, July and August.

Figure 3.1 Box plots of urban -rural differences in daily maximum (left) and minimum (right) temperatures. The box encompasses 50 % of the data; the horizontal line is the median, the circle the mean, and the ends of the vertical lines represent maximum and minimum values. Monthly data for 1991 - 1994.

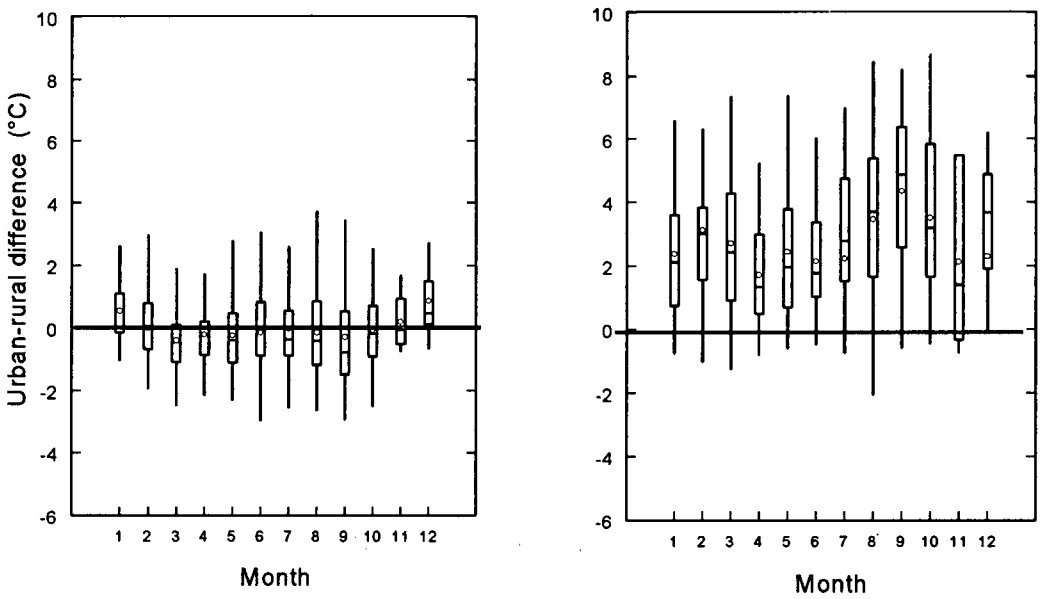

The plot of urban - rural differences in minimum daily temperatures gives a clearer picture of the urban effect on temperature. Unlike maxima, differences in minima are significantly different from zero, with monthly mean and median differences ranging from 1 to 5 °C. Monthly

minimum temperature differences range from -2 to 9 °C, with more than 75% of the data greater than zero (the vertical line below the box plot represents the lower quartile of the data).

Seasonal variations in minimum temperature differences also seem to be present in Figure 3.1. Through most of the year the mean and median differences are in the range of 2 - 3 °C, but the August, September and October values are slightly larger, ranging from 3.5 - 5 °C. These three months also have the largest extreme differences, with urban minimum temperatures exceeding the rural by 8 °C. As these data are from all days and include significant synoptic variability, the larger summer values may simply be a reflection of the increased probability of good weather and favourable heat island conditions in these months. However, they may also reflect the dryness of rural soils and their lower thermal admittance, which allows greater rural cooling. The effect of thermal admittance on heat island magnitude is examined in more detail in Chapter 5.

3.3 Maximum and Minimum Daily Heat Islands

The seasonal patterns of maximum and minimum heat islands (ΔT_{U-R}) in Figure 3.2 are similar to the patterns in differences of minimum and maximum temperatures in Figure 3.1. Based on other studies (Hage, 1972; Lee, 1979; Unwin 1980) the time of minimum heat island magnitude is probably close to the time of maximum daily temperature. The time of maximum heat island magnitude (typically a few hours after sunset) is less likely, however, to correspond to the time of minimum daily temperature.

The seasonal pattern of maximum heat islands shows a minimum value in April, and a steady increase until September, followed by a decline, as did the urban-rural differences in minimum daily temperatures. The only obvious difference between the heat islands and the temperature differences is that the heat island magnitudes are larger than the temperature

differences. This means that the increased warmth of Vancouver's urban area does not affect the daily temperature range as much as it affects simultaneous urban - rural temperature differences. Differences in median maximum temperatures are between 1 and 0 °C, whereas median minimum heat islands range from approximately -0.5 to 2 °C. The median differences in minimum daily temperatures vary between 1 and 5 °C, while the median maximum heat islands are between 2 and 6 °C.

Figure 3.2 Box plots of maximum and minimum daily heat island magnitudes. Refer to Figure 3.1 for an explanation of the plot. Monthly data for 1991 - 1994.

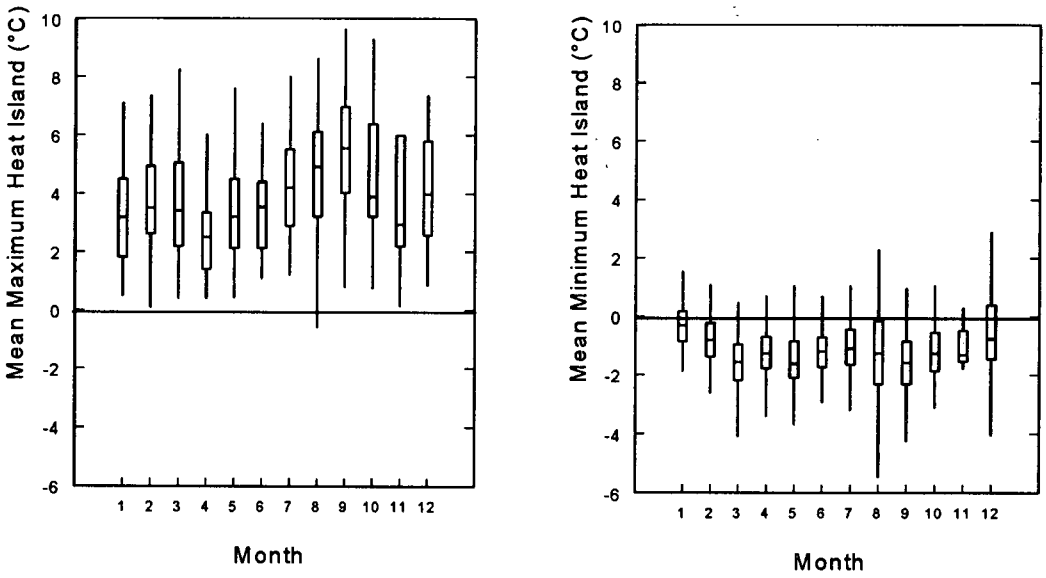

If the magnitude of a heat island were simply a function of the rural area warming faster by day, and cooling faster at night, it might be expected that seasonal variations of the rural warming/cooling rate would result in mirror-image seasonal patterns for daily maximum and minimum heat islands. That is, the maximum rural cooling should occur at the same time of year as the maximum rural warming.

The seasonal patterns displayed in Figure 3.2 clearly show two different seasonal patterns for the maximum (nocturnal) and minimum (daytime) heat islands. Minimum (daytime) heat islands are largest in fall and winter, and are lowest in the summer. Maximum (nocturnal) heat islands have two periods of increasing magnitudes (summer and winter) and two periods of decreasing magnitudes (fall and spring). This lack of symmetry suggests that daytime and nighttime heat islands are not simple functions of rural warming and cooling ability, and the processes driving them have different seasonal cycles.

The urban effect on air temperatures is clearly different by day and night. The following section analyzes heat island magnitudes on an hourly basis to determine the relative frequency of different heat island 'types.'

3.4 Frequency of Positive and Negative Heat Islands

Atwater (1977) defined an urban heat island classification scheme based on whether the heat island is positive or negative by day and night. For example, 'Type 1' heat islands were defined to be those where the rural area is warmer by day and the urban area is warmer at night. Four types are defined from all possible combinations. Unwin (1980) expanded upon Atwater's 4 types to include neutral categories, or occasions when there is no significant urban - rural temperature difference. This type of categorization is straightforward when the temperature data consist of one day-time and one night-time temperature. However for Vancouver, hourly temperature observations reveal that negative and positive heat islands can be present at different times during both the day and night. Classifying a particular day as a specific 'type' is therefore entirely dependent on the time the heat island observations are made. Therefore the Vancouver data have been analyzed on an hourly basis to show the relative frequencies of positive, negative and neutral heat islands by both day and night (Table 3.2). 'Neutral' was defined as a heat island

magnitude within 0.5 °C of zero. Hourly heat island calculations for the period December 1991 to September 1994 were used.

Table 3.2 Frequency of heat island types for Vancouver.

Heat Island Type (Relative Temperatures)		Number of hours	% frequency
Day:	**Rural > Urban**	2472	24
	Urban > Rural	5382	52
	Neutral	2500	24
Night:	**Rural > Urban**	592	7
	Urban > Rural	6744	77
	Neutral	1428	16

Urban > rural temperature is clearly the dominant heat island type by both day and night. About one half of the daytime hourly heat island observations find the urban area to be warmer. Rural > urban temperatures by day are as likely as the neutral case (no urban - rural difference). Warmer urban temperatures are by far the most dominant heat island type at night, representing about three-quarters of the data. Rural nocturnal temperatures were larger than urban temperatures only 7 percent of the time.

The preceding sections have shown that Vancouver's urban heat island is different by day and night, and also changes from hour to hour. Section 3.5 examines the typical daily cycle of Vancouver's urban heat island.

3.5 Daily Cycle of the Urban Heat Island

Figure 3.3 (a) shows the ensemble average of hourly heat island intensities for the period December 1991 to September 1994. Observation times were normalized to sunset to allow for seasonal differences in the timing of the onset of nocturnal cooling. Because the calculations are

from simultaneous temperature observations, the difference represents a true measure of the urban heat island as it is usually defined.

As expected from the previous discussion of maximum and minimum daily temperatures, the heat island magnitude is largest at night (2.4 °C) and smallest in the afternoon (0 °C). On 'ideal' heat island nights it has been observed that the maximum heat island intensity occurs a few hours after sunset and gradually declines thereafter (Hage, 1972; Oke and Maxwell, 1975). The Vancouver ensemble average also shows maximum heat island intensity occurs 4 hours after sunset, but the magnitude remains near the maximum until 8 hours after sunset. The fact that heat island intensity does not decline after reaching its peak at 4 hours after sunset as it has been observed to do on calm, clear nights, may be due to the averaging process which includes all days with different weather conditions. Heat island dynamics are not as well behaved under variable weather conditions as they are for calm, clear nights when cooling proceeds to its full potential. Different night lengths throughout the year result in longer cooling periods in the winter which could also influence the timing of maximum heat island intensity.

On average, heat island intensity begins to decrease 8 hours after sunset, although timing on individual days is controlled by the time of sunrise. Heat island magnitude continues to decrease until the urban - rural difference is eliminated at 4 hours before sunset. This 'zero' heat island is not maintained for long, however, as the magnitude immediately begins to increase, reaching half of the maximum value by sunset. Heat island growth continues at the same rate following sunset until the maximum occurs 4 hours later. The growth of the heat island prior to sunset indicates that significant cooling occurs before sunset, and therefore, simple nocturnal radiative cooling is not the only process driving heat island development.

Figure 3.3 Daily variation of Vancouver's heat island magnitude. Hourly heat island observations are averaged for 1991 - 1994. The horizontal line represents the mean heat island magnitude for the period. Times are normalized to sunset only, (a), and sunset and sunrise (see text) (b). Heat island magnitude has also been normalized to largest and smallest value on a scale of 0 to 1.

(a)

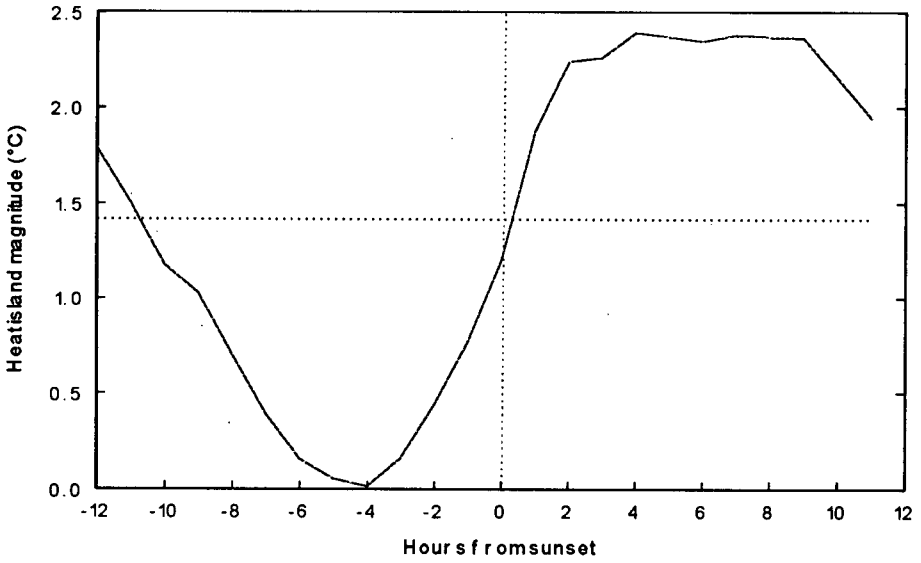

(b)

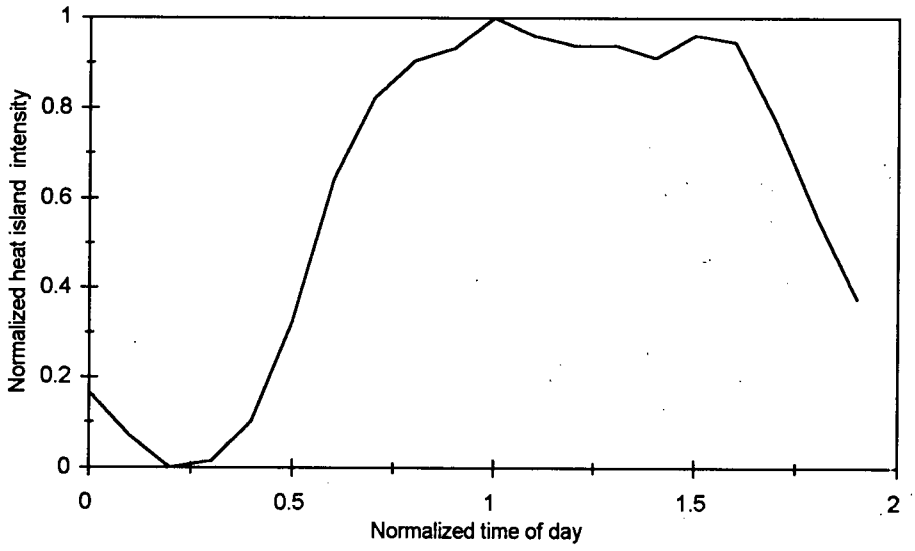

To account for the effect of night length on the timing of the daily heat island cycle, the data of Figure 3.3 (a) have been normalized for both sunset and sunrise as shown in Figure 3.3 (b). The 24 hour day has been normalized on scale of 0 to 2, with 0.5 and 1.5 representing the times of sunset and sunrise respectively, while 0 and 1 represent the mid-points between sunset and sunrise, or 'mid-day' and 'mid-night' respectively. The heat island intensity has also been normalized to the minimum and maximum observed values on a scale of 0 to 1.

Figure 3.3 (b) shows essentially the same pattern of daily heat island intensity as Figure 3.3 (a). Heat island growth begins in the middle of the 'afternoon' and has reached approximately 35 percent of its maximum value by sunset. The maximum heat island intensity occurs in the middle of the night, and decreases slightly after. A second peak in intensity occurs around sunrise which is not visible in Figure 3.3 (a). The intensity decreases rapidly following sunrise until the middle of the afternoon.

3.5.1 Seasonal Variations in the Daily Heat Island Cycle

Figures 3.4 (a) and (b) show the same data as Figure 3.3 (b) except they have been separated by season. Figure 3.4 (a) is a plot of heat island intensity normalized to the minimum and maximum values for each season and therefore shows the relative timing of features in each season. Figure 3.4 (b) gives the heat island intensity normalized to the fall minimum and maximum intensities, since the fall had the lowest and highest intensities of all seasons. This figure illustrates the relative magnitudes of intensities in different seasons.

Figure 3.4 (a) shows that heat island growth begins earliest in the winter and latest in the fall. By sunset, the winter intensity is about 50 percent of its maximum value, while the spring

Figure 3.4 Seasonal variations in the daily heat island cycle. Timing is normalized to sunset and sunrise (see text) and heat island magnitude is normalized to (a) the maximum and minimum values for each season, and (b) the fall maximum and minimum values.

(a)

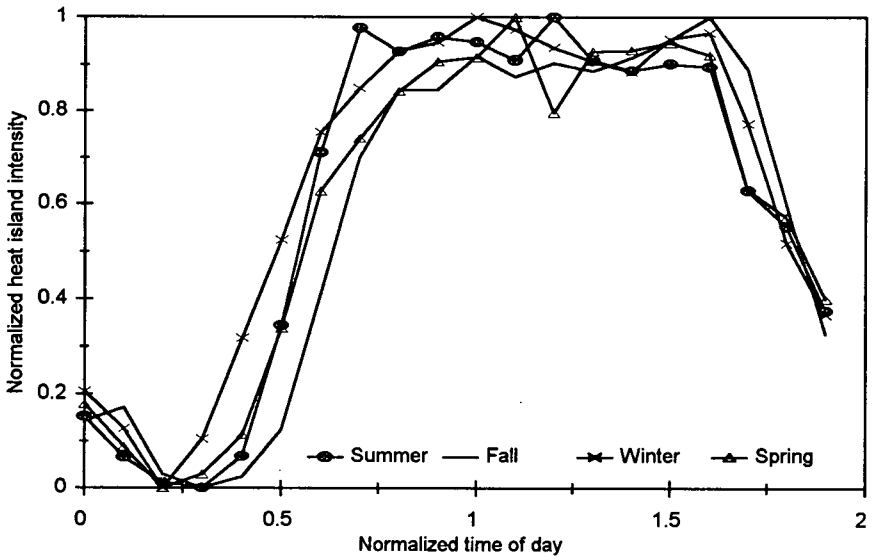

(b)

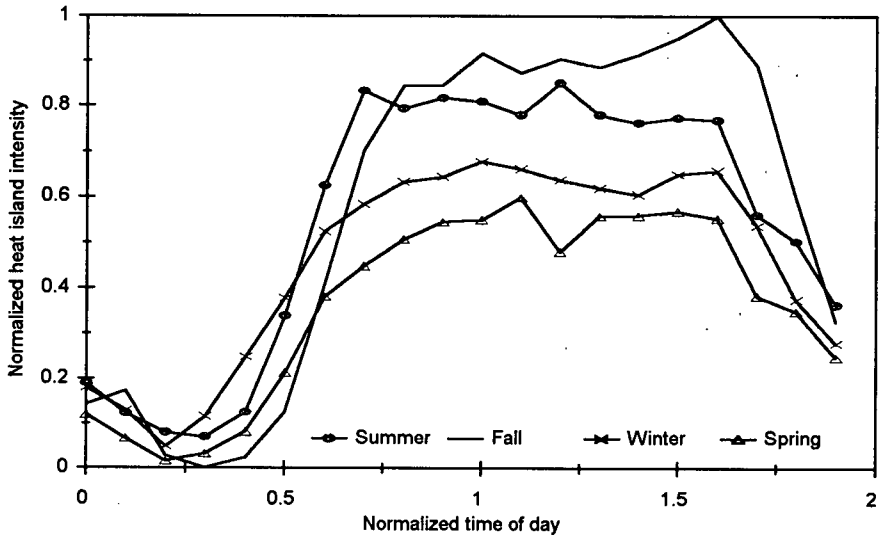

and summer intensities are approximately 35 percent of their maxima, and the fall intensity is only 10 percent of its maximum. In winter, spring and summer, heat island intensity reaches its maximum value around the middle of the night. However in the fall, the intensity grows gradually over the course of the night and does not reach its maximum until around sunrise. These early morning heat islands in the fall are discussed further in Chapter 4; they are probably the result of early morning fog delaying the onset of warming at the rural site. The winter and spring intensities also indicate a secondary peak around sunrise. In all seasons, 80 percent of the maximum intensity is reached by shortly after sunset, and is maintained for the rest of the night. Intensity decreases rapidly after sunrise and reaches its minimum value around mid-afternoon. The fall minimum occurs somewhat later than in the other seasons.

Figure 3.4 (b) shows the relative magnitudes of the heat island intensities in each season. In order of decreasing nocturnal heat island intensity, the seasons are fall, summer, winter and spring. The spring nocturnal intensity is approximately 50 percent of the fall maximum intensity. Minimum heat island intensity is also smallest in the fall. Summer minimum intensity is about 10 percent larger than the fall minimum value, while winter and spring minima are only slightly higher than the fall minimum.

This analysis shows that seasonal variations are present in the daily heat island cycle. Both the magnitude and timing of maximum heat island intensity, as well as the timing of the start of heat island growth vary seasonally. Because times are normalized relative to sunset and sunrise, these differences are not a function of different night lengths, but must be due to some other factor which changes seasonally. Further evidence of seasonal variations in Vancouver's heat island is presented in the following section.

3.6 Seasonal Variations of Heat Island 'Events'

Unwin (1980) defined the concept of a heat island 'event' as a heat island magnitude greater than 1 standard deviation above zero. Because averaging all of the data leads to small heat island magnitudes and small variations from month to month, an analysis of individual 'events' exceeding a certain magnitude can lead to interesting conclusions about a city's heat island climatology. Hourly heat island intensities for the periods December 1991 to December 1992, and February 1993 to February 1994 were used to obtain two full years of data. However, no November data were available for either year.

The mean value of hourly nocturnal urban heat islands is 3.4 °C and the standard deviation is 2.0 °C. A 1σ event is therefore defined as a heat island observation greater than 2 °C, a 2σ event exceeds 4 °C, and a 3σ event exceeeds 6 °C. Figure 3.5 shows the frequency of these events in each month. In order to account for differences in the number of observations, the number of events has been normalized by the number of observations for each month.

The figure shows that 1σ events should perhaps not be considered 'events' at all, as heat islands in excess of 2 °C occur 60 to 80 percent of the time. One interesting feature of the 1σ event is that the frequency drops noticeably in April. (See also Figure 3.1 and 3.2). The 2σ event distribution is more informative. Again, April shows almost no 2σ events, but the frequency increases throughout the summer to a high of 70 percent in September. The frequency decreases to 20 to 40 percent during the winter.

3σ events are relatively rare, occurring less than 10 percent of the time between December and July. The frequency begins to increase by August, reaches a maximum of 40 percent in September, then decreases to 20 percent in October. It is clear that summer and early fall conditions favour larger heat island intensities, with September having the greatest frequency of heat islands in excess of 6 °C. Although the favourable weather conditions are likely to make

larger heat island intensity more probable in the summer and early fall, it does not explain why September experiences nearly 4 times as many 3σ heat islands as July and August. It is possible that the marked increase in large magnitude events is related to the progressive drying-out of rural soils. In the Vancouver region soils reach their minimum thermal admittance, and maximum cooling potential before the rainy season begins in October or November (Chapter 5). Another possible explanation for large heat islands in the fall is that early morning fog in the rural area tends to delay rural warming. This possibililty is discussed in more detail in Chapter 4.

Figure 3.5 Frequency of heat island 'events' with magnitudes greater than 2 °C in each month, 1991 - 1994.

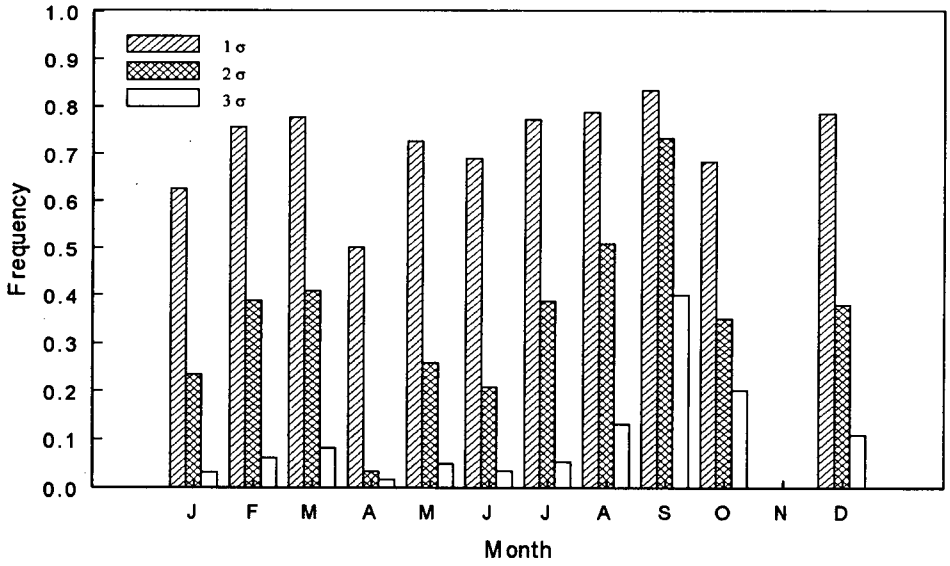

3.7 The Effect of Weather Conditions on Heat Island Intensity

As discussed in Chapter 1, weather is an important control of urban heat island intensity. In particular, wind speed and cloud amount and type have both been shown to influence heat island intensity (Sundborg, 1950; Chandler, 1965; Ludwig, 1970; Oke, 1973; Field, 1973; Lee, 1975). This section uses data from June 1992 to April 1994 to explore the relationship between

weather conditions and Vancouver's nocturnal heat island magnitude. For ease of analysis, and in order to maintain consistency of the time of heat island occurrence, wind speed, cloud conditions, and the maximum heat island intensity occurring between 2200 and 2400 hours, LAT are used.

3.7.1 Wind Speed

The data were initially stratified by cloud amount in order to examine the relationship between nocturnal maximum heat island magnitude and wind speed. Figure 3.6 (a) shows this relationship for clear skies. Although there is significant scatter, there is a trend of decreasing heat island magnitude with increasing wind speed. Figure 3.6 (b) shows a box plot of the same data. The horizontal line represents the median, the rectangle is 50 percent of the data, and the vertical lines show the maximum and minimum values for different ranges of wind speed. The width of each rectangle represents the relative number of observations in each category. The trend of decreasing heat island magnitude with increasing wind speed is now even clearer. Oke (1973) suggested heat island magnitude varies as a function of the inverse square root of wind speed ($u^{-1/2}$), A regression analysis performed on mean heat island intensities and the inverse square root of wind speed (Figure 3.6 (c)) suggests the relationship is essentially linear, with a slope of 5.7, an r^2 value of 0.95 and a standard error of 0.3 °C. These data clearly support Oke's (1973) suggestion.

Figure 3.6 The relationship between nocturnal maximum heat island magnitude and wind speed for clear skies. (a) shows the relationship for all data; (b) and (c) show heat island magnitude averaged for wind speed categories. (b) is a box plot (see explanation for Figure 3.1) showing the range of data. (c) shows the results of a linear regression of heat island magnitude and $u^{-1/2}$.

(a)

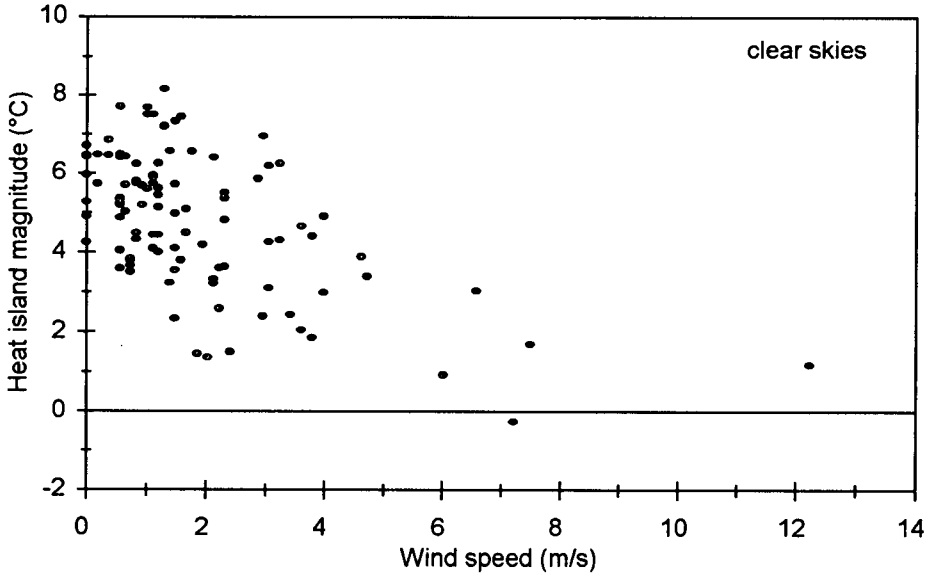

(b)

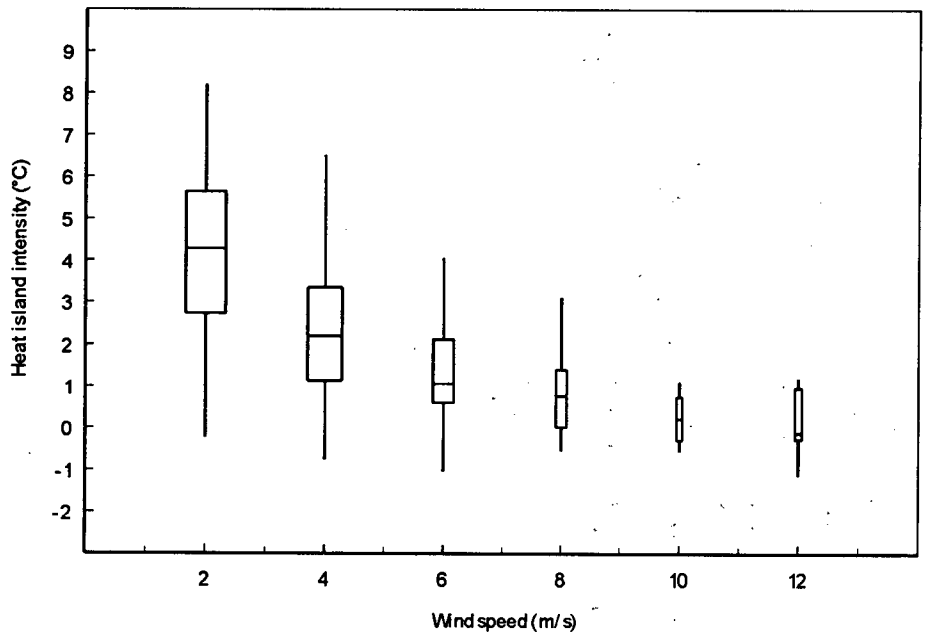

(c)

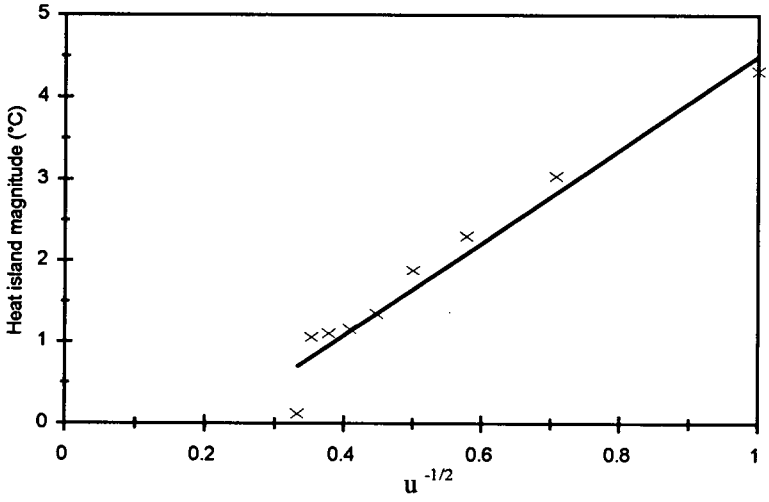

The relationship between heat island intensity and wind speed for overcast conditions (Figure 3.7) has greater scatter than for clear conditions (Figure 3.6 (a)), but the decrease of heat island intensity with increasing wind speed is still evident, and the $u^{-1/2}$ relationship is reasonable. The data have also been stratified by cloud type (or height). In general, for a given wind speed, heat island intensity is greater with high cloud, and smallest with low clouds. These results agree with Field (1973).

Figure 3.7 Relationship between maximum heat island magnitude and wind speed under overcast conditions of high, middle and low cloud.

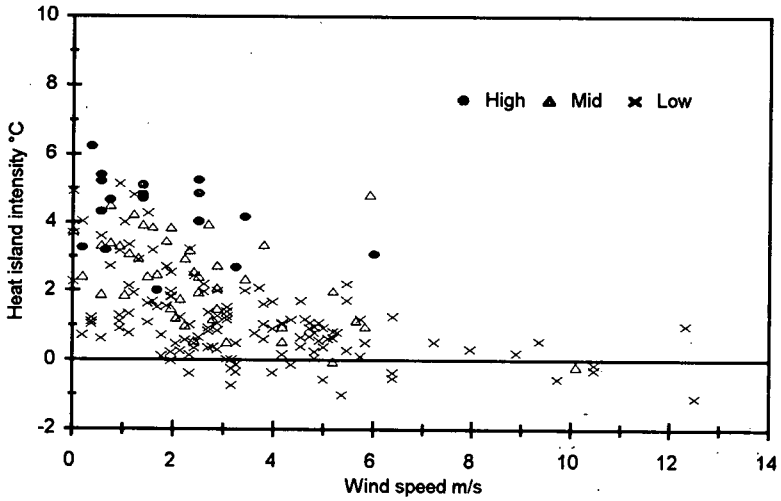

3.7.2 Cloud

Clouds influence the nocturnal heat island intensity by altering the surface net long-wave radiation budget, *i.e.* reducing the radiative cooling. Oke (1995, personal communication) suggests this may be appropriately handled by use of the Bolz cloud correction formula:

$$L^* = L^*_{(0)}(1\text{-}kn^2) \qquad (3.1)$$

where L^* is the net radiation under cloudy conditions, $L^*_{(0)}$ is the clear sky net radiation, k is a coefficient which accounts for decreasing cloud temperature with height, and n is the fraction of sky covered by cloud (on a scale of 0 to 1) (Oke, 1987). For this analysis k values were averaged for low, middle and high clouds. The factor of $(1\text{-}kn^2)$ therefore accounts for both cloud amount and type.

Figure 3.8 Variation of maximum heat island magnitude with cloud amount and type $(1\text{-}kn^2)$ for different wind speed classes.

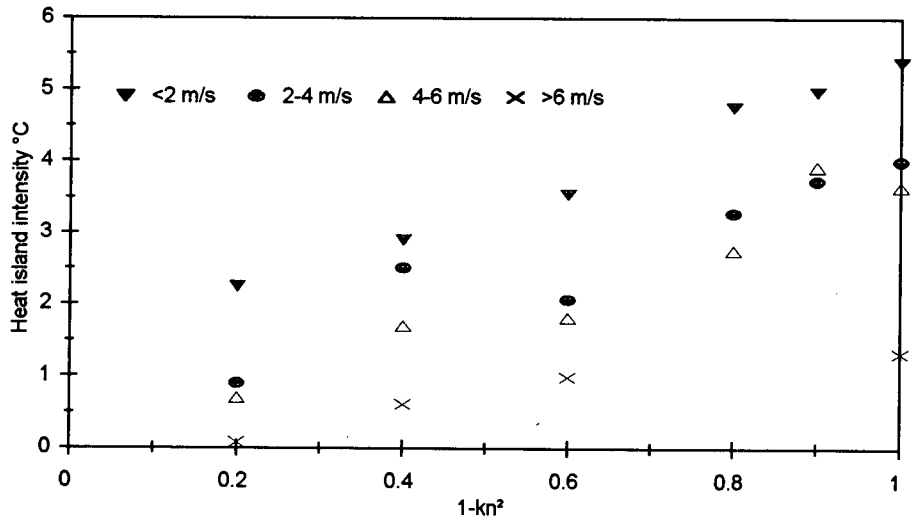

The relationship between heat island intensity and $(1\text{-}kn^2)$ is shown in Figure 3.8. Data have been stratified by wind speed, and heat island intensities have been averaged for certain ranges of $(1\text{-}kn^2)$. Small values of $(1\text{-}kn^2)$ imply cloudy conditions, and a value of 1 means

completely clear skies. The relationship between maximum heat island magnitude and $(1\text{-}kn^2)$ appears to be almost linear, with heat island intensity increasing with the value of $(1\text{-}kn^2)$, *i.e.* as cloud cover decreases. This form is evident for all 4 classes of wind speed. For a given cloud condition, the heat island intensity is greater for lower wind speeds. However, the slopes of the regression lines for different wind speed classes do not display a clear relationship to the wind speed.

3.7.3 Effects of Wind and Cloud Combined

Given these relationships between maximum heat island intensity, wind speed and cloud conditions, it should be possible to predict heat island intensity for known weather conditions. Figure 3.9 combines the results of Figures 3.6 and 3.8 by linking heat islands of equal intensities for combinations of $u^{-1/2}$ and $(1\text{-}kn^2)$. Maximum heat island magnitudes have been normalized on a scale of 0 to 1. The contours are surprisingly regular except for one point which disrupts the 0.4 and 0.5 contours. There is an obvious relationship between the three variables, with heat island intensity decreasing in a predictable manner as $u^{-1/2}$ decreases (wind speed increases) and as $(1\text{-}kn^2)$ decreases (cloudiness increases).

For extreme weather conditions, it appears that only one of the variables is important. That is, for $(1\text{-}kn^2)$ values less than 0.5, heat island intensity is independent of wind speed. Likewise, for very strong winds, heat island intensity is independent of cloud amount. It appears that it should be possible to predict the size of Vancouver's maximum heat island intensity given wind speed, cloud amount and cloud type.

Figure 3.9 Contours of maximum normalized heat island intensity in relation to wind speed and cloud conditions.

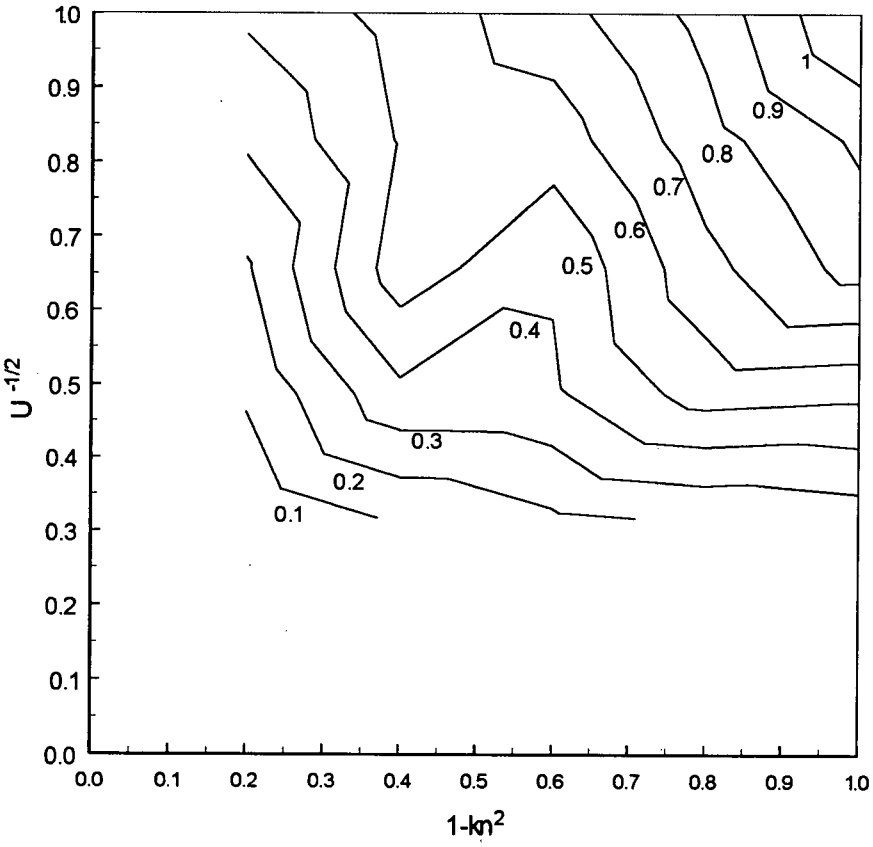

However, Figures 3.6 (c), 3.8, and 3.9 are generated from average maximum nocturnal heat island intensities for certain classes of wind speeds or cloud conditions. Figure 3.10 shows that individual heat island events are not as well behaved. It shows the results of a multiple regression analysis for the entire data set, with $1\text{-}kn^2$ and $u^{-1/2}$ as independent variables. Observed nocturnal maximum heat island intensity is plotted against the heat island intensity predicted by regression. Clearly, individual heat island events are not as predictable as mean values. There is significant scatter with observed heat islands being as much as 5 °C larger or smaller than predicted for the observed wind and cloud conditions. The size of predicted heat island magnitude is limited by the fact that $(1\text{-}kn^2)$ and $u^{-1/2}$ both have a maximum value of 1.

Figure 3.10 Observed and predicted heat islands, where predictions are made from wind speed and cloud amount and type based on multiple regression analysis.

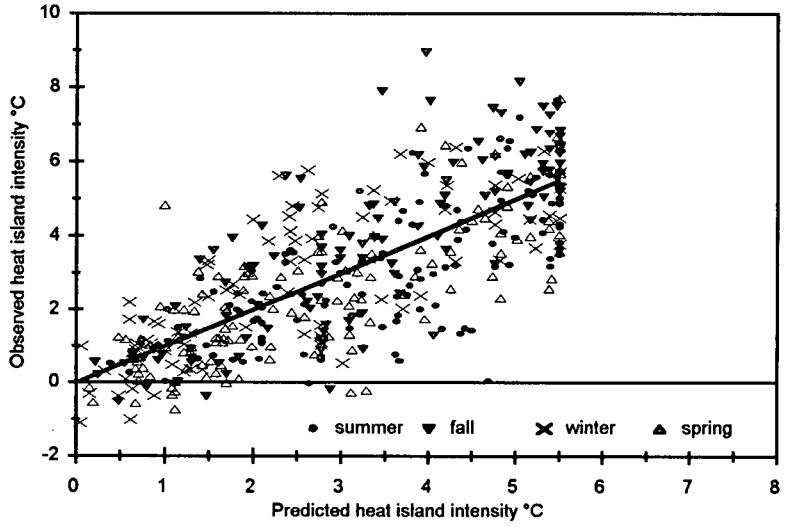

The heat island intensities have also been stratified by season, but this appears to be of little benefit in explaining the variability. Although there is a slight tendency for under-prediction of fall heat island intensities and over-prediction of summer heat island intensities, the scatter is similar in all seasons. Closer examination of the weather conditions reveals that precipitation occurred during the day preceding most of the anomalously low heat island magnitudes. Most of the unusually large heat islands occurred following several days without precipitation.

Surface moisture therefore appears to play a role in determining heat island intensities, but the physics of this influence are not known. Surface wetness could affect air temperatures, and therefore heat island magnitudes in several ways. Increased moisture availability at the urban surface could divert heat into latent rather than sensible forms, thereby reducing daytime heat storage, and the urban surface's ability to offset nocturnal cooling. The reduction in sensible heat might also lead to lower daytime temperatures in both urban and rural settings, so that the amount of nocturnal cooling would be reduced.

Substantial precipitation following a dry spell could also increase the thermal admittance of the more permeable rural surface and reduce the amount of nocturnal cooling, leading to

smaller heat island intensities. Similarly, dry spells in otherwise wet seasons (such as the 18 days without rain preceding the relatively large heat island (4.5 °C) on February 28, 1993) could result in lower than seasonal rural thermal admittances, and larger heat island intensities. This is a reasonable conclusion given that the effect of dew on soil moisture was observed to lead to 10 percent changes in the calculated thermal admittance (Chapter 2).

Alternatively, the fact that precipitation occurred on days preceding small heat islands may indicate cloudy, or completely overcast conditions during the day, and a consequent decrease in solar radiation. This would decrease daytime heat storage. Nocturnal cooling at the rural surface is likely to be reduced, while urban cooling may be enhanced, leading to small heat islands.

To try to incorporate these effects into an explanation of the variability of heat island magnitude, a second multiple regression was performed, this time using $(1-kn^2)$, $u^{-1/2}$, the number of days since precipitation, and the average cloud amount between 1000 and 1500 hours during the preceding day as independent variables. Observed and predicted magnitudes are shown in Figure 3.11. While there appears to be a slight improvement in the scatter from Figure 3.10, this may be due to the fact that the predicted values are no longer limited, since the independent variables can exceed 1. Nor is this relationship physically meaningful, since the number of days since rain is not a physically relevant measure. A true measure of surface wetness might improve the scatter somewhat, and be more physically meaningful.

Heat island intensities were also examined on the basis of wind direction (observed at Vancouver International Airport), to determine if winds from certain directions resulted in unusually high or low heat island intensities. This analysis did not reveal more insight into the nature of the variability of heat island intensity. Approximately 80 percent of the nights when winds were from the north-east, south-east and north-west quadrants experienced 'predictable' heat island intensities, while approximately 10 percent had unusually high, and 10 percent

unusually low magnitudes. Winds from the south-west quadrant appear to result in predictable heat islands most of the time, with only 1 night having an unusually large magnitude. However, south-west winds are relatively rare, and therefore it may be somewhat misleading to make comparisons with the other wind directions which have larger sample sizes.

Figure 3.11 Observed and predicted heat island magnitudes, where predictions are made from multiple regression of heat island intensity as a function of wind speed, cloud amount, number of days since last rainfall and cloud amount in the preceding day.

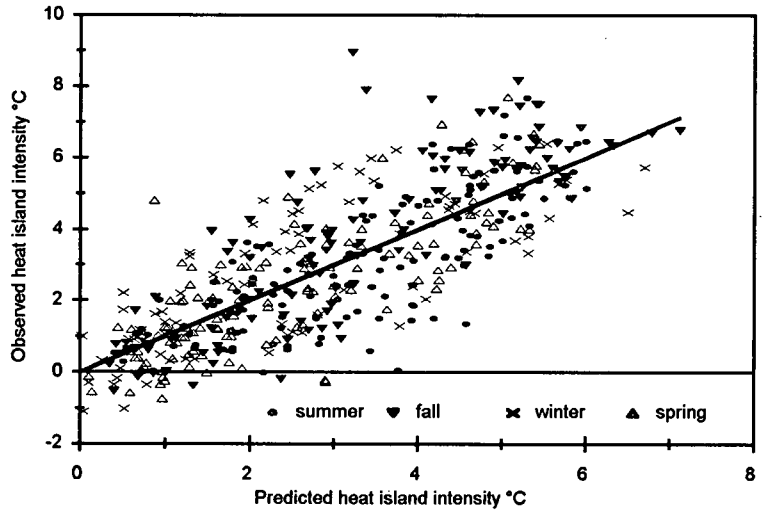

It seems reasonable to conclude that the anomalously high and low heat island magnitudes are not caused by regional air flow advecting unusually warm or cold air to the sites and disrupting the normal cooling process. The question of what explains the remaining variability of heat island intensity, after wind and cloud effects have been accounted for, remains to be answered. It appears that surface wetness and/or solar radiation on the preceding day may be significant, but these data were not available. Another possibility is that the weather observations made at the airport are not representative of both the urban and rural sites. It is known that cloudiness tends to increase northwards across the region, as a result of uplift at the north-shore

mountains (Oke and Hay, 1994). It is also possible for fog to be present at either site, but not at the airport. Since fog can have a strong influence on the temperatures, it is likely to be the cause of at least some of the unexplained variability in heat island intensities.

It also appears that there may be an element of randomness in heat island magnitude which implies that it may be possible to predict heat island intensity very well on average, but not on individual occasions. This lack of predictability which is present even after accounting for wind and cloud suggests that it might be necessary to continue to deal with only 'ideal' conditions, when this variability should be reduced. This possibility is investigated in the following section.

3.8 Heat Island Magnitude for 'Ideal' Conditions

Because nocturnal heat island magnitudes are usually largest on calm, clear nights when the rural surface can cool freely, it is expected that heat island magnitudes on 'ideal' nights should reflect seasonal variations in rural cooling potential, assuming that urban surface cooling potential remains fairly constant throughout the year. Surface cooling is controlled by the surface thermal admittance, which is in turn affected by soil moisture. Assuming that air cools in proportion to surface cooling, and all other factors remain constant, it is expected that heat island magnitudes on calm, clear nights should be largest in the summer or early fall when soil moisture is low and the rural surface has a large cooling potential.

Cloud observations for the period July 1992 to September 1994 from the Vancouver International Airport, and wind speeds from the rural site were used to identify 'ideal' heat island nights in this period. The criteria used to identify ideal nights were as follows: hourly cloud observations between sunset and sunrise never exceed 6/10 cirrus, 3/10 cirrostratus or 2/10 other types; cloud amount during the preceding day less than 5/10; and hourly wind speeds observed at the rural site never exceed 1.5 m s^{-1} between sunset and sunrise. On this basis, 40 ideal nights

were identified, but further examination of the temperatures revealed that on some nights cooling stopped, and occasionally warming occurred, perhaps due to frost, dew or fog which is not apparent in the airport data. These nights were eliminated from the data set leaving 30 'ideal' nights.

Maximum nocturnal heat islands observed on these nights are shown in Figure 3.12. Surprisingly, no systematic seasonal variability is apparent. Heat islands at all times of the year range between 5 and 9 °C. In fact, even less seasonal variability is apparent than in Figure 3.2 which included averaged heat islands from all weather conditions. Figure 3.12 indicates that 'ideal' nights in winter can experience heat islands as large as those on ideal nights in the summer. Further, the smallest 'ideal' heat islands occur in late summer and fall. This is the opposite of what is expected from the lower thermal admittance, and higher cooling potential at this time of year.

Figure 3.12 Nocturnal heat island magnitudes under 'ideal' (calm, clear) conditions.

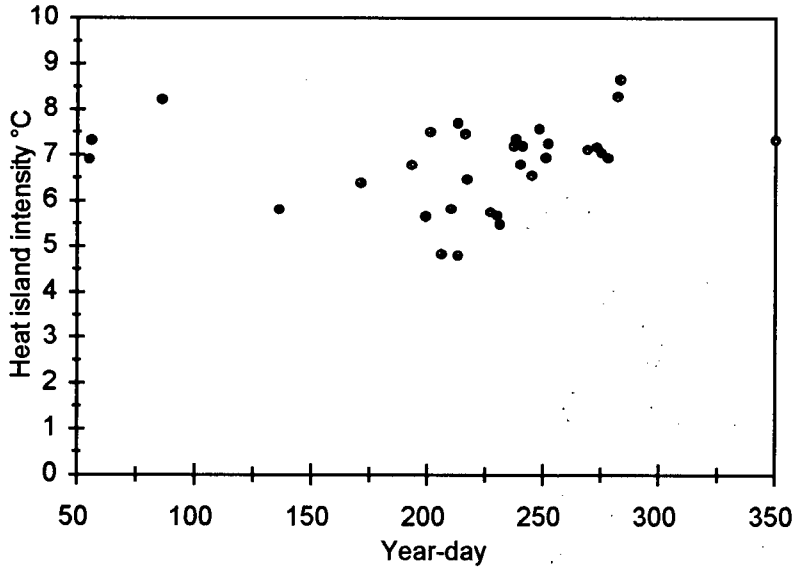

The reasons why heat island magnitudes on ideal nights do not conform to the expected seasonal pattern are not obvious. Because some of the months are represented by only one or two observations it is possible that the true seasonal variability is not represented. The analysis of Section 3.6, which looked at the frequency of heat island events, is perhaps a better method to illustrate seasonal variations. Apparently the absolute magnitude of heat islands on 'ideal' nights is independent of the season, whereas the frequency of occurrence of large heat islands does vary seasonally. Nevertheless, Figure 3.12 shows unexpectedly large winter heat islands, and unusually small summer heat islands on 'ideal' nights. Clearly, rural cooling is not the only factor influencing heat island magnitudes on calm, clear nights.

Unusually large winter heat islands may be the result of anthropogenic heat from space heating which could boost the urban nighttime temperature. The possibility of the influence of antecedent weather conditions was also examined as a cause of the relatively small summer heat islands. That is, cloud and rain preceding the 'ideal' night could lead to low heat island intensities by limiting daytime heat storage and favouring latent heat through evaporation over the wet surface. However, since these 30 days were selected to ensure the preceding day was relatively clear (less than 5/10 cloud cover), and because no precipitation occurred in the preceding 24 hours, and only minimal precipitation within 48 hours preceding only a few nights, antecedent weather conditions (rain and cloud cover) are not considered important on any of these occasions.

Alternatively, advection of cold air in the winter, or warm air in the summer to the rural site would mask the effect of surface cooling and lead to large winter and small summer heat islands. However, advection does not appear to be a likely cause, given the discussion on the effect of wind direction in Section 3.7, unless it is extremely localized to either site. Vancouver's proximity to mountains and the ocean complicates the apparently simple process of nocturnal

cooling. Perhaps cities in less complicated terrain might display more straightforward seasonal patterns

Despite the lack of seasonal pattern in the heat island magnitudes on 'ideal' nights, the other analyses in this chapter indicate that the urban effect on air temperature displays seasonal variations which may be related to seasonal variations in rural cooling potential. Chapter 4 explores this relationship further by examining seasonal variations of urban and rural cooling rates and their implications for heat island magnitude.

Chapter 4

URBAN AND RURAL COOLING

4.1 Introduction

Differences between urban and rural cooling rates are the driving force in the development of the nocturnal heat island (Hage, 1972; Oke and Maxwell, 1975; Lee, 1979). In studying nocturnal cooling in both Vancouver and Montreal, Oke and Maxwell (1975) found that at sunset rural cooling was significantly greater than urban cooling, but it later decreased and eventually approached the small, and nearly constant, urban cooling. Maximum heat island intensity therefore occurred 3 to 5 hours after sunset. On calm clear nights, rural cooling decreased with the square root of time, whereas the urban cooling rate was nearly linear.

Both radiative geometry and the thermal properties of the urban surface affect its cooling potential. Tall buildings reduce the sky-view factor in urban street canyons and thereby reduce the surface net radiative loss. Also, the urban surface thermal which is usually larger than that of the rural area, more readily allows stored heat to be released to offset radiative cooling. Rural surfaces with lower thermal admittances and lesser heat stored by day experience greater decrease of temperature even with the same radiative loss. However, because the thermal admittance of rural surface changes with the amount of soil moisture, it has the potential to increase during the wet season. The urban surface is likely to undergo much smaller seasonal variations because its surface is mainly made up of impermeable construction materials which are less affected by soil moisture.

When urban and rural thermal admittances are similar, nocturnal cooling rates should also be similar and relatively small heat islands should develop. This hypothesis is based on the assumption that surface cooling controls air temperature. This assumption is probably acceptable except when advection is significant. The analysis in Chapter 3 indicates that in Vancouver smaller urban heat islands occur in the winter when rural soils are relatively wet. Chapter 4 looks for evidence of thermal admittance effects on the annual heat island cycle by exploring the nature of urban and rural cooling rates.

4.2 Urban and Rural Cooling Rates: The Daily Cycle, Effects of Weather, and Seasonal Variations

4.2.1 The Daily Cycle

Temperature data for the entire observation period (December 1991 to September 1994) have been used to calculate hourly cooling rates for the urban and rural sites. Maximum observed warming and cooling rates are summarized in Table 4.1.

Table 4.1 Comparison of urban and rural warming and cooling rates.

Maximum Rates °C h^{-1}	Urban Warming	Rural Warming	Urban Cooling	Rural Cooling
All conditions	0.6	0.9	0.5	1.3
Ideal conditions	0.8	1.7	0.7	2.4
Summer	0.8	1.2	0.5	1.8
Winter	0.4	0.7	0.3	0.7

The rates have been averaged for each hour relative to sunset and are presented in Figure 4.1. The results generally agree with those of Oke and Maxwell (1975). Approximately 4 hours before sunset the urban and rural sites both begin to cool. The rural cooling rate increases quickly to 1.3 °C h^{-1} by sunset, while the urban cooling rate reaches approximately 0.5 °C h^{-1} by 1 hour

before sunset, and remains fairly constant for most of the night. Following sunset, the rural cooling rate decreases progressively until 4 hours after sunset, at which time it equals the urban rate. Both rates remain the same for the rest of the night.

Figure 4.1 Hourly warming/cooling rates averaged for the period 1991 - 1994.

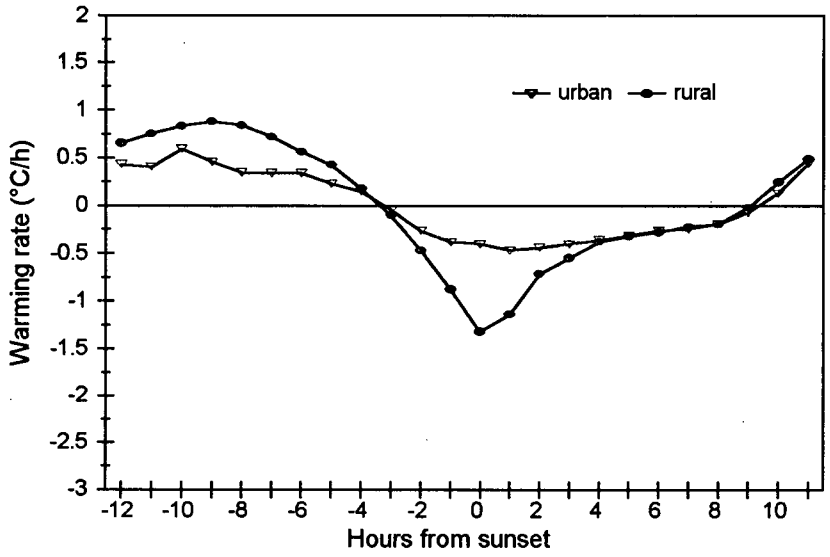

On average warming begins at both sites approximately 9 hours after sunset. Of course the onset of warming is entirely dependent on the time of sunrise, and therefore varies seasonally. The rural warming rate is initially only slightly larger than the urban rate, but by 12 hours after sunset, the rural warming rate is approximately 0.3 °C h^{-1} greater and remains larger for most of the day. The maximum rural warming rate reaches 0.9 °C h^{-1}, and the maximum urban rate is 0.6 °C h^{-1}. The urban warming rate by day is fairly constant, as it is at night, whereas the rural warming rate seems to more closely related to the solar forcing cycle.

The important features of the cooling can be summarized as follows. First, both urban and rural areas begin to cool at the same time (4 hours before sunset); that is, urban cooling is not

delayed, it is merely smaller than the rural cooling. Second, the cooling rates diverge starting 4 hours before sunset, reaching their maximum difference at sunset, then converge to become equal at about 4 hours after sunset. This is consistent with the finding that the maximum heat island intensity occurs 4 hours after sunset (Figure 3.3 a). Third, following the convergence, urban and rural rates are the same for the rest of the night. This implies that after 4 hours from sunset the air cools at a rate which is independent of the surface. Fourth, both urban and rural temperatures begin to increase at approximately the same time and at similar rates, but by three hours after the start of warming, the rural rate is greater. This contrasts with Lee's (1979) findings, who showed the rural area began warming while the urban area was still cooling. The cooling/warming rates are consistent with the development of large positive heat islands at night, and smaller, negative heat islands by day.

4.2.2 Warming and cooling under calm, clear conditions

As outlined in Section 3.8, 30 'ideal' heat island nights were identified in the data set. The average warming and cooling rates on these nights are presented in Figure 4.2. The plot shows essentially the same pattern as the average for all days (Figure 4.1). Both urban and rural temperatures begin to cool 4 hours before sunset but under 'ideal' conditions the rural cooling rate increases more rapidly and reaches a maximum value of 2.4 °C h^{-1} at sunset. The maximum rural cooling rate is maintained for 1 hour following sunset, but decreases and equals the urban rate 4 hours after sunset. The urban cooling rate is essentially the same under 'ideal' conditions (0.6 °C h^{-1}) as it is for the average of all conditions (0.5 °C h^{-1}).

Warming begins 10 hours after sunset under 'ideal' conditions. Both urban and rural temperatures begin warming at the same rate, but by 12 hours after sunset, the rural rate exceeds the urban rate by approximately 0.4 °C h^{-1}. Both urban and rural warming rates are slightly higher

under 'ideal' than average conditions. For the 'ideal' days, rural warming reaches a maximum of 1.7 °C h^{-1}, compared to only 0.9 °C h^{-1} under all conditions. The urban maximum warming rate is about 0.8 °C h^{-1} under 'ideal' conditions and 0.6 °C h^{-1} under all conditions.

Figure 4.2 Hourly averaged warming/cooling rates for calm, clear conditions.

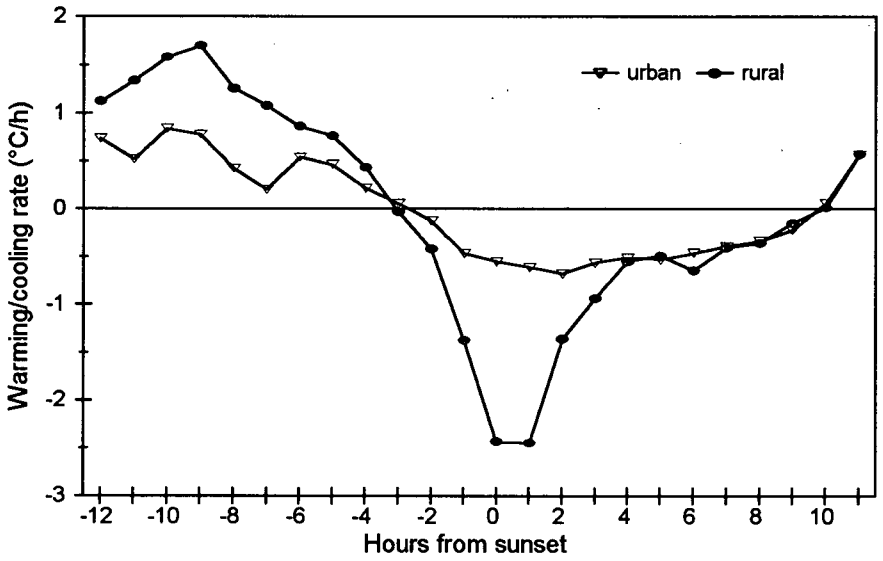

Comparison of Figures 4.2 and 4.1 reveals that under 'ideal' conditions the rural warming and cooling rates are significantly larger than those for all weather conditions. The urban warming and cooling rates are essentially unaffected by weather conditions. This finding agrees with Ludwig's (1970) suggestion that urban cooling rates should be less dependent on wind and cloud than rural cooling rates, since the wind and sky are partially blocked by buildings. Weather conditions do not appear to affect the timing of the daily cycle of warming and cooling rates, except that the maximum cooling rate at sunset was maintained longer under ideal conditions.

Figure 4.3 Hourly warming/cooling rates during summer months (July, August, September).

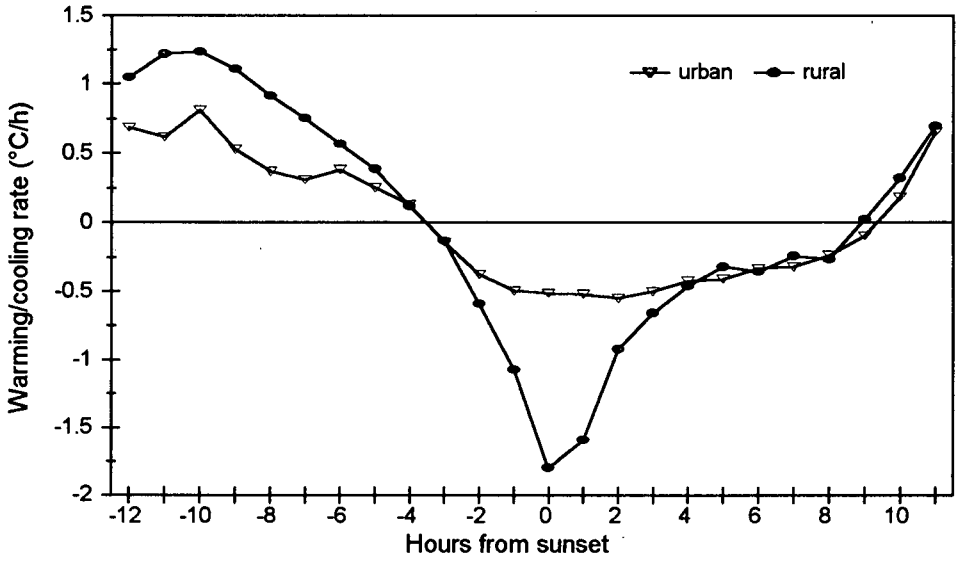

Figure 4.4 Hourly warming/cooling rates for winter months (December, January, February).

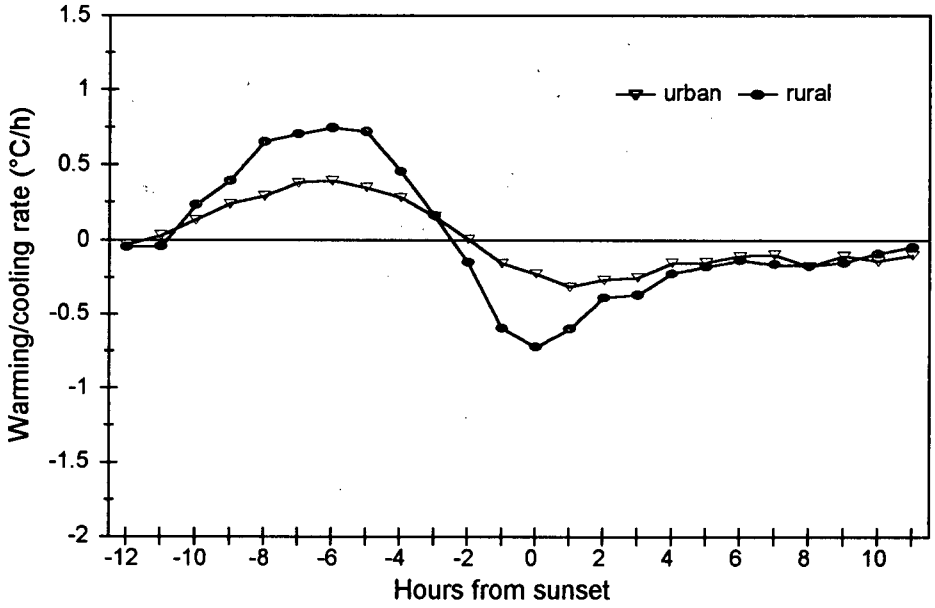

4.2.3 Seasonal Variations of Warming and Cooling Rates

In Chapter 3 it emerged that nocturnal urban-rural temperature differences tend to be largest in the late summer, and smallest in the winter. Figures 4.3 and 4.4 show the warming/cooling rates for the two periods which encompass the observed maximum and minimum urban-rural temperature differences: 'summer' (July, August and September) and 'winter' (December, January, February).

The rural summer warming and cooling rates are significantly larger than the winter rates, while the urban warming and cooling rates show little variation with season. Therefore the cause of larger summer heat islands is apparent: it is due to the significantly greater rural cooling potential in summer.

A small difference between urban and rural cooling rates is maintained slightly longer in the winter than summer, but because the difference is small at all times, the resulting effect on the heat island magnitude is also small. Warming also begins later in the winter, which is simply a reflection of longer winter nights. Urban temperatures actually begin to warm slightly before rural temperatures in the winter, but the rural warming rate increases more quickly and surpasses the urban warming rate by 10 hours before sunset. The maximum urban warming rate is slightly higher in the summer (0.8 °C h^{-1}) than in the winter (0.4 °C h^{-1}).

The fact that rural cooling rates are distinctly different in summer and winter, while the urban cooling rates are relatively constant throughout the year, indicates that controls on cooling rates (*e.g.* thermal admittance) have significant seasonal variability in the rural area, but not in the urban area. In the following section seasonal differences in cooling following sunset are analyzed in order to estimate the annual range of rural thermal admittances.

4.3 Cooling and Thermal Admittance

Brunt (1932) developed the following equation which predicts surface temperature change following a step change in heat flux (e.g. a step change in heat flux is assumed to occur at sunset):

$$\Delta T/L^* = 2t^{1/2} (\pi^{1/2}\mu)^{-1} \qquad (4.1)$$

ΔT is the temperature change following the step change in heat flux, L^* is the net radiation, assumed constant for the night, t is time, and μ is the thermal admittance of a semi-infinite homogeneous medium (in this case, the soil). The equation implies three things: following sunset, temperature decreases as a function of the square root of time; the smaller the net radiative drain, and/or the larger the thermal admittance, the smaller the resulting temperature drop. If the temperature decrease is plotted against the square root of time it yields a straight line so that surface thermal admittance can be estimated from the slope.

Seasonally-averaged air temperature change following sunset on calm, clear nights is shown in Figures 4.5 and 4.6 for both rural and urban sites. Analysis of the cooling has been limited to 8 hours following sunset, since the shortest night length in this region is 8 hours. Seasonal differences in night length and their effect on cooling are therefore eliminated. The graphs show that rural temperatures decrease with the square root of time, whereas urban temperatures decrease linearly with time. Therefore, it is possible to estimate thermal admittances for the rural surface, but not the urban surface. This finding agrees with Oke and Maxwell (1975).

4.3.1 Rural Cooling

The differing slopes of the rural cooling curves in Figure 4.5 imply seasonal variations in thermal admittance if all other controls on cooling remain similar. The least amount of cooling occurs in the winter (December, January, February), and therefore the thermal admittance is

Figure 4.5 Seasonal variations of rural cooling on calm, clear nights.

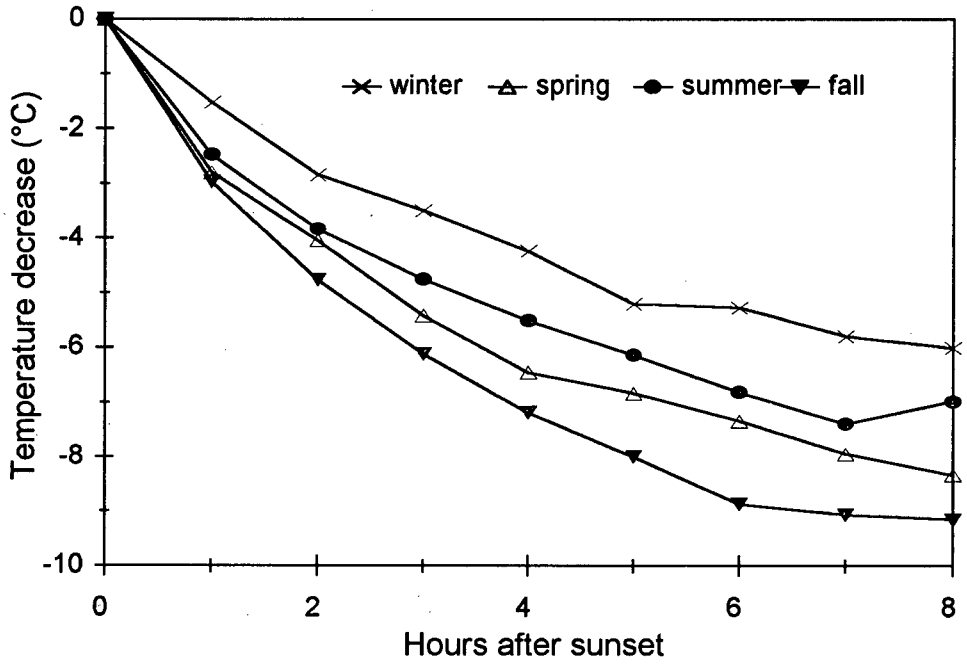

Figure 4.6 Seasonal variations of urban cooling on calm, clear nights.

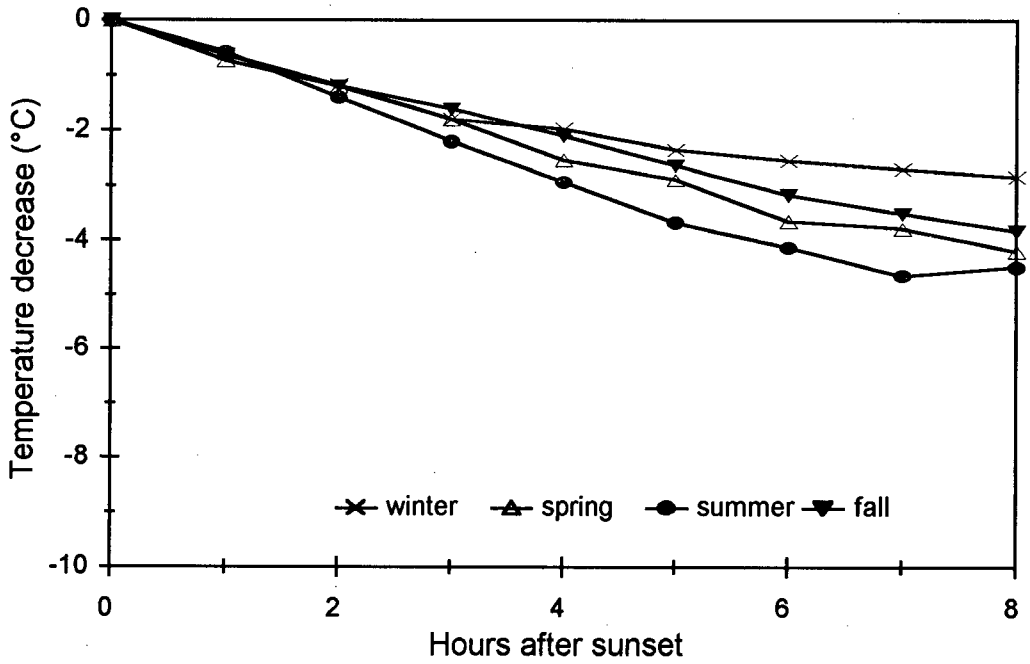

relatively large, while the greatest amount of cooling occurs in the fall (September, October), implying a lower thermal admittance. The spring (March and May) and summer (June, July, August) cooling curves are intermediate. The summer curve shows less cooling (and a higher thermal admittance) than expected. Because of the drying of soils, the summer curve was expected to lie between the fall and spring cooling curves.

A few explanations for the unexpected summer cooling are possible. First, only 2 nights were included in the spring cooling curve and therefore it may not be representative. Second, certain difficulties arise in attempting this type of analysis using summer data because significant cooling occurs well before sunset. Because of longer summer days, temperatures begin to decrease after the maximum occurs in late afternoon (often by 1600 LAT in July and August) whereas sunset does not occur until 2100 LAT. Thus, at least half of the total temperature decrease has occurred by sunset. As a result cooling following sunset may not be any larger than on some winter or spring nights. In fact, on most July nights, the cooling no longer varies with the square root of time, but takes on a more linear form similar to the later parts of the other curves. On the other hand, in winter and spring, the maximum daily temperature often occurs only 1 to 2 hours before sunset, and therefore cooling following sunset includes essentially all of the daily cooling. Therefore it seems that the summer cooling curve in Figure 4.5 should actually begin some time before the true sunset, but the Brunt equation would then no longer apply. Nevertheless, the extremes of cooling in winter and fall agree with the findings of large heat island magnitudes in September, and small heat islands in the winter.

The cooling curves in Figure 4.5 were analyzed to obtain estimates of relative thermal admittances. The estimates are very general, since the curves are based on average temperatures, and the calculation of thermal admittance strongly depends on net radiation which was not measured directly. For the calculations net radiation was estimated from

$$L^* = \sigma T_a^4(\varepsilon_a - 1), \qquad (4.2)$$

where ε_a is the atmospheric emissivity which was taken to be

$$\varepsilon_a = 0.005T_a + 0.72, \qquad (4.3)$$

where T_a is in °C (Campbell, 1977). T_a was the average air temperature at sunset on the days used to construct each cooling curve.

Table 4.2 Estimated net radiation values and calculated thermal admittances from the Brunt equation.

	Estimated L* ($W\ m^{-2}$)	**Slope of ΔT vs $t^{1/2}$**	**Thermal Admittance $J\ m^{-2}\ s^{-1/2}\ K^{-1}$**
Winter	-87	0.0356	2750
Spring	-76	0.0502	1700
Summer	-68	0.0448	1700
Fall	-76	0.0574	1500

The estimated values lie close to the range of thermal admittances for wet and dry soils listed in Oke (1981) (600 to 2550 $J\ m^{-2}\ s^{-1/2}\ K^{-1}$). They are slightly larger than those calculated from soil moisture observations (Chapter 5: 1000 to 2400 $J\ m^{-2}\ s^{-1/2}\ K^{-1}$), but this is to be expected because the Brunt analysis applies to surface rather than near-surface air cooling. The use of air temperatures should slightly overestimate the thermal admittance. Nevertheless, they indicate that significant seasonal variations in rural thermal admittance are present at the rural site and are consistent with expectations.

4.3.2 Urban Cooling

As Figure 4.6 shows, the urban cooling curves are essentially linear. Although thermal admittances cannot be calculated using equation (4.1) , investigation of the seasonal variations of urban cooling will help to explain aspects of the annual heat island cycle.

Comparison of Figures 4.5 and 4.6 reveals that urban cooling is significantly smaller than rural cooling at all times of the year. In 8 hours following sunset the maximum urban cooling is 4 °C, whereas rural temperatures may decrease up to 9 °C.

Relatively small seasonal differences in the urban cooling rates, which were not apparent in Figures 4.3 and 4.4, are present. Cooling is similar in all seasons for the first 3 hours following sunset. After this time, winter experiences the least cooling after sunset, followed by fall, spring, and summer. By 8 hours after sunset, summer temperatures have cooled 2 degrees more than winter temperatures on average. Winter cooling may be reduced because of slightly higher anthropogenic heat inputs than at other times of the year and the fact that the evening rush hour is at or near sunset.

A comparison of the seasonal order of cooling magnitudes at the urban and rural sites reinforces the point that it is necessary to consider processes at both locations to adequately explain heat island dynamics. Figure 4.7 shows the potential growth of the nocturnal heat island determined from the difference in urban and rural cooling for each season (Figures 4.5 and 4.6). Heat island growth is largest in the fall, since rural cooling is greater than in other seasons, while urban cooling is relatively limited. Heat island growth potential is also potentially high in the spring, since rural cooling is slightly less, and urban cooling slightly greater, than in the fall. Heat island growth potential is small in both summer and winter. In the summer rural cooling is small, while urban cooling is greater than at other times of the year. In winter, both rural and urban cooling rates are less than at other times of the year, resulting in small heat island potential. Although seasonal variations in urban cooling rates are small, their relative magnitudes differ from the rural case.

This analysis shows that nocturnal heat island intensity is not controlled by urban and rural cooling rates alone. Figure 4.7 suggests that heat island intensity is expected to be largest in the

fall, followed by spring, with winter and summer being smallest and nearly equal. However, in Chapter 3 it was determined that on average heat island intensity is largest in the fall, followed by summer, winter, and spring. As previously noted, summer heat islands predicted

Figure 4.7 Seasonal variations in heat island growth following sunset, based on urban and rural cooling curves.

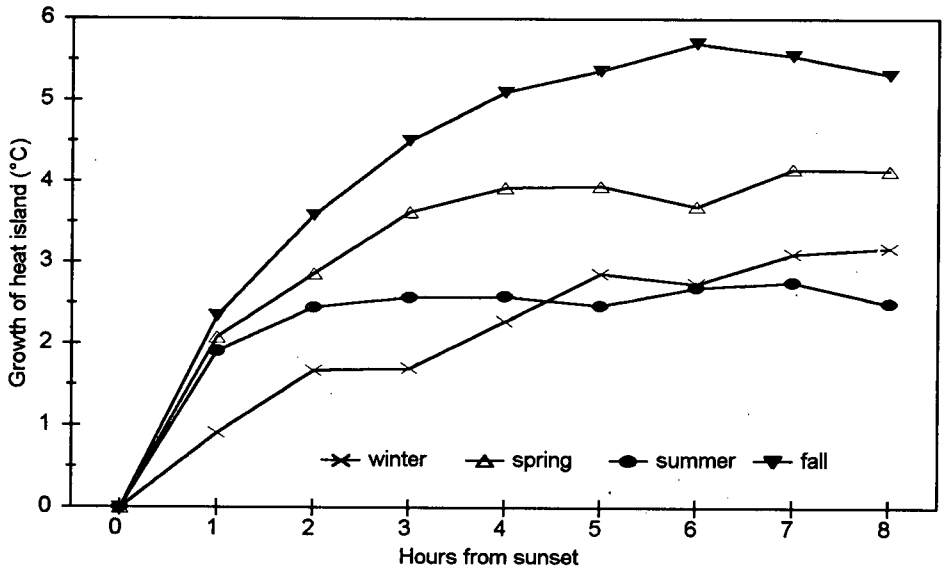

from cooling after sunset may be smaller than observed because significant cooling occurs before sunset in the summer. However, the reason for the relatively small observed spring heat islands compared to the large predicted potential is not apparent.

4.4 Warming and Cooling and Early-Morning Heat Islands

Before leaving the discussion of urban and rural warming and cooling rates, an interesting observation concerning heat islands following sunrise is presented. Although the largest heat islands in most cities tend to occur a few hours after sunset on calm clear nights, analysis of the maximum heat island magnitudes observed here reveal that of the 20 heat islands larger than

8°C, only 4 occur on calm, clear nights. Four occur between sunset and sunrise on nights eliminated from the 'ideal' set because cloud exceeded the threshold during the night. The remaining 12 large heat islands all occurred at 8 am LAT between late August and October. Examination of the cooling/warming rates near sunrise on these occasions showed a common feature: urban warming began 2 to 3 hours earlier than at the rural site. Figure 4.8 shows warming rates characteristic of most of the 12 mornings. It shows both urban and rural cooling rates are nearly equal and small at 5 am. By 6 am urban temperatures begin to increase, but the rural area continues to cool. The rural area does not begin to warm until 8 am, at which time the urban warming rate is nearly 1 °C h^{-1} . Thereafter the rural rate increases quickly and exceeds the urban rate by 2 °C h^{-1} at 9 am. The heat island magnitude on this morning reached 8.3 °C at 8 am. Large magnitudes are possible because temperatures at the relatively warm urban site begin to increase while the cooler rural area continues to cool. This creates larger temperature differences than when both areas are cooling.

Figure 4.8 Urban and rural warming rates, and heat island magnitude on the morning of September 23, 1993.

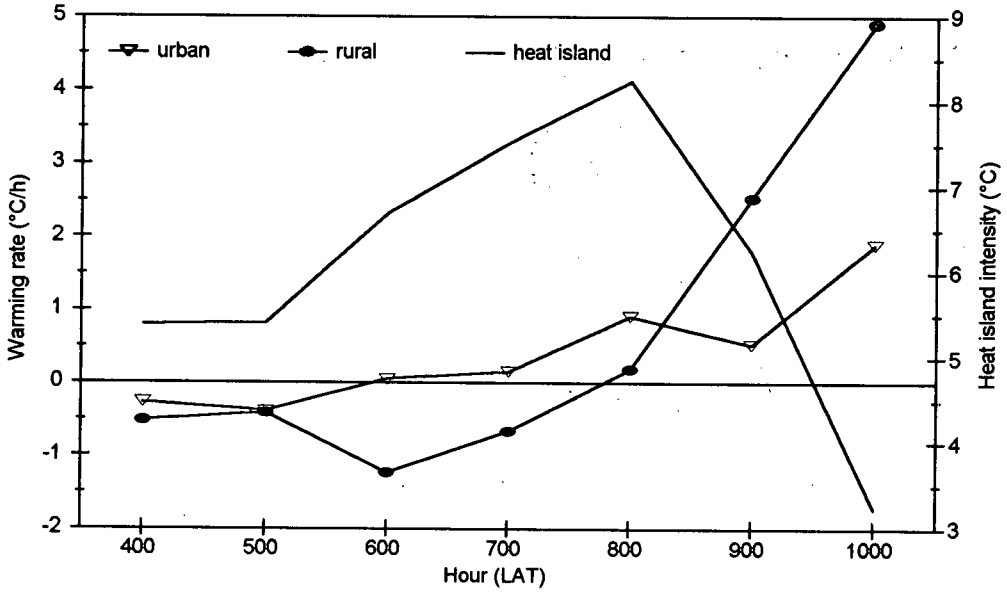

The pattern of warming on these days differs from the average rates of Figure 4.1 which show urban and rural warming to begin at the same time. They also disagree with Lee's (1979) observations in London, that the rural area begins to warm while the urban area continued to cool, which he attributed to a delay in heating caused by the urban haze layer. Also, the shading effects of buildings might be expected to delay urban warming.

The anomaly on most of these 12 days in Vancouver does not, however, appear to be due to early urban warming, but delayed rural warming. 8 am is well past sunrise in the early fall in Vancouver, and so rural temperatures should be increasing before this time. The fact that they do not could be explained by cloud effects. The existence of a fog layer before sunrise at the rural site would delay the onset of warming. At this time of year fog is common, and has often been observed early in the morning at this rural site. The fog may be localized, so no record would occur in the airport weather data. Support for the existence of fog is available from the rural humidity readings. Relative humidities observed around sunrise on these mornings ranged from 98 to 102 percent.

It is interesting that all of these anomalously large heat islands occurred at 8 am. Heat released from the morning rush hour traffic may also contribute to the earlier urban warming and large heat island magnitudes. Whatever the cause, these early morning heat islands are intriguing because they represent the largest urban-rural temperature differences recorded between 1991 and 1994. Their magnitude is larger than for those on calm, clear nights. Therefore, they represent a separate class of urban heat islands with different causes and characteristics.

The analyses in this chapter demonstrate the importance of both urban and rural cooling rates in heat island development. Seasonal variation of heat island magnitude is clearly linked to the rural cooling potential, which is in turn controlled by the soil thermal admittance, but other factors (urban and rural) are also at work. Preliminary estimates of the annual range of thermal

admittance from seasonally averaged cooling curves and the Brunt equation give values close to those expected. Chapter 5 goes beyond this relatively qualitative description of urban and rural cooling and attempts to determine more accurate estimates of thermal admittance from cooling curves on individual calm, clear nights, and to estimate seasonal variations of thermal admittance from soil properties.

Chapter 5

THE THERMAL ADMITTANCE OF THE RURAL ENVIRONS OF VANCOUVER

5.1 Introduction

In Chapters 3 and 4 it was demonstrated that seasonal variations in Vancouver's heat island intensity and rural cooling potential follow a pattern related to expected variations in the rural surface thermal admittance. In Chapter 4 estimates of the annual range of the thermal admittances of the rural area were made using seasonally averaged cooling curves and the Brunt (1932) equation. The range of values was slightly larger but similar to those of soils with varying moisture content (Oke, 1981). Because rural thermal admittance appears to be one of the controls of the heat island intensity of Vancouver, it is worthwhile to understand its variability.

This chapter compares two methods of estimating thermal admittance. The first, introduced in Chapter 4, uses the Brunt equation and observations of surface cooling after sunset under ideal conditions to calculate thermal admittance for individual nights. These estimates are then compared to calculated values from estimated heat capacity and thermal conductivity based on soil composition and soil moisture. The strengths and shortcomings of both methods are discussed, and the pattern of annual variations of thermal admittance is presented.

5.2 Estimates of Thermal Admittance from the Brunt Equation

The Brunt (1932) equation predicts surface temperature change (ΔT_s) following a step change in heat flux as a function of the square root of time. Under calm and clear nocturnal conditions, when the only significant non-radiative term in the energy balance is the soil heat flux, (*i.e.* $L^* = Q_g$), the temperature change is given as

$$\Delta T_s = -2L^* t^{1/2} (\pi^{1/2} \mu)^{-1} \qquad (5.1)$$

where μ is the soil thermal admittance and t is time after sunset. If the temperature change is known, then μ can be calculated from the slope of a plot of $\Delta T / L^*$ vs $t^{1/2}$. This approach has been used by Kagawa (1968) and Reiter (1951) to determine rural thermal admittance values using air temperature. Oke (1981) and Spronken-Smith (1994) derived thermal admittances of scale model surfaces using surface temperature observations. The estimates were in agreement with known values of the model materials.

Determining accurate thermal admittance values by this method in the field proved to be more difficult. One of the main problems encountered in the present study is the availability of the necessary observations (surface temperature and net radiation) on nights which experience strong and steady cooling. Because of equipment failure and/or unusual cooling patterns (linear cooling, or occasional bursts of warming) the necessary observations were obtained on only a few days. Sample results are presented to illustrate how this method can be used to estimate thermal admittance when the data are available.

5.2.1 The Effect of Non-constant Net Radiation

A criticism of the Brunt equation is that it assumes net radiation remains constant during the cooling period. This is only an approximation, even on ideal nights. Groen (1947) modified

Brunt's equation to allow the net radiation to change linearly as a function of temperature. A simplified form of Groen's equation is given in Lyons (1983) as

$$\Delta T_s = -L_o^*/f \{\exp (f^2/\mu^2)\mathrm{erfc}(f\, t^{1/2}/\mu)-1\} \qquad (5.2)$$

where t is time after sunset, L_o^* is net radiation at sunset, μ is the thermal admittance of the surface and f is the rate of change of net radiation as a function of temperature.

To determine the effect of assuming constant net radiation on the calculated thermal admittances, results from both equations were compared. Equation (5.1) was used to estimate surface thermal admittances from the surface and air cooling curves for the night of August 26, 1994. Plots of $\Delta T_s/L^*$ vs $t^{1/2}$ for this night are shown in Figure 5.1. The value of L* used was the average for the night (-41.6 W m^{-2}). The relationships are essentially linear, with r^2 values of 0.93 and 0.95 for air and surface temperatures respectively. The estimated thermal admittances were 940 ± 12 J m^{-2} $s^{-1/2}$ K^{-1} using air temperature, and 1255 ±15 J m^{-2} $s^{-1/2}$ K^{-1} using surface temperature. In reality, the uncertainties associated with these estimates are significantly larger due to measurement error and assumptions which are discussed in the following sections.

These thermal admittances and the observed change of net radiation with temperature (f = 3.569 for air, f = 4.596 for surface temperature) were then used in equation (5.2) to predict temperature change following sunset. Cooling predicted from equation (5.2) (solid lines) and the observed surface and air temperature cooling (symbols) are shown to be in very good agreement (Figure 5.2). Similar calculations for the nights of July 21 and September 21, 1994 also show good agreement between predicted and observed temperatures. Therefore the assumption of constant net radiation does not significantly affect the thermal admittance estimates from equation (5.1). Lyons (1983) suggested this to be the case, since the variation of L* with time is small relative to the magnitude of the thermal admittance in the real world case.

Figure 5.1 Brunt analysis to determine surface thermal admittance on August 26, 1994. The straight lines represent best fit lines determined from regression analysis.

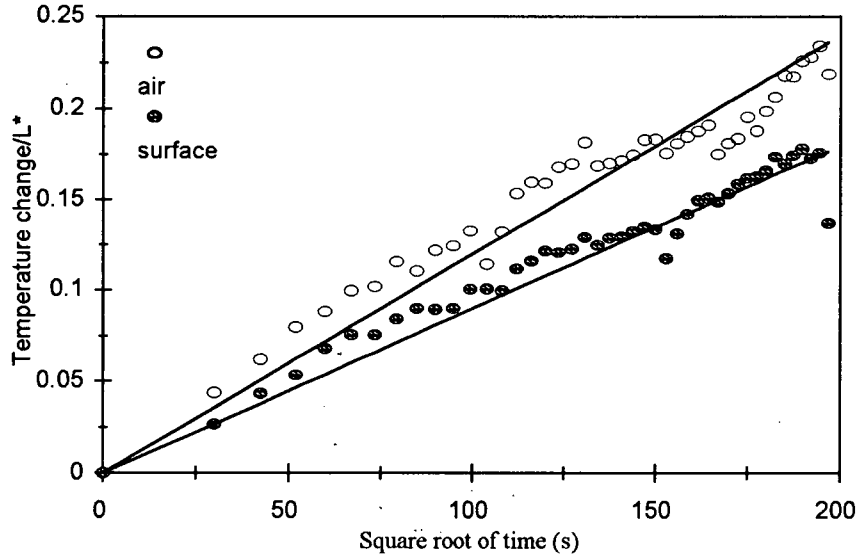

Figure 5.2 Observed and predicted (from Groen, 1947) cooling for August 26, 1994.

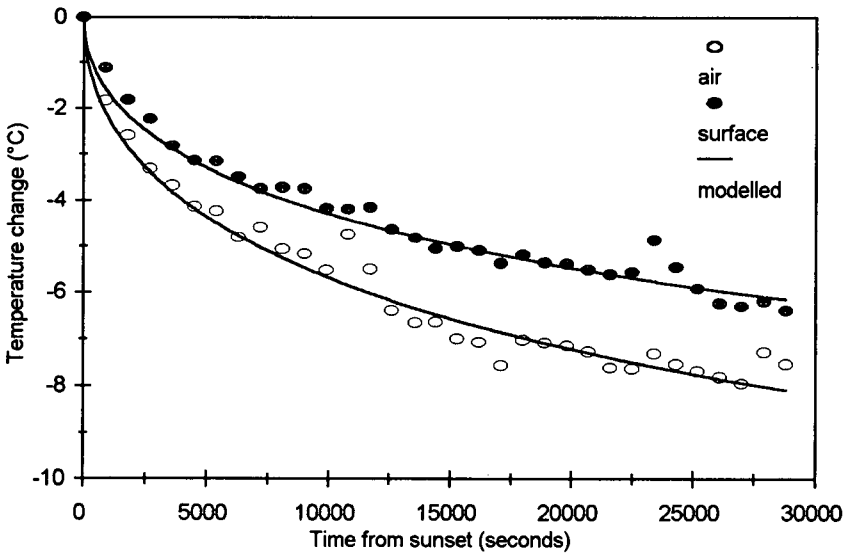

5.2.2 The Use of Air Temperatures Rather Than Surface Temperatures

Strictly the Brunt equation applies to surface, not air temperature change. The primary data set used in this study contains only air temperatures, and it is hoped that they can be substituted for surface temperatures to estimate soil thermal admittances. Under calm, clear conditions when Brunt analysis is possible, surface cooling is expected to drive air temperature cooling as well.

Because surface temperatures have a larger diurnal amplitude than air temperatures, it is expected that air temperatures will show slightly less cooling and therefore overestimate the surface thermal admittance, but that the seasonal range of thermal admittances should be similar using either temperature. However, as Figure 5.2 and observations on other occasions show, the air often cooled more than the surface following sunset, and therefore the use of air temperature in the Brunt equation may lead to a slight underestimation of the thermal admittance. However, it is encouraging that the thermal admittance calculated from soil moisture for the same night (Section 5.3) is intermediate between the estimates from air and surface temperatures (1042 ± 200 J m^{-2} $s^{-1/2}$ $K^{-1)}$. Therefore, it appears that under calm, clear conditions the use of air rather than surface temperatures does not significantly change the estimated thermal admittances.

5.2.3 The Role of Atmospheric Thermal Admittance

A further limitation of the Brunt equation is its assumption that the soil heat flux is the only significant non-radiative component of the surface energy balance at night. In practice both the atmosphere and the soil can supply heat to the surface to offset radiative cooling at night. A 'surface' can only be defined by the two different adjacent media: in this case the soil and the atmosphere. Therefore both media should be involved in assigning surface values.

The surface temperature change (ΔT_s) for a semi-infinite homogeneous medium (the soil) is given by the Brunt equation as

$$\Delta T_s = -2Q_s t^{1/2} \ (\pi^{1/2} \mu_s)^{-1} \qquad (5.3)$$

where Q_s is the soil heat flux and μ_{soil} is the soil thermal admittance. However, since the atmosphere may also be considered a semi-infinite homogeneous medium whose thermal properties control temperature change at its surface, equation (5.3) can be re-written for the atmosphere as

$$\Delta T_s = -2Q_h t^{1/2} \ (\pi^{1/2} \mu_a)^{-1} \qquad (5.4)$$

where Q_h is the sensible heat flux from the atmosphere and μ_a is the thermal admittance of the atmosphere given as

$$\mu_a = C_a K_h^{1/2} \qquad (5.5)$$

where C_a is the heat capacity of air and K_h is the eddy conductivity of the atmosphere. From the surface energy balance,

$$Q^* - Q_e = Q_s + Q_h. \qquad (5.6)$$

and rearranging and substituting (5.3) and (5.4) into (5.6) gives

$$\Delta T_o = -2(Q^*-Q_e)t^{1/2} \ [\pi^{1/2}(\mu_s + \mu_a)]^{-1}. \qquad (5.7)$$

The surface temperature decrease following sunset is therefore inversely proportional to the sum of the atmospheric and soil thermal admittances, rather than the soil thermal admittance alone. At night Q_e is considered negligible. Estimates of Q_e (by residual) on calm, clear nights found it to be less than 10 percent of Q^* until just before sunrise when it became large and negative, corresponding to the formation of dew.

When wind speeds and K_h are large, the calculated atmospheric thermal admittance is also large (equation 5.5) and therefore is significant to the temperature decrease. However, under

very calm, clear conditions when the Brunt equation applies, the value of K_h may be small enough to make μ_a insignificant relative to μ_s. Estimates of K_h were made on such nights in order to verify this statement.

5.2.4 Estimates of Atmospheric Thermal Admittance

Assuming a heat capacity of 1200 J m^{-3} K^{-1} for air in equation (5.5), then the atmospheric thermal admittance at any time depends on the value of the eddy conductivity, K_h. Since

$$Q_h = -C_a K_h \frac{\overline{\partial\theta}}{\partial z} \approx -C_a K_h \frac{\overline{\Delta\theta}}{\Delta z} \qquad (5.8)$$

K_h can be determined if the sensible heat flux, Q_h, and the vertical temperature gradient, $\overline{\partial\theta}/\partial z$, are known. In practice, the finite difference approximation, $\overline{\Delta\theta}/\Delta z$, is used rather than the true gradient. Therefore K_h applies at the log mean height.

The necessary measurements to determine K_h and μ_a were made on several calm, clear nights during the summer of 1994 (Chapter 2). Observations for the night of July 21, 1994, which experienced calm, clear conditions (wind speeds less than 1.5 m s^{-1}, cloud cover less than 3/10) are used to estimate K_h from equation (5.8) and then in (5.5) to calculate hourly values of μ_a for the night of July 21, 1994 (Figure 5.3). A moving average over 1 hour was used in order to eliminate occasional negative K_h values which arise from anomalous positive heat fluxes at time scales of 15 minutes.

The hourly averaged atmospheric thermal admittance (μ_a) on July 21, 1994 was greatest (148 J m^{-2} $s^{-1/2}$ K^{-1}) at 2200 hours, approximately 1 hour after sunset. During the remainder of the night μ_a was near or less than 100 J m^{-2} $s^{-1/2}$ K^{-1}, averaging approximately 78 J m^{-2} $s^{-1/2}$ K^{-1}, *i.e.* about an order of magnitude smaller than the soil thermal admittance. Similar calculations on other calm clear nights gave μ_a estimates of less than 100 J m^{-2} $s^{-1/2}$ K^{-1}. It appears therefore, that

the Brunt equation is applicable, and μ_a is small enough relative to μ_s to be only a minor influence on surface temperature change. Therefore equation (5.1) can be used to estimate μ_s instead of (5.7) with an uncertainty of approximately 100 J m^{-2} $s^{-1/2}$ K^{-1}. It is systematic, however, so the neglect of μ_a always contributes in one direction.

Figure 5.3 Calculated atmospheric thermal admittances (J m^{-2} $s^{-1/2}$ K^{-1}) for July 21-22, 1994.

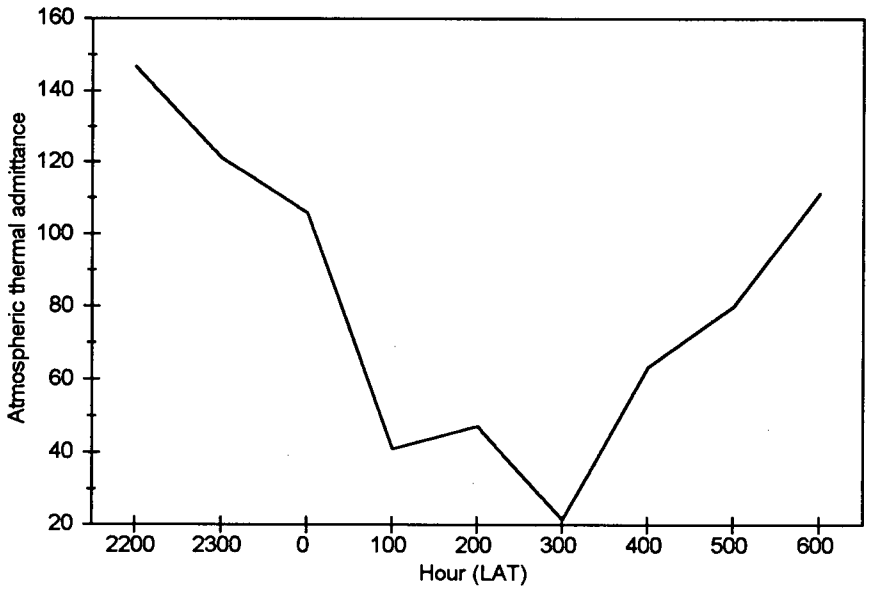

5.3 Estimating Thermal Admittance from Soil Properties

The thermal admittance (μ_s) of a homogeneous substance can be determined if the heat capacity (C_s) and thermal conductivity (k_s) are known since $\mu_s = (C_s k_s)^{1/2}$. The heat capacity and thermal conductivity of soil are not easily determined because soil consists of mineral and organic matter, air, and water in proportions which vary vertically, horizontally and temporally. For the purposes of this research, the soil composition was considered homogeneous in the upper 0.15 m and horizontally. This is considered acceptable because the soil is worked several times during the year, although there may be some variation of moisture with depth (Chapter 2). It was

thought adequate to consider only the upper 0.15 m of soil, since Byrne and Davis (1980) found from remote sensing measurements that a layer thicker than 0.1 m behaves like an infinite layer with respect to the diurnal temperature wave. Soil moisture observations were also made to a depth of 0.15 m.

De Vries (1963, 1975) presents equations to calculate the heat capacity and thermal conductivity of soils. Heat capacity is simply the sum of the weighted fractions (x_i) of the heat capacities of each of the soil components (i): mineral (m), organic (o), air (a) and water (w). Because the heat capacity of air is negligible, it is not necessary to include it in the calculation. The heat capacity of the soil is therefore

$$C_{soil} = x_m C_m + x_o C_o + x_w C_w \qquad (5.9)$$

The soil thermal conductivity is more complex. It depends not only on the relative proportions of each soil component, but also on the shape of the particles and the air pockets. The soil is considered to consist of water as a continuous medium in which soil grains and air pockets are distributed. Thermal conductivity is given as

$$k = \frac{x_w k_w + x_a k_a \lambda_a + x_{mq} k_{mq} \lambda_{mq} + x_{mo} k_{mo} \lambda_{mo} + x_o k_o \lambda_o}{x_w + x_a \lambda_a + x_{mq} \lambda_{mq} + x_{mo} \lambda_{mo} + x_o \lambda_o} \qquad (5.10)$$

In this case, the subscript mq stands for quartz minerals, and the subscript mo stands for other minerals. Because the heat capacities of quartz and other minerals are virtually the same, this distinction was not necessary in (5.9).

In equation (5.10), λ represents the ratio of the space average of the temperature gradient in each type of soil grains to that of the water, which in turn depends on the thermal conductivity and the shape of the enclosure

$$\lambda_{ij} = (1 + (k_i/k_w - 1)g_i)^{-1} \qquad (5.11)$$

where the subscript i denotes the soil component, j denotes the direction of the temperature gradient along 3 axes of an ellipsoid, and g is the shape factor. The equation can be simplified if the soil particles and air pockets are considered spherical, so that the temperature gradient is the same in all directions, then

$$\lambda_i = 2/3\ (1+(k_i/k_w\ -1)g_i) + (3(1+(k_i/k_w\ -1)(1-2g_i)))^{-1} \qquad (5.12)$$

(van de Griend *et al*, 1985).

The values of the properties of each soil component are listed in Table 5.1.

Table 5.1 Properties of soil components.

Soil Component	λ	Reference for λ	C 10^6 J m^{-3} K^{-1}	k W m^{-1} K^{-1}
Air	3.2	van de Griend *et al* (1985)	0.0012	0.025
Organic matter	1.253	De Vries (1963)	2.5	0.25
Quartz	0.246	De Vries (1963)	2.0	8.8
Other minerals	0.505	De Vries (1963)	2.0	2.9
Water	--	--	4.2	0.57

De Vries (1975) estimated this method yields an accuracy of 5 per cent or better, but it does not apply at volumetric moisture contents less than 10 per cent. Moisture contents this low were not encountered in the field.

The soil was analyzed to determine its composition. Burning off the organic matter at 350 °C for 8 hours showed the average organic content to be 10 per cent by volume. X-ray diffraction showed the remaining mineral portion of the soil was 90 percent quartz, and 10 per cent other.

Equations 5.9 and 5.10 were used to calculate soil heat capacity and thermal conductivity on all days for which soil moisture measurements are available between August 1992 and September 1994. Figure 5.4 (a) shows the complete record of soil moisture at the rural site and 5.4 (b) shows monthly averages to illustrate seasonal variations. Over the 2 year period, soil

Figure 5.4 Soil moisture observations at the rural site from August 1992 to September 1994. Individual observations, (a), and monthly averages, (b).

(a)

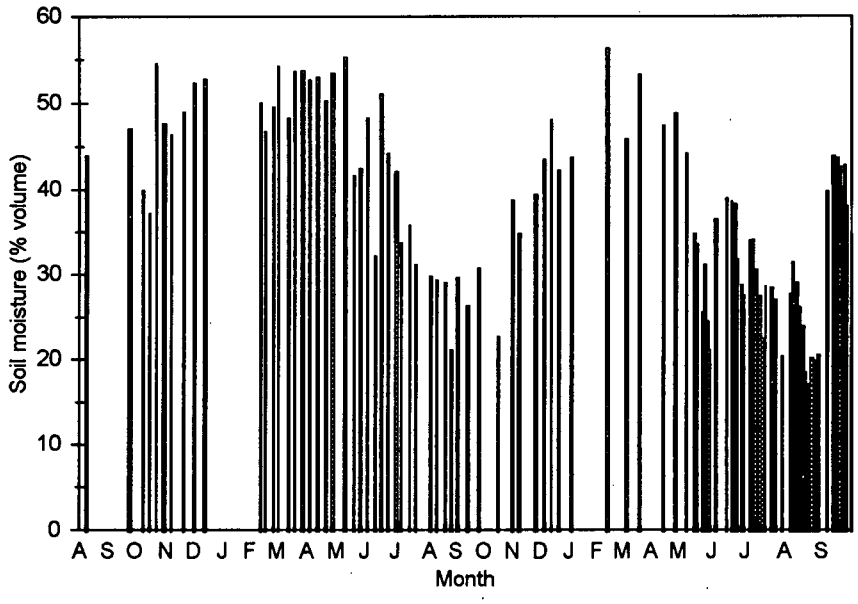

(b)

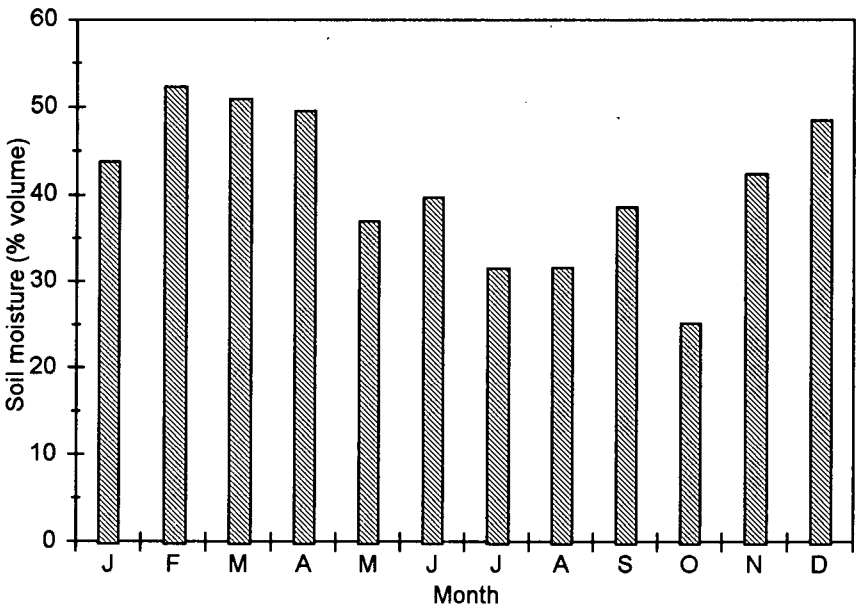

Figure 5.5 Soil thermal admittance (J m^{-2} $s^{-1/2}$ K^{-1}) calculations based on soil properties for August 1992 to September 1994. Individual calculations, (a), and monthly averages, (b).

(a)

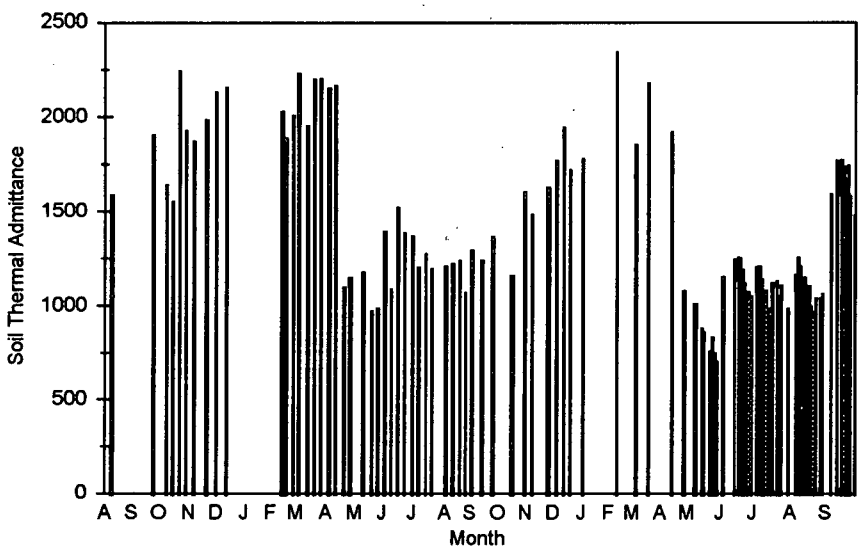

(b)

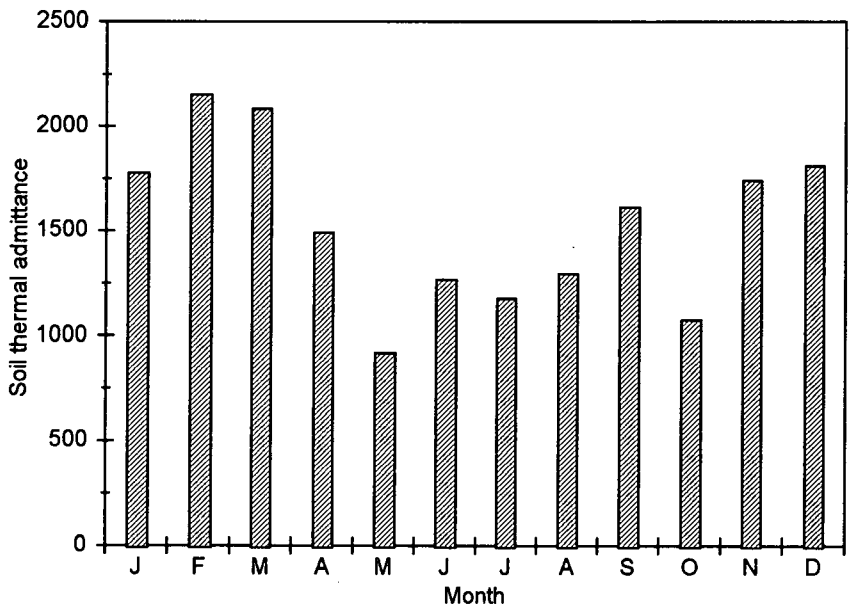

moisture values ranged from 18 to 55 per cent; a large enough range to expect significant variations in soil thermal properties. Seasonal patterns are apparent, with soil moisture high for most of the winter, decreasing rapidly in the spring to minima in the summer or early fall, and increasing again in the late fall. In addition to seasonal variations, there are short-term changes of about 10 per cent, which could also introduce significant variability in the calculated thermal properties.

The calculated thermal admittances based on the heat capacity and thermal conductivity from equations 5.9 and 5.10 are given in Figures 5.5 (a) and (b). Because soil moisture is the main control on the thermal admittance variations, seasonal values largely follow the pattern of soil moisture variation (Figure 5.4). Estimated thermal admittances range from a low of 700 J m^{-2} $s^{-1/2}$ K^{-1} in the spring of 1994 to a high of 2300 J m^{-2} $s^{-1/2}$ K^{-1} in the winter of 1993-94. Novak and Black (1983) calculated thermal admittances for silt-loam soils with different bulk densities. They found the admittance of the soil with lower bulk density (870 kg m^{-3}) to be 690 ± 100 J m^{-2} $s^{-1/2}$ K^{-1} during dry, summer conditions. This agrees with the spring time (low bulk density, dry soils) value of 700 J m^{-2} $s^{-1/2}$ K^{-1} noted above. They also calculated the thermal admittance of the soil with higher bulk density (1030 kg m^{-3}) to be 1330 ± 160 J m^{-2} $s^{-1/2}$ K^{-1} for wet, summertime conditions, which is also in agreement with the summer thermal admittances of approximately 1300 J m^{-2} $s^{-1/2}$ K^{-1} shown in Figure 5.5 (b). Since both bulk density and soil moisture would be larger in the winter, the calculated value of 2300 J m^{-2} $s^{-1/2}$ K^{-1} seems reasonable.

The thermal admittance shows distinct seasonal variations, but also significant short-term variations. Soil moisture observations on consecutive evenings and mornings in July 1994 showed that even without precipitation soil moisture in the upper 0.15 m could increase by as much as 6 per cent overnight due to wetting by dew. This results in thermal admittance variations

of up to 120 J m^{-2} $s^{-1/2}$ K^{-1} , or approximately 10 per cent. Therefore thermal admittance estimates can vary significantly over the course of the day. For this reason, as well as errors involved in calculating soil moisture (the conversion from gravimetric to volumetric contents, spatial variations of moisture in the field, different observers and techniques etc.), these thermal admittance estimates have an error of at least ± 200 J m^{-2} $s^{-1/2}$ K^{-1} . Seasonal variations of the soil thermal admittance greater than this are present, and may be expected to cause seasonal variations in rural nocturnal cooling and the urban heat island intensity.

5.4 Comparison of Thermal Admittance Estimates from Both Methods

It was hoped that agreement between thermal admittance estimates from both methods would indicate some confidence in the ability to measure thermal admittance. However, equipment failure and less than ideal cooling patterns made it possible for only 4 estimates of thermal admittance from the Brunt equation. As discussed in Section 5.2, agreement between the two methods is good for the night of August 26, 1994. The estimate from soil properties is between the estimates using air and surface cooling. However, this was the most 'ideal' night of the 4, with strong and steady cooling throughout. Cooling curves on the other three nights displayed some irregularities, and little confidence can be placed in the derived estimates of thermal admittance.

Comparisons of estimates at other times of the year when the thermal admittances are significantly higher or lower would be helpful, but it was not possible to obtain sufficient data for the Brunt method. Therefore it is not possible to determine which, if either, of the methods provides the best estimates. However, there is some agreement between the methods, and it seems reasonable to use the thermal admittances determined from the soil properties method to characterize seasonal variations.

5.5 Implications of Rural μ Variations on Heat Island Intensity and Cooling

Figure 1.3, which shows the results of several simulations from the Surface Heat Island Model (SHIM) (Oke *et al.*, 1991), can be used to estimate the range of heat island magnitudes expected from the variations in rural thermal admittance estimated from soil properties. Assuming a sky view factor of approximately 0.4 for Vancouver (Steyn, 1980), an urban thermal admittance of 2200 J m^{-2} $s^{-1/2}$ K^{-1} (the largest shown in Figure 1.3) and rural thermal admittances of 2200 and 600 J m^{-2} $s^{-1/2}$ K^{-1} for winter and summer conditions respectively, then heat island magnitudes (*i.e.* maximum growth after sunset) are expected to vary between 3° C in winter to 9 °C in the summer. These magnitudes are in line with the observed variation of heat island magnitude (Chapter 3), although the observed seasonal variations are less.

Seasonally averaged values of thermal admittances estimated from soil properties are listed in Table 5.2 together with those estimated from the seasonal cooling curves in Table 4.2. The thermal admittances calculated from soil properties are lower, and do not show as much seasonal variability as those from the cooling curves. Based on the cooling curves, thermal admittance differences of 1250 J m^{-2} $s^{-1/2}$ K^{-1} are expected between early fall and winter. The values calculated from soil moisture show the summer thermal admittance to be lowest, with the winter values only 650 J m^{-2} $s^{-1/2}$ K^{-1} larger. Given the earlier comments on the variability of thermal admittance calculations even over the course of a day, seasonal averages are perhaps of limited meaning, particularly since the soil moisture measurements are less frequent in the winter. As observations on individual days show, the thermal admittance can vary between 700 and 2300 J m^{-2} $s^{-1/2}$ K^{-1} at different times of the year. This difference of 1600 J m^{-2} $s^{-1/2}$ K^{-1} is more in line with the variability estimated from seasonal cooling curves.

Table 5.2 Seasonal averages of rural soil thermal admittance, estimated from soil properties (this Chapter), and from seasonal cooling curves (Chapter 4).

	μ from soil properties $J\ m^{-2}\ s^{-1/2}\ K^{-1}$	μ from seasonal cooling $J\ m^{-2}\ s^{-1/2}\ K^{-1}$
Winter	1900	2750
Spring	1500	1700
Summer	1250	1700
Fall	1350	1500

Figure 5.6 shows monthly averaged thermal admittances and nocturnal heat island intensities represented as deviations from their mean values. Positive values indicate months with above average rural thermal admittances or heat island magnitudes; negative values are months with below average values. Of the 22 months of data available, 13 months (60%) fit the expected pattern. That is, larger than average heat islands occur when thermal admittances are smaller than average, and *vice versa*. Of the remaining 9 months which did not fit the expected pattern, 3 show both larger than average heat islands and thermal admittance: February 1993, March and September 1994; and 6 experienced smaller than average heat islands and thermal admittances: May to July 1993 and April to June 1994. Of the deviations from the expected pattern, the heat islands, rather than the thermal admittances appear to be the anomaly. Large heat islands in February and March, and small heat islands in late spring and early summer are not expected. While there appears to be some evidence that on average, large heat islands occur when rural thermal admittance is small, this is not always the case. Since these averages encompass a wide range of weather conditions, the variability is perhaps not surprising.

Figure 5.6 Monthly averaged thermal admittance and heat island intensity deviations from annual means. August 1992 to September 1994.

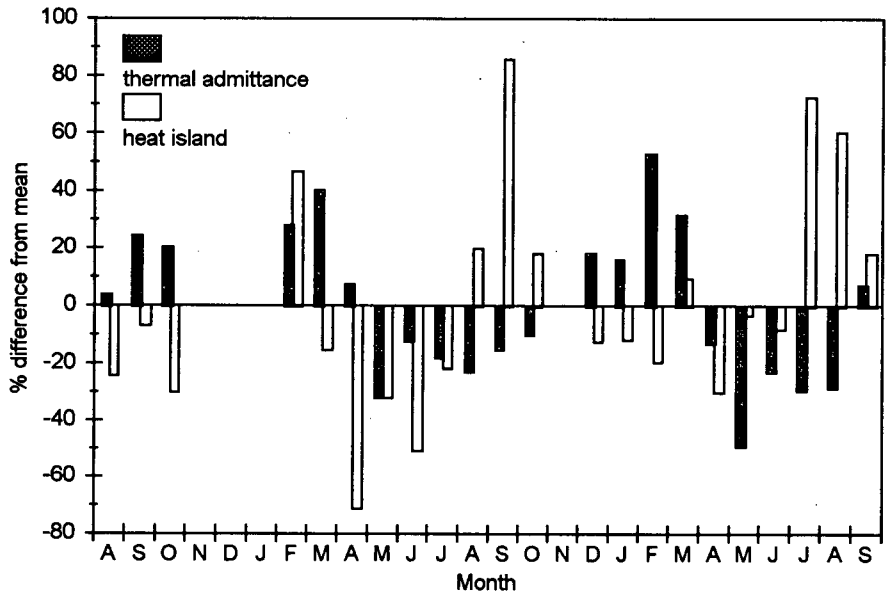

Figure 5.7 shows maximum nocturnal heat island intensities and rural thermal admittances for individual nights. As discussed in Chapter 2, it was not possible to reliably interpolate thermal admittances between soil moisture observations. Hence, only heat island magnitudes on nights preceding the soil moisture observations are included. The data have been stratified by weather conditions, that is, by the product of $(1\text{-}kn^2)$ and $u^{-1/2}$ since Figure 3.9 showed these variables to be of approximately equal importance in affecting heat island magnitude. Large values of this product represent near 'ideal' heat island conditions, while low values indicate high wind speeds and/or significant cloud.

The weather conditions clearly explain most of the variability in Figure 5.7, *i.e.* heat island magnitude decreases with increasing wind speed and cloud at a given value of thermal admittance. However, there is surprising little variation of magnitude with thermal admittance. Even for the nearly 'ideal' case heat island magnitudes of approximately 6 °C occur with rural thermal

admittances ranging from 900 to 1900 J m^{-2} $s^{-1/2}$ K^{-1}. The largest magnitude (≈ 8 °C) occurs at an intermediate thermal admittance of 1400 J m^{-2} $s^{-1/2}$ K^{-1}. The other weather conditions also show relatively large heat island magnitudes at large thermal admittances, despite the fact that rural cooling is clearly limited. It appears that although on average thermal admittance variations are correlated to variations in heat island magnitude, rural thermal admittance is of little benefit in explaining the variability of heat island magnitude on individual nights (*e.g.* Figures 3.10, 3.11).

Figure 5.7 Heat island magnitude and rural thermal admittances for individual nights with varying wind speed and cloud conditions. The four categories represent the value of $(1\text{-}kn^2)\cdot u^{-1/2}$, with 0.1 being very windy and/or cloudy, and 1 being calm and clear.

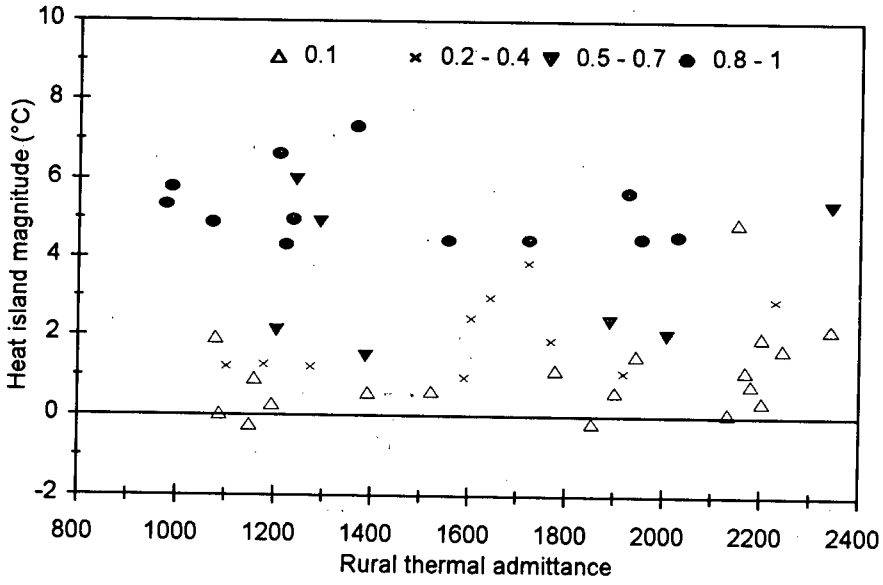

This chapter shows that there is significant seasonal variability in the rural thermal admittance which model calculations indicate should be capable of producing significant variations in rural nocturnal cooling and heat island intensity. Larger than average heat island intensities are associated with smaller than average thermal admittances, and smaller than average heat island

intensities occur with larger than average thermal admittances. However, when averaged on a seasonal basis, the calculated thermal admittances do not agree with those expected from the strength of nocturnal cooling (Chapter 4). Nor does the heat island magnitude on any individual occasion appear to be limited by the value of the thermal admittance.

These results imply that while rural thermal admittance may be a control on rural cooling, it is just one of many factors producing variations in nocturnal cooling and heat island intensity. The relationship between thermal admittance and heat island intensity is complicated by other undetermined influences. Therefore, even after accounting for variable weather conditions, rural thermal admittance is not the only factor which determines heat island magnitude on individual nights in a given city.

Chapter 6

CONCLUSIONS

This thesis presents the results of an analysis of the characteristics and dynamics of Vancouver's urban heat island. The roles of weather conditions and seasonal factors in controlling heat island magnitude are examined. In particular, the role of thermal admittance of the rural surface as a significant control on seasonal variations of nocturnal cooling and heat island magnitude is investigated.

6.1 Summary of Conclusions

- The urban heat island effect as given by urban - rural air temperature differences is present in Vancouver most of the time, and averages 1.4 °C annually. The heat island effect is largest at night, averaging 2.4 °C on an annual basis. A maximum magnitude of 8.9 °C was observed in this study.
- The daily cycle of heat island growth shows that on average the magnitude increases rapidly a few hours before sunset, peaks a few hours after sunset, remains high during the night, then decreases rapidly after sunrise and is essentially eliminated by mid-afternoon. This agrees with previous findings (Oke and Maxwell, 1975). The timing of the daily cycle changes seasonally, with the growth of the heat island occurring earlier in winter and latest in the fall. As a result about half of the maximum nocturnal heat island magnitude is reached by sunset in winter, while only 10 percent of the maximum is reached by sunset in the fall. The maximum magnitude also occurs later in the fall (closer to sunrise).

- On average, wind speed and both cloud amount and height are significant controls on the heat island. Its magnitude varies linearly with the inverse square root of wind speed, as shown by Oke (1973). It also decreases with $(1\text{-}kn^2)$, where k is a coefficient related to cloud height, and n is the cloud amount in tenths. It is therefore possible to predict the average maximum heat island magnitude expected (as a fraction of the maximum observed value) from wind speed and cloud amount and type. However, these weather variables do not explain the significant variability of magnitude observed on individual occasions.
- Nocturnal heat island magnitudes are largest in the fall, followed by summer, winter and spring. The frequency of occurrence of heat islands larger than 6 °C is also greater in the fall.
- Nocturnal heat island magnitudes under 'ideal' (calm and clear) conditions showed surprisingly little seasonal variability compared to those averaged for all weather conditions. This fact, combined with large day-to-day variability which cannot be accounted for by wind and cloud indicates that other factors are present which exert significant control on heat island magnitude on any particular occasion.
- Differences in urban and rural cooling and warming rates are clearly related to the daily cycle of heat island growth, but seasonal variations in cooling rates do not explain the observed variations in nocturnal heat island magnitudes. On average, both urban and rural sites begin cooling approximately 4 hours before sunset, but rural cooling is significantly greater until 4 hours after sunset (when the maximum heat island intensity occurs). For the rest of the night the cooling rates are similar. Warming begins at approximately the same time at both sites, but the rural warming rate is greater throughout the day. Urban cooling rates are largely unaffected by wind and cloudiness, whereas the maximum rural cooling rate is doubled under calm, clear conditions. Urban cooling rates also display relatively little seasonal variability compared to rural cooling. Based on potential nocturnal cooling alone, heat island

magnitudes are expected to be largest in fall, followed by spring, winter and summer. The observed order is fall, summer, winter, spring.

- The largest heat island magnitudes observed in this study occur shortly after sunrise in early fall. They result from warming at the urban site occurring while the rural site continues to cool. This delayed rural warming is probably due to the presence of fog at the rural site.
- Two methods to estimate rural thermal admittance are explored. The agreement between the two methods is difficult to determine since comparisons were only possible on a few occasions. The seasonal variability of rural thermal admittance estimated from observed soil moisture is significant enough to produce heat island magnitude differences of 3 to 9 °C under ideal conditions according to model results (Oke *et al.*, 1991). However, as noted above, the observed heat island magnitudes on ideal nights do not vary as much.
- Furthermore, seasonally averaged thermal admittances do not vary as much as expected from seasonally averaged nocturnal cooling, indicating that thermal admittance is not the only significant control on nocturnal cooling. As it is noted that seasonal variations in rural cooling do not fully explain variations in heat island magnitude, it is perhaps not surprising that a clear relationship between rural thermal admittance and heat island intensity is not observed. Only 60 percent of the months show larger (smaller) than average heat island magnitudes occur when rural thermal admittance is smaller (larger) than average. In the remaining months, the heat island magnitudes, rather than thermal admittances, appear anomalous. Observations of heat island magnitudes and rural thermal admittances on particular nights do not indicate any obvious relationship between the two variables, even after wind and cloud effects are accounted for.

6.2 Recommendations for Further Research

Perhaps the most curious aspect of this research is the finding that the relationships between heat island magnitude and the most obvious physically relevant controls are clearly defined and predictable on average, but not on any individual occasion. The day-to-day variability of heat island magnitude cannot be explained by weather conditions or the thermal admittance of the rural soil which determines the amount of cooling. Random temperature fluctuations at each site as well as experimental errors may contribute to this variability. A network of urban and rural stations, rather than single sites might eliminate some of this variability.

It also appears that other significant controls on heat island magnitude are probably at work. Further investigation of the role of solar radiation, wind speed and surface wetness during the day may help to explain some of this variability, or perhaps other controls can be identified. A similar study in another city with less complex topography, (*e.g.* without the complications of sea breezes and valley-channeled flow) might also help to identify the important controls on heat island magnitude.

This study is unable to find conclusive evidence that rural thermal admittance is a significant control on heat island magnitude, despite the obvious physical relevance of thermal admittance to the cooling process. Measurement of the necessary variables to estimate thermal admittance from Brunt's (1932) equation at different times of the year and over a greater range of thermal admittances would be helpful to understand this relationship better. It would also allow better understanding of the relationship between thermal admittance determined by the Brunt method and that estimated from soil properties. Alternative practical measures of thermal admittance might also be investigated.

The surprising lack of seasonal variability in heat island magnitude, especially on calm and clear nights might simply be a function of the relatively small seasonal variability of temperatures

in Vancouver's maritime setting. Again, a similar study in a city with greater seasonal variations in climate and significant variations in rural thermal admittance might help to understand the relationship between these two variables.

A further approach to establish the relationship between heat island intensity and rural thermal admittance would be to obtain reasonable estimates of the thermal admittance of the rural surroundings at the time of maximum observed heat island intensity in a number of cities from around the world. Variations in rural thermal admittances may explain the regional variability in heat island intensity which cannot be accounted for by variations in the sky-view factor alone.

This research has shown that causes and controls of the urban heat island interact in complex, and as of yet, not fully understood ways. Both urban and rural factors are at work producing seemingly random variations in heat island intensity which cannot be explained in terms of the most obvious physical controls. We are still far from being able to predict heat island magnitude on any given occasion, despite the apparent predictability in the mean. These findings should not be considered cause for discouragement, however, but rather as a reminder that this field is still ripe with challenging research opportunities.

REFERENCES

Atwater, M.A. (1977): Urbanisation and pollutant effects on the thermal structure in four climatic regimes. *Journal of Applied Meteorology* **16**, 887-895.

Bahl, H.D. and B. Padmanabhamurty (1979): Heat island studies at Delhi. *Mausam* **30**, 119-122.

Bowling, S.A. and C.S. Benson (1978): Study of the subarctic heat island at Fairbanks, Alaska. Environmental Monitor. Report No. EPA-600/4-78-072, US E.P.A., Research Triangle Park, N.C.

Brunt, D. (1932): Notes on radiation in the atmosphere 1. *Quarterly Journal of the Royal Meteorological Society* **58**, 389-420.

Byrne, G.F. and J.R. Davis (1980): Thermal inertia, thermal admittance, and the effect of layers. *Remote Sensing of Environment* **9**, 295-300.

Campbell, Gaylon S. (1977): *An Introduction to Environmental Biophysics.* Springer-Verlag, New York. 159 pp.

Chandler, T.J. (1965): *The Climate of London.* Hutchinson, London.

de Vries, D.A. (1966): Thermal properties of soils, *in* W.R. Van Wijk, *Physics of Plant Environment*, 2nd edition. North-Holland Publishing Company, Amsterdam.

de Vries, D. A. (1975): Heat transfer in soils, *in* D.A. de Vries and N.H. Afgan (editors), *Heat and Mass Transfer in the Biosphere.* John Wiley & Sons, New York, 5-28.

Emslie, J.H. (1972): Surface temperature field Greater Vancouver, B.C. Technical Memoranda. Atmospheric Environment Service, Department of the Environment, Canada.

Estournel, C., R. Vehil, D. Guedalia, J. Fontan and A. Druilhet (1983): Observations and modelling of downward radiative fluxes (solar and infrared) in urban/rural areas. *Journal of Climate and Applied Meteorology* **22**, 134-142.

Field, W.J. (1973): The effect of overcast cloud on the Vancouver heat island, unpublished project, Department of Geography, University of British Columbia.

Groen, P. (1947): On radiational cooling of the earth's surface during the night, especially with regard to the prediction of ground frosts. *Koninklijk Nederlands Meteorologisch Instituut De Bilt, No. 125: Mededelingen en Verhandelingen Serie B Deel I, No. 9*, 34 pp.

Hage, K.D. (1972): Nocturnal temperatures in Edmonton, Alberta. *Journal of Applied Meteorology* **11**, 123-129.

Howard, L. (1833): *The Climate of London*, Vols. I-III, London.

Jauregui, E., L. Godinez and F. Cruz. (1992): Aspects of heat-island development in Guadalajara, Mexico. *Atmospheric Environment* **26B**, 391-396.

Jauregui, E. (1986): The urban climate of Mexico City, *in* Oke, T.R. (ed):, *Urban Climatology and its applications with special regard to tropical areas.* WMO No. 652, World Meteorological. Organization, Geneva, 63-86.

Kagawa, N. H. (1968): An evaluation of Brunt's cooling formula for minimum temperature prediction at five prairie locations. TEC 667, Met. Branch, Department of Transport, Canada, 20 pp.

Lee, D.O. (1975): Rural atmospheric stability and the intensity of London's heat island. *Weather* **30**, 102-109.

Lee, D.O. (1979): Contrasts in warming and cooling rates at an urban and a rural site. *Weather* **34**, 60-66.

Lowry, W. P. (1977): Empirical estimation of urban effects on climate: a problem analysis. *Journal of Applied Meteorology* **16**, 129-135.

Ludwig, F.L. (1970): Urban air temperatures and their relation to extra-urban meteorological measurements, *in* Papers presented at the Symposium on Survival Shelter Problems, American Society of Heating, Refrigerating, and Air Conditioning Engineers, New York. Document SF-70-9, pp. 40-48.

Lyons, T.J. (1983): Comments on 'Canyon geometry and the nocturnal urban heat island: comparisons of scale model and field observations.' *Journal of Climatology* **3**, 95-101.

Novak, M.D and T.A. Black (1983): The surface heat flux density of a bare soil. *Atmosphere-Ocean* **21**, 431-443.

Oke, T.R. (1973): City size and the urban heat island. *Atmospheric Environment* 7, 769-779.

Oke, T.R. (1976): The distinction between canopy and boundary-layer urban heat islands. *Atmosphere* **14**, 268-277.

Oke, T.R. (1981): Canyon geometry and the nocturnal urban heat island: comparison of scale model and field observations. *Journal of Climatology* **1**, 237-254.

Oke, T.R. (1982): The energetic basis of the urban heat island. *Quarterly Journal of the Royal Meteorological Society* **108**, 1-24.

Oke, T.R. (1987): *Boundary Layer Climates*, 2nd Edition. Methuen, London, 435 pp.

Oke, T.R. (1995): The Heat Island of the Urban Boundary Layer: Characteristics, Causes and Effects, *in* J.E. Cermak *et al.* (editors), *Wind Climate in Cities.* Kluwer Academic Publishers,Netherlands, 81-107.

Oke, T.R. and G.B. Maxwell (1975): Urban heat island dynamics in Montreal and Vancouver. *Atmospheric Environment* **9**, 191-200.

Oke, T.R., G.T. Johnson, D.G. Steyn and I.D. Watson (1991): Simulation of surface urban heat islands under 'ideal' conditions at night Part 2: Diagnosis of causation. *Boundary-Layer Meteorology* **56**, 339-358.

Oke, T.R. and J.E. Hay (1994): *The Climate of Vancouver* 2nd Edition. B.C. Geographical Series, Number 50.

Philip, N., E. Daniel and K. Krishnamurthy (1973): Seasonal variation of surface temperature distribution over Bombay. Proceedings for the Symposium on Environmental Pollution, New Delhi, 308-317.

Reuter, H. (1951): Forecasting minimum temperatures. *Tellus* **3**, 141-147.

Spronken-Smith, R. A. (1994): *Energetics and Cooling in Urban Parks.* Ph.D. Thesis, Department of Geography, University of British Columbia, Vancouver, B.C.

Steyn, D.G. (1980): The calculation of view factors from fisheye-lens photographs. *Atmosphere-Ocean* **18**, 254-258.

Sundborg, A. (1951):. Climatological studies in Uppsala with special regard to the temperature conditions in the urban area. *Geographica*, Geographical Institute Uppsala No. 22, 111 pp.

Tyson, P.D., W.J.F. Du Toit and R.F. Fuggle (1972): Temperature structure above cities: review and preliminary findings from the Johannesburg Urban Heat Island Project. *Atmospheric Environment* **6**, 533-542.

Unwin, D.J. (1980): The synoptic climatology of Birmingham's urban heat island, 1965-74. *Weather* **35**, 43-50.

van de Griend, A.A., P.J. Camillo and R.J. Gurney (1985): Discrimination of soil physical parameters, thermal inertia, and soil moisture from diurnal surface temperature fluctuations. *Water Resources Research* **21**, 997-1009.

van Wijk, W.R. and W.J. Derksen (1966): Sinusoidal temperature variation in a layered soil, *in* W.R. van Wijk (editor), *Physics of Plant Environment* 2nd Edition. North Holland Publishing Company, Amsterdam, p. 191.